Projecting Climate Change in the United States

A Technical Document Supporting the Forest Service 2010 RPA Assessment

Linda A. Joyce, David T. Price, David P. Coulson, Daniel W. McKenney, R. Martin Siltanen, Pia Papadopol, and Kevin Lawrence

Joyce, Linda A.; Price, David T.; Coulson, David P.; McKenney, Daniel W.; Siltanen, R. Martin; Papadopol, Pia; Lawrence, Kevin. 2014. **Projecting climate change in the United States: A technical document supporting the Forest Service RPA 2010 Assessment**. Gen. Tech. Rep. RMRS-GTR-320. Fort Collins, CO: U.S. Department of Agriculture, Forest Service, Rocky Mountain Research Station. 85 p.

ABSTRACT: A set of climate change projections for the United States was developed for use in the 2010 USDA Forest Service RPA Assessment. These climate projections, along with projections for population dynamics, economic growth, and land use change in the United States, comprise the RPA scenarios and are used in the RPA Assessment to project future renewable resource conditions 50 years into the future. This report describes the development of the historical and projected climate data set. The climate variables are monthly total precipitation in millimeters (mm), monthly mean daily maximum air temperature in degrees Celsius (°C), and monthly mean daily minimum air temperature in degrees Celsius (°C). Downscaled climate data were developed for the period 2001-2100 at the 5-arcminute grid scale (approximately 9.3 km by 7.1 km grid size at 40 degree N) for the conterminous United States. These data were also summarized at the U.S. county level. Computed monthly mean daily potential evapotranspiration (mm) and mean grid cell elevation in meters (m) are also included in the data set. The scenarios used here from the IPCC Special Report on Emissions Scenarios are A1B, A2, and B2. The A1B and A2 scenarios were used to drive three climate models: the Third Generation Coupled Global Climate Model, version 3.1, medium resolution; the Climate System Model, Mark 3.5 (T63); and the Model for Interdisciplinary Research on Climate, version 3.2, (T42), all used in the Fourth IPCC Assessment. The B2 scenario was used to drive three earlier generation climate models: the Second Generation Coupled Global Climate Model, version 2, medium resolution; the Climate System Model, Mark 2; and the UKMO Hadley Centre Coupled Model, version 3, all used in the IPCC Third Assessment. Monthly change factors were developed from global climate model output using the delta method. The coarse-resolution change factors were downscaled to a 5-arcminute resolution grid using ANUSPLIN. The 30-year mean historical climatology (1961-1990) was developed using the Parameter-elevation Regressions on Independent Slopes Model (PRISM) data at 2.5-arcminute resolution and aggregated to the 5-arcminute resolution grid. The downscaled change factors were combined with the PRISM observed climatology to develop nine future climate projections for the conterminous United States. These projection data and the change factor data are available through the U.S. Forest Service data archive website (http://www.fs.usda.gov/rds/archive/).

Keywords: Climate scenario, downscaling, PRISM, natural renewable resource assessments, RPA Scenarios.

Authors

Linda A. Joyce, U.S. Department of Agriculture, Forest Service, Rocky Mountain Research Station, Fort Collins, Colorado.

David T. Price, Northern Forestry Centre, Natural Resources Canada, Canadian Forest Service, Edmonton, Alberta.

David P. Coulson, U.S. Department of Agriculture, Forest Service, Rocky Mountain Research Station, Fort Collins, Colorado.

Daniel W. McKenney, Great Lakes Forestry Centre, Natural Resources Canada, Canadian Forest Service, Sault Ste. Marie, Ontario.

R. Martin Siltanen, Northern Forestry Centre, Natural Resources Canada, Canadian Forest Service, Edmonton, Alberta.

Pia Papadopol, Great Lakes Forestry Centre, Natural Resources Canada, Canadian Forest Service, Sault Ste. Marie, Ontario.

Kevin Lawrence, Great Lakes Forestry Centre, Natural Resources Canada, Canadian Forest Service, Sault Ste. Marie, Ontario.

Acknowledgments

We acknowledge the modeling groups, the Program for Climate Model Diagnosis and Intercomparison, and the World Climate Research Programme's (WCRP) Working Group on Coupled Modelling for their roles in contributing and willingness to share the WCRP Coupled Model Intercomparison Project phase 3 (CMIP3) multi-model dataset through the Program for Climate Model Diagnosis and Intercomparison web-based data portal. Support of this dataset is provided by the Office of Science, U.S. Department of Energy.

Further, we greatly appreciate the availability of data provided by:

The Canadian Centre for Climate Modelling and Analysis

The Australian Commonwealth Scientific and Industrial Research Organisation, particularly M. Collier, M. Dix, and T. Hirst of the Marine and Atmospheric Research Division

In Japan, the Center for Climate System Research, together with the University of Tokyo, the National Institute for Environmental Studies, and the Frontier Research Center for Global Change.

The Hadley Centre for Climate Prediction and Research, UK.

We acknowledge the use of PRISM (Parameter-elevation Regressions on Independent Slopes Model) climate mapping system, developed by Chris Daly, PRISM group director, and colleagues for the characterization of historical climate. We also acknowledge the support of the USDA Forest Service and Natural Resources Canada, Canadian Forest Service. We greatly appreciate the time and effort by reviewers for technical review: David Wear, Michael Bowker, Ashley Askew, Matt Reeves, Jim Morrison, Jeff Lukas, Tom Brown; for statistical review, Scott Baggett; for editorial review, Lane Eskew and Loa Collins.

You may order additional copies of this publication by sending your mailing information in label form through one of the following media. Please specify the publication title and number.

Publishing Services

Telephone	(970) 498-1392
FAX	(970) 498-1122
E-mail	rschneider@fs.fed.us
Web site	http://www.fs.fed.us/rmrs
Mailing Address	Publications Distribution Rocky Mountain Research Station 240 West Prospect Road Fort Collins, CO 80526

Contents

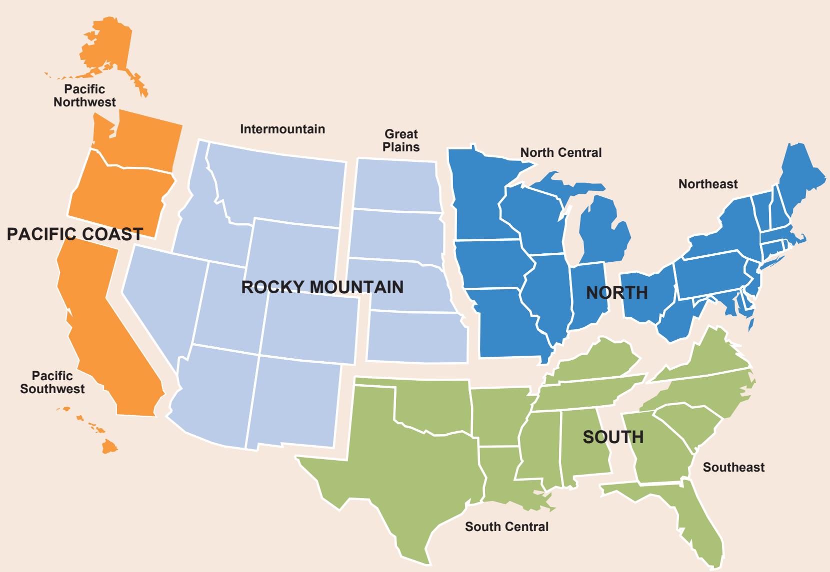

Pacific Northwest
Intermountain
Great Plains
North Central
Northeast
PACIFIC COAST
ROCKY MOUNTAIN
NORTH
Pacific Southwest
SOUTH
Southeast
South Central

Introduction

Climate influences the long-term dynamics of forests and rangelands across the United States and the production of renewable natural resources from these public and private lands. Human communities across the United States are dependent upon ecosystem services from forests and rangelands. Such services range from clean water for human consumption to commodity products such as timber to biodiversity of plants and animals. Increasingly, the potential effects of climate change have become a concern for resource managers.

The Resource Planning Act (RPA) Assessment produced by the USDA Forest Service provides a snapshot of current U.S. forest and rangeland conditions and trends on all ownerships, identifies drivers of change, and projects 50 years into the future (see USDA Forest Service 2012a). This Assessment is produced every 10 years as required by the Forest and Rangeland Renewable Resources Planning Act (RPA) of 1974. In addition, the Act specifically requires an analysis of the potential effects of climate change on U.S. forests and rangelands (Joyce and Birdsey 2000). The 2010 RPA Assessment uses a scenario-based approach that integrates the individual resource analyses with particular emphasis on links to alternative world economic outlooks, population growth, and associated climate change (USDA Forest Service 2012a,b). Such an approach allows the RPA assessment to analyze a range of possible futures, including climate change, for U.S. renewable resources.

Criteria for selecting scenarios to be used in the RPA Assessment specified that the scenarios be globally consistent, scientifically credible and well documented, and include key driving forces of resource change such as population, economic growth, land use change, energy use, and climate (USDA Forest Service 2012a). The scenarios used in Intergovernmental Panel on Climate Change (IPCC) Third and Fourth Assessment reports met these criteria, particularly in the areas of documentation and data availability (IPCC 2001a, 2007a). Described in the Special Report on Emissions Scenarios (SRES) (Nakicenovic and Swart 2000), these scenarios integrate socioeconomic driving forces as well as climate change. Three SRES scenarios (A1B, A2, and B2) were identified that would provide the RPA Assessment with a wide range of possible futures (USDA Forest Service 2012a). Socioeconomic and climate data were available at the global and macro-regional level from the IPCC scenario-based projections; however, RPA resource analyses are typically conducted using U.S. county or finer scale data. Procedures used to develop national and sub-national projections of population, economic growth, income, bioenergy use, and land use change can be found in Gen. Tech. Rep. RMRS-GTR-272 (USDA Forest Service 2012a). Development of the finer-spatial-scale projections of climate is the focus of this report.

The requirement of a nationally consistent set of scenario-based climate projections at the county spatial scale necessitated a process to retrieve and downscale global climate model output to the scale of 5-arcminutes for the conterminous United States and Alaska. This task was undertaken through a cooperative effort between the Canadian Forest Service and the USDA Forest Service (Price and others 2011a; Joyce and others 2011; this General Technical Report). We use the downscaling methods of Price and others (2011a) and Joyce and others (2011) and the historical gridded climatology based on PRISM (Parameter-elevation Regressions on Independent Slopes Model) to provide a suite of future climate scenarios for the conterminous United States for use in the RPA Assessment. In this report, we describe the downscaling approach and development of the climate projection data at the 5-arcminute resolution. We present a series of graphics to describe and interpret the climate projections for the conterminous United States. These data are publicly available through the U.S. Forest Service archive website (http://www.fs.usda.gov/rds/archive/) and are described using internationally accepted standards for metadata documentation (Coulson and Joyce 2010a,b; Coulson and others 2010a,b,c,d; Price and others 2011b,c). These climate data are being used in the RPA analyses of forest condition, wildlife habitat, water yield/use, recreation participation, and effects of natural amenities on rural population migration (e.g., Bowker and others 2012; Cordell and others 2011; Foti and others 2012; Greenfield and Nowak 2013; Wear and others 2013). The intended audiences for this report are those individuals who are interested in modeling the ecological and socio-economic effects of climate change and need climate projection data. These data may also be useful input for other applications exploring the impact of climate change on resource management issues.

Linking Population and Economic Drivers With Global Climate

Briefly, the process of constructing alternative world futures undertaken by the IPCC and the climate modeling community requires integrating the socioeconomic global driving forces; estimating greenhouse gas emissions resulting from these forces as well as the effects of the emissions on atmospheric chemistry; and finally determining the effects of that changing atmospheric chemistry on the global climate (Figure 1). Global driving forces include

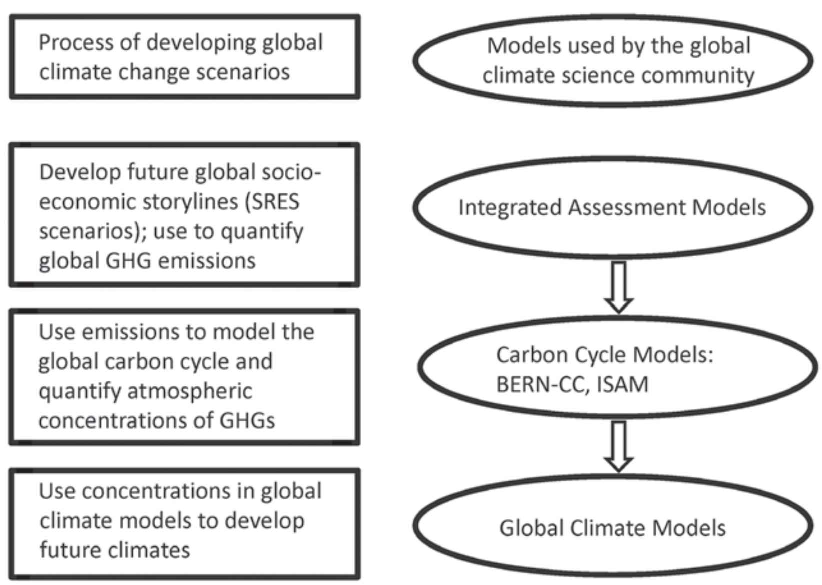

Figure 1. Process used by the global climate science community to develop socio-economic global driving forces and to quantify the effects of those forces to future greenhouse gas emissions and future climates for the Intergovernmental Panel on Climate Change.

demographic shifts, technological changes, energy development, economic interactions, and environmental considerations associated with land use changes. Storylines describing trends in these future global forces were developed in the Special Report on Emission Scenarios (SRES) for the Third IPCC Assessment and were also used in the Fourth IPCC Assessment (Nakicenovic and Swart 2000). For example, the A1 storyline describes a future world of very rapid economic growth, low population growth, and rapid introduction of new and more efficient technologies (Table 1). Within the A1 storyline, three sub-storylines focus on alternative directions of technological change in the energy sector. The A1B storyline reflects a balanced future use of fossil fuel and non-fossil energy sources. The A2 storyline describes the future world as very heterogeneous, where economic development is regionally oriented and though fertility rates vary, global population growth is relatively high. The B2 storyline envisions a world where emphasis is on more local solutions to achieve economic, social, and environmental sustainability, and economic growth is intermediate. These storylines do not include policies to limit greenhouse gases or implement adaptation strategies. No single storyline is considered more or less likely than another, and all include aspects that may be considered desirable or undesirable.

Table 1—Summary characteristics of the four storylines developed by the Special Report on Emissions (modified from Parry and others [2007]).

SRES storyline	World	Economy	Population	Governance	Technology
A1	Market-oriented	Fastest per capita growth	2050 peak, then decline	Strong regional interactions, income convergence	Three sub-storylines: A1FI – fossil intensive A1T – non-fossil energy sources A1B – balanced across all sources
A2	Differentiated	Regionally oriented; lowest per capita growth	Continuously increasing	Self-reliance with preservation of local identities	Slowest and most fragmented development
B1	Convergent	Service and information based; lower growth than A1	Same as A1	Global solutions to economic, social and environmental sustainability	Clean and resource-efficient
B2	Local solutions	Intermediate growth	Continuously increasing at lower rate than A2	Local and regional solutions to environmental protection and social equity	More rapid than A2, less rapid, more diverse than A1/B1

The qualitative storylines were then used to develop global emission scenarios (Nakicenovic and Swart 2000). Population and economic trends were quantified and six integrated assessment models (IAMs) were used to estimate the global greenhouse gas emissions that would result from these socioeconomic driving forces over the next 100 years. Marker scenarios were identified as results from specific IAMs that were illustrative of a particular storyline (Figure 2). The integrated assessment models estimated, for each scenario, the total amounts (metric tons) of greenhouse gases emitted per year into the atmosphere at 10-year intervals (http://www.ipcc-data.org/ddc_co2.html). These emissions are the total amounts of greenhouse gases that would result from future global economic activity and population growth. In order to determine the impact of these emission levels on climate, the quantities in total metric tons emitted (output from the IAMs) must be converted to atmospheric concentrations through time.

Emissions of carbon dioxide (CO_2) gas enter the global carbon cycle where carbon is cycled through plants, soil, and bedrock within the terrestrial ecosystem, through water, plants, ocean bottom within ocean ecosystems, and through the atmosphere. Activities such as deforestation and fossil fuel combustion return CO_2 to the atmosphere. Once emitted into the atmosphere, CO_2 and other greenhouse gases interact with atmospheric chemistry, the vegetated land surface, and other components of the global carbon cycle. Those dynamics determine

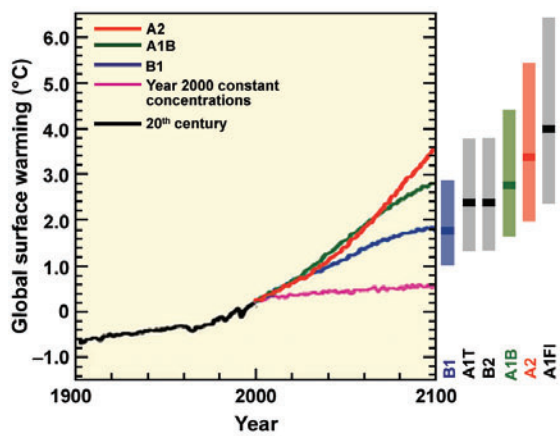

Figure 2. Solid lines are multi-model global averages of surface warming (relative to 1980-1999) for the SRES scenarios A2, A1B, and B1, shown as continuations of the 20th century simulation. The orange line is for the experiment where concentrations were held constant at year 2000 values. To the right of the graph, the vertical colored bars indicate the best estimate of surface warming (solid black line within each bar) and the likely range assessed for the six SRES marker scenarios at 2090-2099 relative to 1980-1999. The assessment of the best estimate and likely ranges includes results from the Atmosphere-Ocean General Circulation Models (AOGCMs) shown in the left part of the figure, as well as results from a hierarchy of independent models and observational constraints (Figure 3.2 Synthesis Report AR4, downloaded January 8, 2013).

the atmospheric concentration of the gases over time. Two different carbon cycle models were used to project future CO_2 concentrations based on the SRES scenarios (Figure 1): the Integrated Science Assessment Model (ISAM) and the Bern Carbon Cycle model (Bern-CC). Though simplified, these carbon cycle models contain ocean and terrestrial ecosystem feedbacks to the atmosphere consistent with more process-based models and allow for uncertainties in climate sensitivity and in ocean and terrestrial responses to CO_2 and climate (Prentice and others 2001). Atmospheric CO_2 concentrations associated with the SRES scenarios A1B, A2, and B2—based on output from the Bern-CC and ISAM models—are given in Appendix I. Nitrogen oxide (NO_x) emissions were also computed in the integrated assessment models (http://www.ipcc-data.org/ddc_co2.html) and are given in Appendix I. In contrast to CO_2, which is a well-mixed gas globally and one atmospheric concentration is reasonably representative of conditions around the entire globe, regional concentrations of nitrogen gases vary. Nitrogen gases have been spatially distributed across the global grid for the A2 scenario (Lamarque and others 2005).

Global climate models use these projections of atmospheric concentrations of CO_2 and other greenhouse gases to estimate their effects on global climate (Meehl and others 2007a; see also http://www.ipcc-data.org/ddc_co2.html). The published results of these analyses are synthesized in IPCC reports (most recently, IPCC 2007a). Storylines influence global emissions (Table 1) and, consequently, the global climate. For example, the B1 scenario (Table 1) assumes a future where economic growth is low and there is emphasis on clean and resource-efficient energy technology. The projected global average surface warming based on several models using the B1 scenario is 1.8 ^{o}C by the 2090-2099 period (relative to 1980-1999, IPCC 2007a). In contrast, when the high per-capita growth and fossil intensive energy technology of the A1FI scenario is analyzed, a surface warming of 4.0 ^{o}C is projected for the 2090-2099 period. The exploration of these scenarios with several climate models shows the range of projected future temperatures (Figure 2). Projected global temperatures do not differ appreciably among the emissions scenarios until after 2030 (Figure 2), which indicates that the world is already committed to warming of about 1.0 ^{o}C, relative to the 1990s, regardless of any mitigation efforts. This commitment is caused by the thermal lag of the oceans, which will continue to absorb extra heat for several decades because of the additional greenhouse gases already present in the atmosphere.

The future climates projected by the climate modeling groups vary among scenarios and climate models. All models are based on physical principles, and implementation of those principles is nuanced by understandings of the climate modelers and their experience projecting climate dynamics. Climate models depict the global climate using a three-dimensional grid over the globe, typically having a horizontal resolution of between 250 and 600 km, 10 to 20 vertical layers in the atmosphere, and in some cases, as many as 30 layers in the ocean. Given the horizontal dimensions of the grid cells, each grid cell typically covers a vast area. The results from these models are generated at a scale too coarse for assessing U.S. climate change effects in the RPA Assessment, where the spatial scale of analysis is typically the size of a U.S. county or smaller. Hence, there is the need to downscale the climate projections to the spatial scales used for the RPA Assessment, namely the U.S. counties and the 5-arcminute grid (approximately 9.3 km north-south by 7.1 km east-west at 40 degrees N, approximately at mid-conterminous United States).

Methods

Selection of Climate Models

RPA Scenarios

The requirement of a diverse set of population and economic futures for the RPA Assessment led to the initial choice of SRES scenarios A1T, A1FI, A2, and B2 (see Table 1 for the varying population and economic assumptions) (USDA Forest Service 2012a). The protocols for climate experiments and archival procedures varied between the Third IPCC Assessment (TAR) and the Fourth IPCC Assessment (AR4). For the TAR, climate model projection data from varying experiments that modeling groups across the world conducted were archived through the Data Distribution Center (DDC) of the IPCC. In contrast, the climate model community agreed to structure a consistent series of experiments to explore climate dynamics for the AR4 report (Meehl and others 2007a). The archiving process, overseen by the Program for Climate Model Diagnosis and Intercomparison (PCMDI), provided a standardization of terms and output across models. However, the final set of modeling experiments for the AR4 included only the SRES scenarios A1B, A2, and B1 (Meehl and others 2007a). Thus, no climate projections for A1T, A1FI, and B2 scenarios were archived through PCMDI (http://www-pcmdi.llnl.gov/ipcc/data_status_tables.htm). Identifying a priority to use the AR4 model results from PCMDI, the RPA process selected the A1B scenario in place of the A1T and A1FI scenarios. Projections in the AR4 associated with A2 were available from the PCMDI web portal, and we turned to archived projections for the B2 scenario from the TAR at the IPCC data portal. Hence, the RPA Scenarios are based on the SRES scenarios of A1B, A2, and B2 (USDA Forest Service 2012a,b).

Climate Models and Output

For each of the three scenarios (A1B, A2, and B2), output from three climate models was used to develop the downscaled projections (Table 2). For scenarios A1B and A2, the same three models were selected: the Third Generation Coupled Global Climate Model, version 3.1, medium resolution [CGCM3.1(T47)]; the Climate System Model, Mark 3.5 [CSIRO-MK3.5(T63)]; and the Model for Interdisciplinary Research on Climate, version 3.2, medium resolution [MIROC3.2(T42)]. For the B2 scenario, the three models selected were the Second Generation Coupled Global Climate Model, version 2, medium resolution [CGCM2]; the Climate System Model, Mark 2 [CSIRO-MK2]; and the Hadley Centre Coupled Model, version 3 [HadCM3] (Table 2). The CGCM and CSIRO models were used in all scenarios, however the versions used for the B2 scenario are associated with the TAR, and are separated by several years of model development from the versions used the AR4 report (see Discussion section for more information on these models).

Scenarios A1B and A2. The climate models were chosen for emissions scenarios A1B and A2 based on the availability of projections in the PCMDI Third Coupled Model Intercomparison Project (CMIP3) database at the time this study started, and the availability of variables needed for the RPA Assessment, and climate assessments being done in Canada (see Discussion section for the broader set of scenarios/models available now). Output data (projections from the climate models) were obtained primarily from the CMIP3 data portal, which

Table 2—Climate models used in the 2010 RPA Assessment.

	Climate Models			
Scenarios	Coupled Global Climate Model (CGCM)	Climate System Model	Hadley Centre Model	Model for Interdisciplinary Research on Climate (MIROC)
B2	Second General Coupled Global Climate Model, version 2, medium resolution (T47) [CGCM2]	Climate System Model, Mark 2, [CSIRO-MK2]	Hadley Centre Coupled Model version 3 [HadCM3]	
A1B and A2	Third Generation Coupled Global Climate Model, version 3.1, medium resolution (T47) [CGCM3.1(T47)]	Climate System Model, Mark 3.5 (T63) [CSIRO-MK3.5 (T63)]		Model for Interdisciplinary Research on Climate, version 3.2, medium resolution [MIROC3.2(T42)]
Climate Modeling Research Centers	Canadian Centre for Climate Modelling and Analysis, Canada	Commonwealth Scientific and Industrial Research Organization (CSIRO), Australia	Hadley Centre for Climate Prediction and Research, UK	Japanese Center for Climate System Research, University of Tokyo; National Institute for Environmental Studies, and Frontier Research Center for Global Change, Japan

offers standardization of format, variable names, units, and other aspects facilitating comparisons among models (Table 3). In addition to output for A1B and A2 projections, climate model output for the 20th century simulations (20C3M) were also obtained. The 20th century simulations (1961-1990) were used to normalize the global climate projections. Global projections can be biased; combining the normalized values with observed climatological data at the scale of interest corrects the bias in the global projections. Variables included monthly mean daily minimum air temperature (at 2 m above surface), monthly mean daily maximum air temperature (at 2 m above surface), and monthly total precipitation (Table 4). The CMIP3 catalogue numbers of the individual model runs (also called realizations) associated with the AR4 models used in this study are given in Appendix II. This information can be important when comparing climate projections used in this study with other climate projections of the same models.

Scenario B2. Three climate models using the B2 scenario in the TAR were chosen from the suite of climate models that had been downscaled by Price and others (2004) using the same approach as for the AR4 scenarios by Price and others (2011a) and this study. The downscaling of these B2 scenarios was part of the VINCERA (Vulnerability and Impacts of North American Forests to Climate Change: Ecosystem Response and Adaptation) project (Price and others 2004; Price and Scott 2006; Bachelet and others 2008; Lenihan and others 2008).

Table 3—Climate model output data for the historical simulation for the 20th century (20C3M) from period 1961-2000 and the scenarios A1B and A2 from period 2001-2100 (used in the Intergovernmental Panel on Climate Change Fourth Assessment report) were obtained from the WCRP Coupled Model Intercomparison Project phase 3 (CMIP3) multi-model dataset and obtained through the Program for Climate Model Diagnosis and Intercomparison (PCMDI) web-based data portal.

Climate model version, modeling center	Nominal cell size	Source of the model data
CGCM3.1(T47), Third Generation Coupled Global Climate Model, version 3.1, medium resolution (T47), developed by the Canadian Centre for Climate Modelling and Analysis http://www.cccma.bc.ec.gc.ca/models/cgcm3.shtml	3.75 degrees latitude by 3.75 degrees longitude at the equator	CMIP3 data in PCMDI portal - Majority of the climate model/scenario/variable data were obtained from the CMIP3 data portal. https://esg.llnl.gov:8443/index.jsp CCCma data portal for CGCM3 model data (http://www.cccma.bc.ec.gc.ca/data/cgcm3/cgcm3.shtml). [Daily tmin/tmax data as CMIP3 did not have these data for the CGCM3 model.]
CSIRO-MK3.5, Climate System Model, Mark 3.5 (T63), developed by Commonwealth Scientific and Industrial Research Organization (CSIRO), Australia, http://www.cmar.csiro.au/e-print/open/gordon_2002a.pdf http://www-pcmdi.llnl.gov/ipcc/model_documentation/CSIRO-Mk3.5.htm	1.875 degrees latitude by 1.865 degrees longitude at the equator	CMIP3 data in PCMDI portal
MIROC3.2(T42), Model for Interdisciplinary Research on Climate, version 3.2, medium resolution (T42), developed by the Japanese Center for Climate System Research, University of Tokyo; National Institute for Environmental Studies, and Frontier Research Center for Global Change, http://www.ccsr.u-tokyo.ac.jp/kyosei/hasumi/MIROC/tech-repo.pdf	2.79 degrees latitude by 2.81 degrees longitude at the equator	CMIP3 data in PCMDI portal

Table 4—Variables in the climate model data sets obtained from the Program for Climate Model Diagnosis and Intercomparison data portal used to create the downscaled climate projections in this study. The CMIP3 catalogue numbers of the individual model runs (also called realizations) associated with the AR4 models used in this study are given in Appendix II.

Climate model[a]	SRES scenario(s)	Monthly variable(s)[b]	Source[c]	Time period
CGCM3.1(T47)	20C3M[d], A1B, A2	pr	CMIP3	1961–2100
CGCM3.1(T47)	20C3M, A1B, A2	tas, tasmin, tasmax	CCCma	1961–2100
CSIRO-MK3.5(T63)	20C3M, A1B, A2	tas, tasmin, tasmax, pr	CMIP3	1961–2100
MIROC3.2(T42)	20C3M, A1B, A2	tas, tasmin, tasmax, pr	CMIP3	1961–2100

[a] CGCM3.1(T47) = Third Generation Coupled Global Climate Model, version 3.1, medium resolution; CSIRO-MK3.5(T63) = Commonwealth Scientific and Industrial Research Organisation Climate System Model, Mark 3.5; MIROC3.2(T42) = Model for Interdisciplinary Research on Climate, version 3.2, medium resolution.
[b] Simulated climate variables (as defined by Program for Climate Model Diagnosis and Intercomparison): tas; mean 2m air temperature (K); tasmin: mean daily minimum 2m air temperature (K) (T_{min}); tasmax: mean daily maximum 2m air temperature (K) (T_{max}); pr: monthly precipitation (kg m^{-2} s^{-1}).
[c] The majority of the climate model, scenario, and variable data were downloaded from the WCRP Coupled Model Intercomparison Project Phase 3 (CMIP3) at the data portal hosted by the Program for Climate Model Diagnosis and Intercomparison (PCMDI) at https://eqg.llnl.gov:83443/index.jsp. This "multi-model data set" is archived by the PCMDI project. The major advantage to using CMIP3 data was their standardization of format, variable names, units, and other aspects, which facilitated comparison among models. The Canadian Centre for Climate Modelling and Analysis (CCCma) web site serves data for CGCM3.1(T47) and other Canadian climate models (http://www.cccma.bc.ec.gc.ca/data/cgcm3/cgcm3.shtml). Daily T_{min} and T_{max} data for CGCM3.1(T47) were obtained from this source because they were not available from CMIP3.
[d] The 20C3M refers to the 20th century model simulations.

Price and others (2004) obtained output data for the 1961-2100 period for three models from the IPCC Data Distribution Centre data portal (Table 5). These Third Assessment models are several years older than the models used for scenarios A1B and A2 (see Discussion section). Historical simulation realizations for the 20th century were also obtained and the 1961-1990 period was used to normalize the global projections. The data sets included three monthly climate variables: monthly mean daily maximum and minimum temperature, and monthly total precipitation (Price and others 2004). For CGCM2, multiple ensemble runs had been performed with different initializations, and only results for the second run were used (Price and others 2004).

Downscaling Global Climate Model Projection Data

Downscaling Methods

The development of downscaled climate projection data is an active area of research to meet the needs of the climate impacts analysis community by providing finer-scale climate change projections. Two main approaches to downscaling differ in their complexity (IPCC-TGICA 2007). The more sophisticated approaches include dynamical and statistical downscaling.

Table 5—Climate model output data for the historical simulation for the 20th century (period 1961-2000) and the SRES B2 scenario from the period 2001 to 2100 (used in the Third Assessment report of the Intergovernmental Panel on Climate Change) were obtained from the Intergovernmental Panel on Climate Change data portal.

Climate model version, modeling center	Nominal cell size	Source of the model data
CGCM2, Second Generation Coupled Global Climate Model, version 2, medium resolution (T47), developed by the Canadian Centre for Climate Modelling and Analysis http://www.ec.gc.ca/ccmac-cccma/default.asp?lang=En&n=40D6024E-	3.75 degrees latitude by 3.75 degrees longitude	http://www.ipcc-data.org/sres/gcm_data.html
CSIRO-MK2, Climate System Model, Mark 2, developed by the Commonwealth Scientific and Industrial Research Organisation (CSIRO), Australia http://www.cmar.csiro.au/e-print/open/hennessy_1998a.html#ccm	3.2 degrees latitude by 5.6 degrees longitude	http://www.ipcc-data.org/sres/csiromk2_info.html
HadCM3, Hadley Centre Coupled Model version 3, developed by the Hadley Centre for Climate Prediction and Research UK, http://www.metoffice.gov.uk/research/modelling-systems/unified-model/climate-models/hadcm3	2.5 degrees of latitude by 3.75 degrees of longitude	http://www.ipcc-data.org/sres/hadcm3_info.html

Dynamical modeling uses a nested modeling approach where a finer resolution climate model (typically a regional climate model) is nested within a global climate model. The atmospheric processes occurring within the domain of the regional climate model are forced by boundary conditions generated by the global climate model at its usual time step. Within the domain of the regional climate model, higher-resolution representation of surface topography and more detailed parameterization of some processes allow the model to generate physically consistent simulations of weather and climate. Christensen and others (2007) cite the main drawback of dynamical models as their computation cost, and that in projections of future climate, the parameterization schemes used to represent sub-grid scale processes may be operating outside the range for which they were designed. Recently, projections for the conterminous United States at the 50-km spatial scale have become available (see North American Regional Climate Change Assessment Program, http://www.narccap.ucar.edu/results/rcm3-gfdl-results.html).

In statistical downscaling, a statistical procedure is used to describe climate at a finer spatial scale based on global climate information. This relationship is then used to relate the global model projection output to the finer spatial scale. This approach requires observational data at the spatial scale of interest and over a sufficiently long period in order to develop statistical relationships. Christensen and others (2007) identify drawbacks in this approach, notably in the assumptions about cross-scale relationships remaining stable in a changing climate.

Simpler methods use global climate model (GCM) output directly (e.g., from the closest grid cell node) and spatially interpolate to finer resolution from latitude and longitude coordinates. These methods have been adopted for interpolating both climate observations and climate model output to fine spatial resolutions over large regions where it may be impractical to apply statistical downscaling methods or computationally difficult to use dynamical downscaling. One such method—the delta or change factor method—has been adopted for interpolating climate model output to fine spatial resolutions over large regions (VEMAP members 1995; Hamlet and Lettenmaier 1999; Miller and others 2003; Price and others 2004; McKenney and others 2006a; Rehfeldt and others 2006; Tabor and Williams 2010; Anandhi and others 2011). Global climate model output data are normalized with respect to a historical reference period so that bias in the simulated historical values (i.e., compared to observed data at the same location) can be removed (Price and others 2004; USDI Bureau of Reclamation 2010). In this normalization process, every GCM-projected climate data point within the geographic region of interest is converted to a change factor (or delta value), relative to a particular historical period. For temperature, the change factor is computed as the arithmetic *difference* between the projected monthly temperature variable and the corresponding 30-year mean of the simulated historical temperature variable for that month. For precipitation, the change factor is the *ratio* of the projected monthly value to the corresponding 30-year simulated historical mean for that month. These change factors are estimated for each month and year in the projection period at the scale of the global model. The change factors are then spatially interpolated to the scale of interest. Because climate models typically have very low horizontal resolution, their representation of topographic effects on local climate is necessarily poor. For this reason, the normalized and interpolated climate model data (change factors) are combined with observed climatological data for the reference period interpolated to the same resolution as the change factors. This approach provides a correction for local topographic effects to the downscaled climate projection data. Because historical climate data are interpolated to capture the spatial complexity of local climate (e.g. the result of topography), a possible drawback to this approach is the assumption that causes of spatial variability in past climate will remain unchanged (or will change uniformly) in future climate. In practice, such effects are likely to be small compared to the inherent errors and assumptions built into the climate model simulations. Ultimately all downscaling approaches have advantages and disadvantages that should be recognized and understood by the end user to be sure the results suit their specific purposes (see Daniels and others 2012).

Delta Method and Spatial Interpolation of the Change Factors Using ANUSPLIN

Standardized procedures for processing climate model data sets developed by Price and others (2004) were used by Price and others (2011a) and Joyce and others (2011) to develop change factors with AR4 models for Canada and the United States, respectively. This study uses the downscaled change factors developed by Joyce and others (2011) to develop projections for the conterminous United States. We briefly describe those procedures here and further detail can be found in Price and others (2011a) and Joyce and others (2011).

These procedures were built around interpolation of the climate model output data using ANUSPLIN, the thin plate smoothing spline climate interpolation software tool developed by Hutchinson and coworkers at the Australian National University (Hutchinson 2010). The ANUSPLIN tool was developed for interpolating climate station observations and has been used to carry out interpolations of monthly time series data and time series at shorter timescales (weeks to days) (Price and others 2000, 2004; McKenney and others 2006b; Price and Scott 2006; Rehfeldt 2006; Hutchinson and others 2009; McKenney and others 2011). Here the monthly data values from the climate models were treated as records obtained from a 'virtual climate station' located at the climate model grid-node coordinates. Conversion, extraction, and interpolation processes were run on multiple computers, controlled by UNIX scripts developed in-house by Price and others (2011a) at the Northern Forestry and at the Great Lakes Forestry Centres, Canadian Forest Service. These scripts were edited specifically for each climate model, to account for the different spatial resolutions covering the North American domain (Tables 3 and 5) and for other differences in the contents of the data files (Price and others 2011a). The processing steps were similar for both the AR4 and the TAR climate model output data (Table 6).

Once the data were prepared for the North American grid (steps 1 – 5), monthly values of daily surface temperature (minimum and maximum) and precipitation were used to calculate GCM-simulated 30-year means for the 1961-1990 period using the 20th Century realization (20C3M) at the resolution of each global model (Tables 3 and 5). These monthly mean values were then used to compute the monthly change factors in the following manner. For maximum and minimum temperature, the change factor was computed as the arithmetic difference between the simulated monthly value for each year in the projection period and the corresponding simulated 1961-1990 mean value of the same temperature variable for that

Table 6—Major steps in developing the change factors: downloading, extraction and processing of the climate model output data, as described by Price and others (2011a) and Joyce and others (2011).

Major step	Processes
1	Download global orography data sets for each climate model and create sets of grid cell coordinates for elevation, latitude, and longitude files
2	Download climate model global data files for each climate variable and each of the desired scenarios.
3	Extract data for each climate variable for North America from the global data file and convert to an ASCII format file.
4	Extract data for surface wind components for those climate models with data files containing multiple pressure levels and compute estimates of surface wind velocity
5	Prepare the monthly climate model data for input to ANUSPLIN.
6	Compute vapor pressure from values for specific humidity and sea-level pressure (adjusted to grid cell elevation) as simulated by each climate model
7	Spatially interpolate the normalized monthly change factors for each of the six variables, all scenarios and all climate models
8	Extract rectangles from the North American grid for the conterminous 48 states and Alaska using ARC/INFO.

month. For precipitation, the change factor was the ratio of the monthly projected value to the simulated 1961-1990 mean for that month. Thus for each grid node at the global resolution within the North American domain, there were change factors for each month for monthly mean daily maximum temperature, for monthly mean daily minimum temperature and, for total monthly precipitation over the 2001 through 2100 period.

The monthly change factors associated with each global grid node were spatially interpolated to the 5-arcminute scale. An ANUSPLIN model was generated for each monthly change factor variable, which was then used to create gridded data for that monthly variable covering the conterminous United States and Alaska at a spatial resolution of 5 arcminutes. Because the data were treated as anomalies from the 1961-1990 mean, a fixed signal model, rather than a standard optimization model, was used (McKenney and others 2006a). We note there is no inherent statistical relationship between these GCM-generated anomalies and the independent variables (longitude and latitude). A fixed signal of 60 percent of the data points (climate model grid cell values) produced reasonable results (e.g., to avoid singularities [“bulls eyes”] in the resultant models). Monthly grids of interpolated change factors were generated in ARC/INFO ASCII format, with a cell size of 5-arcminute latitude by 5-arcminute longitude, covering the domain from the 168 degree to 52 degree W and from 25 degree to 85 degree N (1,392 columns by 720 rows, covering all of the continental United States and Canada). This grid resolution matches that of many other climate data products previously produced at the Great Lakes Forestry Center, Canadian Forest Service (McKenney and others 2011). Additional details on the downscaling of the AR4 scenarios (A1B and A2) can be found in Price and others (2011a) and Joyce and others (2011) and for the TAR B2 scenario in Price and others (2004).

Development of the RPA Climate Projections for the Conterminous United States

Development of the Observed Historical (1961-1990) Climate Data Set Using PRISM

The change factor data generated from the GCM projections needed to be combined with gridded observed 30-year climate data to produce physically consistent gridded projections of future climate, corrected both for local topographic effects and for the mean bias in the climate model projections. In this manner, projections integrate the spatial variability observed in present-day climate at the spatial scale of interest with the spatio-temporal variability simulated by each climate model. In addition, the use of a historical climatology on which to base future projections corrects for biases among different climate models and facilitates a direct comparison of their future projections.

The RPA climate projections use a historical climatology based on PRISM data (Daly and others 1994), as these historical climate data were used as climate data in the individual RPA resources analyses (e.g., Bowker and others 2012; Foti and others 2012; Greenfield and Nowak 2013; Wear and others 2013). Several different historical climatologies are available: Kittel and others (2004), Rehfeldt (2006), McKenney and others (2006b,c 2011), and DAYMET (see http://www.daymet.org/default.jsp).

PRISM climate mapping system, developed by Christopher Daly, PRISM Group director, is a knowledge-based system, continuously updated, that uses point measurements of precipitation, temperature, and other climatic factors to produce continuous grid estimates of monthly, yearly, and event-based climatic parameters (Daly and others 1994, 2002; Gibson and others 2002). Point data, a digital elevation model, and expert knowledge of complex climatic extremes, including rain shadows, coastal effects, and temperature inversions are integrated to produce the interpolated climate data set (see http://www.prism.oregonstate.edu/).

Historical climate data (monthly mean daily maximum air temperature, monthly mean daily minimum air temperature, and monthly total precipitation) were obtained by download from ftp://prism.oregonstate.edu/pub/prism/us/grids/. Data are provided in raster files, where each file contains 1,405 columns (longitude) and 621 lines (latitude), resulting in 872,505 grid cells covering the conterminous United States. Each file represents the month and year of a single climate variable. PRISM grid cells are 2.5-arcminutes resolution, referenced by the southwestern corner (left-hand lower corner).

As the change factors were developed at the 5-arcminute scale and PRISM data are at the 2.5-arcminute scale, we aggregated the PRISM historical climate data to the 5-arcminute spatial scale so that these data could be used to construct future climate projections using the downscaled change factors. The PRISM grid scale is one half that of the change factor grid scale, thus, the area of four PRISM grid cells matches the area of one change factor grid cell. The PRISM grid starting point (southwest corner) is offset by 3.75 degrees north and 1.25 degrees east from the change factor grid. This effectively lines up the longitude/latitude center of each change factor grid cell with one PRISM grid cell and portions of eight surrounding PRISM grid cells (Figure 3).

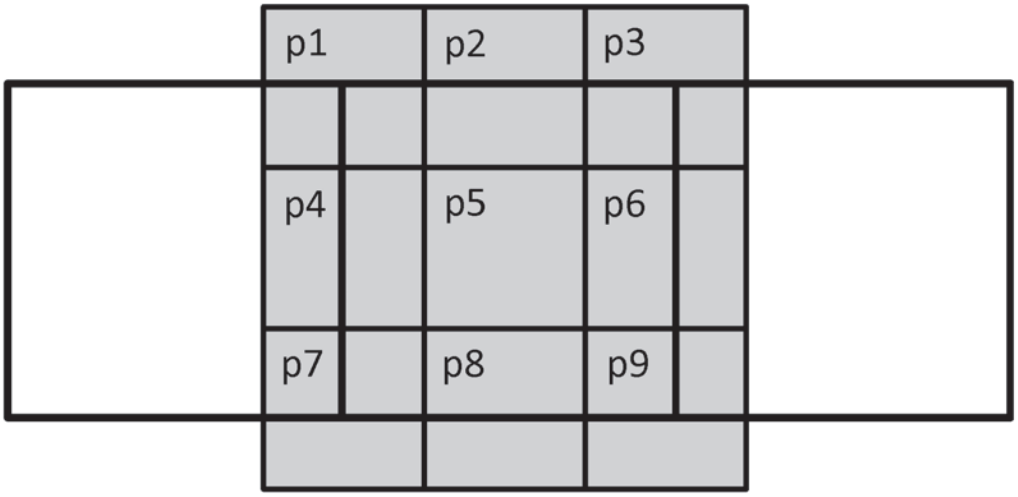

Figure 3. Relationship between the 5-arcminute grid (change factor grid) and the PRISM data grid of 2.5 arcminute (numbered gray grids). Historical data from PRISM were aggregated from the 2.5-arcminute scale to the 5-arcminute scale by matching the grid centers of one 5 arcminute grid with one 2.5 arcminute grid and weighting each of the overlapping nine 2.5-arcminute grids to develop the 5-arcminute values. See text for individual weighting factors.

Using PRISM data, the monthly mean for the 1961 to 1990 period was computed for each monthly climate variable: precipitation, maximum temperature, and minimum temperature within each PRISM grid cell. The area-weighted mean value for each climate variable was calculated for each change factor grid cell using the following formula. One PRISM grid cell (p5 in formula; see also Figure 3) overlaps with the center of the change factor grid cell and portions of eight surrounding grid cells are added to the estimate.

Mean grid cell value =

$$(0.25*p1+0.5*p2+0.25*p3+0.5*p4+p5+0.5*p6+0.25*p7+0.5*p8+0.25*p9)/4,$$

where p1 to p9 are illustrated in Figure 3. In the event an overlapping PRISM grid cell has missing data, the change factor climate variable estimate is the weighted average of those PRISM grid cells with data. These computations produced a historical climate data set at the 5-arcminute grid scale and are used as the historical basis for developing the future climate projections.

Development of Projections Using Change Factors and Observed Historical Climatology

The change factor data at the 5-arcminute spatial scale were combined with the historical climatology data at the same spatial scale. The projected change factor value was multiplied by (precipitation) or added to (temperature) the appropriate historical climate variable, resulting in climate projections for each climate model and each scenario.

Following the use of potential evapotranspiration (PET) in ecological modeling (Bachelet and others 2001, 2003), PET for vegetation was calculated using the mean temperature variable and a modification of Penman's work by Linacre (1977). Here PET is a function of mean monthly temperature, mean monthly temperature adjusted for elevation, elevation, latitude, and to replace dew point temperature an adjustment based on the difference between the means of the hottest and coldest months. The full calculations are given in Appendix III. Potential evapotranspiration is estimated as mm/day. Kingston and others (2009) noted that different formulations of PET can result in large differences in PET values. Although this formulation of PET has minimal climate parameter needs, it relies solely on temperature data and could result in an overestimate of PET for some areas and, when used in hydrological analyses, could produce overestimates of water demand and underestimates of water yield.

The climate projections were subject to a variety of quality checks to ensure the reasonableness of the data. Given that the data in this project are the work of several developers, we describe their quality control and assurance steps as reported in their documentation. The global data from the climate models used in the IPCC Fourth Assessment were obtained from the Program for Climate Model Diagnosis and Intercomparison (PCMDI) Climate Model Intercomparison Project 3 (CMIP3), and for models used in the Third Assessment, the Intergovernmental Panel on Climate Change DDC (http://www.ipcc-data.org/sres/gcm_data.html). Documentation for each climate model is available on the PCMDI website: http://www-pcmdi.llnl.gov/ipcc/model_documentation/ipcc_model_documentation.php. Further, the web links for each climate model used in this study are given in Tables 3 and 5.

Attribute accuracy for the PRISM data can be found at http://www.ocs.orst.edu/prism/docs/meta/temp_103yr.htm. The PRISM developers suggest that care should be taken in estimating temperature values or precipitation values at any single point because temperature or precipitation estimates for each grid cell (2.5 arcminutes) are an average over the entire area of that cell. Thus, point temperature or precipitation can be estimated at a spatial precision no better than half the resolution of a single grid cell. In this study, PRISM data were aggregated across the original scale of the grid cells to a larger spatial scale and thus did not violate this concern.

Price and others (2011a) document quality control issues encountered in the downscaling procedures and the development of the change factors. Data availability was problematic for some projections, resulting in some data needing to be retrieved from the climate modeling centers (instead of from PCMDI or the IPCC DDC). In addition, missing data for some years were addressed (Price and others 2011a; Joyce and others 2011).

During our initial quality checks it was discovered that the CSIRO-MK2 model used for the B2 scenario had some abnormally high projected precipitation values. Precipitation in the historical record can exceed four times a historical mean. However, these projected values seemed to be anomalous as they were associated only with particular years. When these data were developed for the VINCERA project (http://www.environment.uwaterloo.ca/research/vincera/), a filtered data set was produced to correct these data anomalies (Price, personal communication). They did so by "capping" the average deltas (ratios) to five (400 percent change over the simulated historical data) before interpolating the precipitation change factors. We followed this procedure and used their filtered ratios to build the projected precipitation values for the B2 scenario using the CSIRO-MK2 model.

Additional quality assurance tests were made in the development of the projection data where data from the change factor data sets and the 30-year means were manipulated at different spatial scales. In the process of downscaling precipitation, it was discovered that in regions of low precipitation, negative change factors (ratios) were sometimes interpolated. As negative precipitation values are obviously impossible, these values were set to zero.

For some regions of the United States, the difference between the minimum temperature and the maximum temperature can be slight, e.g., northern latitudes or seasonally in winter. It is possible that spatial interpolation of observed climate can result in minimum temperature values greater than maximum temperature, as they are interpolated separately. This result did not occur in the aggregated historical climate data used in this study. However, it was discovered that in some cases, the output from climate models can project greater increases in the minimum temperature than the maximum temperature. This difference could be greater than the difference between the observed minimum and maximum temperatures. Thus when the change factors are imposed on the observed historical climate, the projections could result in the values of minimum temperature being greater than maximum temperature values for an individual grid cell. This anomaly rarely occurs in all but one of the projections, namely the B2 scenario simulated by the CSIRO-MK2 model, especially in winter months and the northernmost latitudes of the conterminous United States. No adjustment was made in the climate projection data set. If the relationship between minimum and maximum temperature is to be included in an analysis with this climate data set, the user should determine whether an adjustment is needed. One possibility would be a function where the maximum temperature is assigned the maximum value of both temperatures and minimum temperature, the minimum value of both temperatures.

County-Level Summarization

For purposes of the RPA Assessment, climate data availability at the county spatial scale is critical. We used the U.S. Forest Service Forest Inventory Analysis (FIA) Survey Unit and County Coverage as the spatial delineation for counties. An overlay file between the 5-arc-minute grid and the county boundaries was developed in ArcGIS 9.2. This ultimately resulted in 120,680 grid cells with climate data within the conterminous United States. This resulting database file was imported into SAS and merged with the projected climate data.

Once merged, the county means for monthly total precipitation, monthly mean daily maximum air temperature, and monthly mean daily minimum air temperature were calculated using an area-weighted mean value of the underlying 5-arcminute grid cells within the county. With the overlay of the county shape file on the grid shape file, some grid cells are assigned to more than one county. During the overlay process, the area of each grid cell falling wholly or partially within the county was calculated. These areas were used as weights to calculate the county means.

Analysis of Climate Projections

The nine projections (three scenarios associated with each of three climate models) describe alternate futures of monthly climate over a 100-year period for three distinct climate variables (i.e., monthly mean daily maximum temperature, monthly mean daily minimum temperature, and monthly total precipitation). Because these data will be used in other analyses as input for renewable resource models, our analysis focuses on comparing and contrasting the trends (spatial and temporal) seen in the scenarios and the nine individual climate model projections at the conterminous U.S. scale. And because the data may be of interest to finer-scale analyses, we explore several different types of analyses that can be performed with the climate data at regional scales within the United States.

The focus of the RPA Assessment is on projections for the 50-year period from 2011 to 2060. Hence we show maps of projected changes at the end of this period, by scenario and model, for the 10-year period surrounding the year 2060, 2055-2064, to avoid the issues of the representativeness of a single year. We also show maps of projected change of the last 30-year period (2071-2100).

Spatial and Temporal Patterns of Temperature and Precipitation for the Conterminous United States

We explore the temporal projections for annual mean daily temperature and annual total precipitation, first by aggregated scenario, and then for all three model projections within each scenario. The projections of maximum temperature and minimum temperature are also examined for all nine projections. For the conterminous United States temporal analysis, we area-weight the grid cell values by grid cell areas, thereby accounting for latitudinal distortions in grid cell area associated with the underlying map projections.

Climates within the United States are highly varied from the cold climates of alpine regions in western United States to the warm and humid climates of southern United States. These latitudinal and elevational differences and the east-to-west gradients caused by the synoptic weather systems and the Rocky Mountains dominate the displays of the conterminous U.S. climate maps. Hence, because the spatial variations in individual and aggregated projections are small compared with these strong climatic gradients, we display change in temperature and precipitation relative to the 1961-1990 period to reveal the differences among the scenarios and projections by the 2060 period and by the 2071-2100 period. We show changes in temperature using degrees Celsius (^{o}C). For precipitation, changes are shown for the 2060 period in both the units of millimeters and as a percent change, and for the 2071-2100 period as percent change only. Percent change in precipitation is computed as the projected precipitation (typically a mean of at least 10 years) minus the historical (1961-1990) precipitation mean divided by the historical precipitation mean. The historical period serves as a benchmark to compare changes in projected climate spatially and temporally across the United States.

We examine relationships between the area-weighted change in annual mean daily mean temperature and the percent change in annual precipitation projected by each climate model for the 2060 period and the 2071-2100 period relative to the 1961-1990 period means. These scatter plots demonstrate how the three climate models (under each of the three scenarios) differ in their projections of climate change for the conterminous United States.

Regional Patterns in Annual and Seasonal Climate Projections

The interpretation of the projected changes in climate may be assisted by different types of analyses and presentations. While the changes in mean daily temperature are often used to quantify the potential impact of climate change, Lobell and others (2007) suggest that it may be possible to improve the exploration of climate change impacts by separating the potential mean temperature changes into minimum temperature and maximum temperature changes, and perhaps by season. Changes in seasonal temperature and precipitation may have a differential effect on vegetation dynamics across a region, particularly in spring when plants are initiating growth or during summer when flowering and fruiting occur. We briefly explore seasonal changes that may influence the ecological response as an example of the types of analyses that can help analysts interpret the change in climate. For the Southeastern regions (the states of Virginia, North Carolina, South Carolina, Georgia, and Florida), we explore spatial patterns in nine projections of maximum mean daily temperature as compared to projections for minimum mean daily temperature. We focus on summer (the months of June, July, and August).

While the spatial display gives a sense of the pattern across the region, we use the frequency distributional changes to assess the magnitude of temporal and spatial change. For the Northern Great Plains region (the states of North Dakota, South Dakota, and Nebraska), we explore the changes in spring temperatures. Warmer temperatures in the spring season potentially project a longer growing season. The occurrence of freezing temperatures is a limiting factor in the initiation of spring vegetative growth and changes in the frequency distribution of spring temperatures (mean and minimum) could facilitate earlier spring vegetative growth. Frequency distributions are constructed for a 30-year period of historical data (1961-1990), and a 30-year period as projected by the climate models (2045-2074). The distribution is described by the seasonal values associated with individual grid cells for each year within the 30-year period. For the Southern Great Plains (the states of Oklahoma and Texas), we explore the changes in spring and summer temperatures. Precipitation is projected to decline slightly or to remain the same in this region. Increasing temperatures could put drought stress on vegetation particularly late in the growing season. As with the Northern Great Plains, the frequency distributions are based on the historical period (1961-1990) and the projected period (2045-2074). Spring is defined as the months of March, April, and May.

Looking at projected temperatures in the context of the historical record offers a comparison that can assist managers and others in planning for climate change. Ray and others (2008) compared historical data from a weather station with the interpolated data for grid cells surrounding the local weather station. This analysis allows a comparison of the historical variability and the projected data. Following Ray and others (2008), we use a 50-year historical record (1950-1999) for the Lamar weather station located in southeastern Colorado and the Lakeview weather station located in eastern Oregon. We aggregate a block of grid cells (five grid cells east to west and three grid cells north to south) surrounding the weather station (approximately a 35-km by 45-km region) and compute the historical annual precipitation and annual mean daily temperature for this region. Projected monthly climatologies are computed for all nine projections for the 20-year period surrounding 2050 (2040-2059), after Ray and others (2008). We compare the observed mean and variability with the nine climate projections.

Price and others (2011a) developed a set of comprehensive tables to provide an outlook for various regions in Canada. Using their technique, we summarize the projected changes during the 21st century for mean daily temperature, mean daily minimum temperature, and total precipitation for the State of Colorado. The 1971-2000 period was selected as baseline because this 30-year period represented the most recent 30-year period (at the time of the study) used by weather and climate scientists to depict 'normal.' The area-weighted mean for each climate variable is the mean of the values projected by the three climate models and therefore represents a central estimate or 'best" guess, assuming that the climate models produce equally plausible results. For each variable, the data are organized across the table in three sets of five columns. Each set of columns in the tables represents a single emissions scenario (in the order A2, A1B, and B2), with the columns containing the means of the three climate model projections of monthly values for spring, summer, fall, winter, and the entire year. The rows are labeled in the leftmost column according to the period represented. "Baseline 1971–2000" refers to the 30-year mean for the period 1971-2000. It is important to distinguish this 30-year period from the period 1961–1990, which was used as the reference period for combining scenario data with observed climate normals for 1961–1990. Although any differences between the periods 1961–1990 and 1971–2000 are probably small, there is evidence of a general warming trend over this entire period that is apparent in many of the graphs shown previously (both in the observed temperature records and in the climate model projections). Changes in precipitation and temperature are computed in the projected 30-year means relative to 1971-2000: change by 2001–2030, change by 2031–2060, and change by 2061–2090. For these changes over time, a positive value indicates an increase, and a negative value indicates a decrease. A "100-year change" is computed and represents the change over the 100 years from 2001 to 2100, as determined by fitting a linear relationship to the data. The "100-year variability (%)" is the coefficient of variation for the slope of the line. Both of these metrics are based on monthly data, thereby not representative of how variability in daily values might change in the future.

The Pacific Northwest region (the states of Idaho, Washington, and Oregon) is a climatically diverse region; the coastal ranges are wet and cool and the interior is dry and warm. Here we explore the changes in precipitation and temperature seasonally and spatially. At the conterminous U.S. scale, we compared the annual mean temperature changes with the annual precipitation changes by scenario and by model and suggested that these graphs could facilitate selecting scenarios where a specific range of projected changes in climate (temperature and precipitation) is desired (e.g. wettest and warmest). For the Pacific Northwest region, we compare the seasonal mean temperature changes with the seasonal precipitation change (as percent) for the 2060 period.

In the Northeastern region of the United States (the states of Maine, Vermont, and New Hampshire), we display the scenario projections for annual mean daily temperature, based on the three model projections within each scenario. These spatial results are then compared and contrasted with the nine individual projections of changes in annual mean temperatures.

The historical and projected climate data can be used to develop indices of interest to the user. We use the aridity index, developed by the United Nations Environmental Program (UNEP) with downscaled climate data from this study. This index is:

Aridity Index (AI) = Precipitation/PET

where Precipitation is total annual precipitation (mm) and PET is annual Potential Evapotranspiration (see Appendix III for calculations). This aridity index was originally developed to identify zones using a common classification:

Zone	Aridity Index values
Hyper-arid	< 0.05
Arid	0.05 - 0.2
Semi-arid	0.2 – 0.5
Dry Humid	0.5 – 0.65
Humid	>0.65

Using annual precipitation and potential evapotranspiration (PET) values from the historical (1971-2000) and the nine projection data sets (2060 period: 2055-2064), we estimate the aridity index for each grid cell.

A common metric to assess consensus or agreement in projections is to compute the number of projections that show the same result. We are interested in whether there is an agreement in the projected changes in aridity. Using the formula above, we estimate the Aridity Index and then use the index to classify each grid cell into an aridity class for the historical period and using each of the nine model projections for the 2060 period (2055-2064). In terms of changes in classification between the historical and the projected period, the three possible cases are: 1) no change in the classification; 2) the grid cell becomes more humid, e.g., from arid (historical) to semi-arid by 2060; and 3) the grid cell becomes more arid, for example from arid (historical) to hyper-arid in 2060. For each grid cell, we count the number of projections that agree for each case; no change, increased aridity, and increased humidity. The change can be more than one class; for this example, we focus only on whether there is a change in classification, not the degree of the change. The scale of 9 would indicate that all projections agreed on the same result, e.g., no change in aridity. We map the aridity zones for the 1961-1990 period and the agreement in 2060 projected changes of increased aridity for the conterminous United States.

Results

Mean Temperature and Total Precipitation Projections for the 2060 Period for the Conterminous United States

At the scale of the conterminous United States, annual mean daily temperatures aggregated by RPA scenario increase above the range of the entire historical 1940-2000 period; however, projected annual precipitation throughout the 21st century nearly always remains within historical variability (Figure 4). The aggregated results show similar increases in temperature across the scenarios until 2070 when temperatures for the A2 scenario begin to diverge from the A1B and B2 projections. By 2100, the annual mean daily temperature increases from the historical (1961-1990) mean of 11.2 ^{o}C to about 15.0 ^{o}C for the B2 scenario, 15.3 ^{o}C for the A1B scenario, and 16.3 ^{o}C for the A2 scenario. By 2060, the A1B scenario shows the greatest increase in mean annual temperature (3.2 ^{o}C); however, differences at the conterminous U.S. scale are very small among the three scenarios (A2, 3.1^{o}C; B2 2.8 ^{o}C). By the end of the 21st

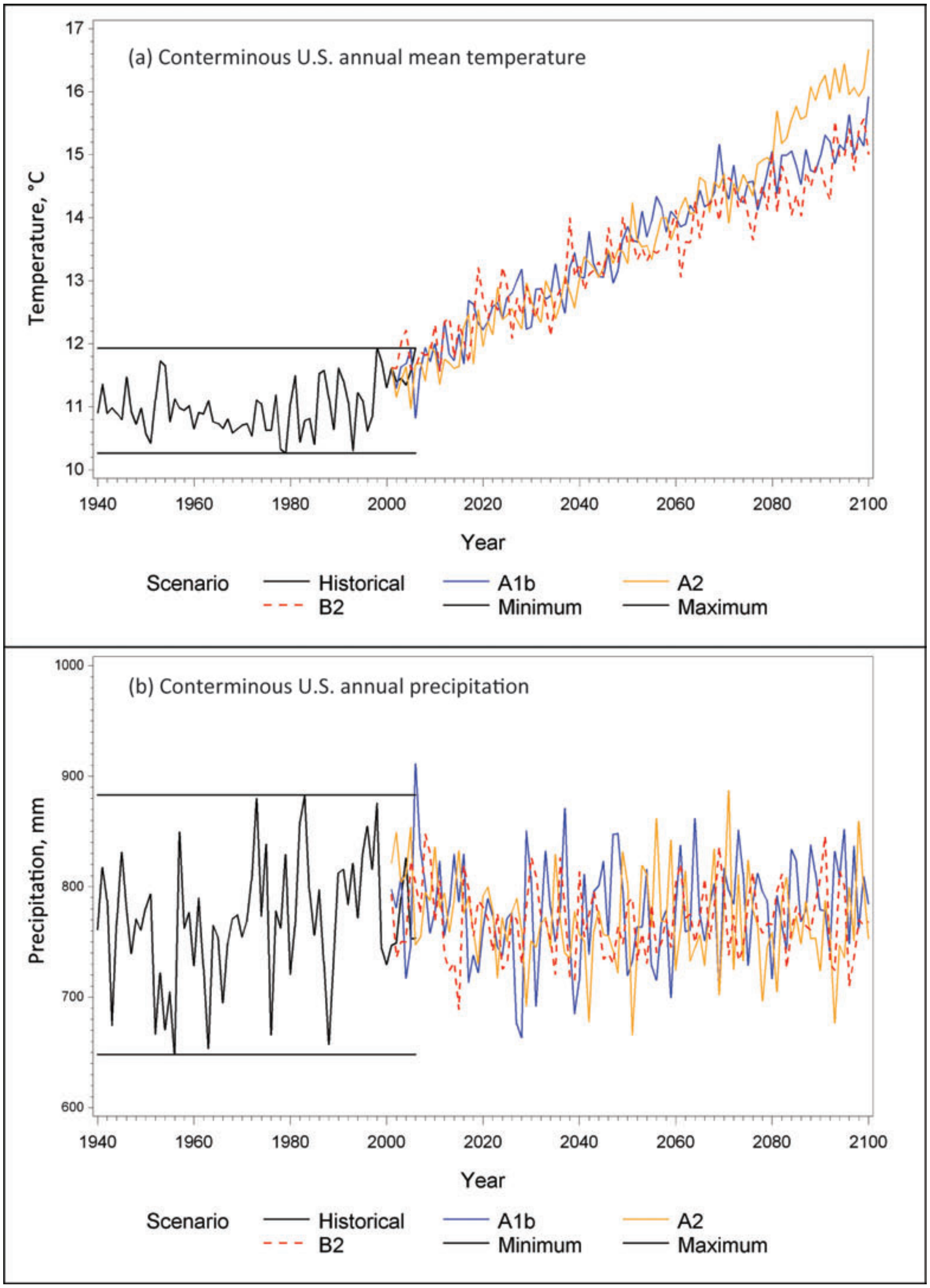

Figure 4. Observed (1940-2006) and projected (2001-2100) annual mean daily mean temperature (°C) (a) and annual precipitation (mm) (b) for conterminous United States and scenarios A1B, A2, and B2. Each projection (colors) is the mean of three climate model projections for each scenario. The solid black line is the historical annual temperature mean (a) and annual precipitation (b). Horizontal lines denote upper and lower range of the historical means.

century, the A2 scenario shows the greatest warming (visible in Figure 4). Precipitation projections for all scenarios are highly variable (Figure 4). Given the challenges in measuring and modeling precipitation, no real differences over time or by scenario can be drawn from these national results for precipitation, in contrast to the temperature projections.

Plots showing the change in annual mean temperature against the change in annual precipitation change have been used to assist in the selection of specific scenarios and projections to use in impact analyses. The graphs show the individual model projections as well as each scenario mean. From the graph, the relative nature of the individual model projections can be seen; for example the model/scenario that is the wettest or warmest in this set of 9 projections (Figure 5). The individual model projected changes span a wide range in both precipitation (increase of 80 mm to a decrease greater than 100 mm) and temperature (greater than 1.0 ^{o}C

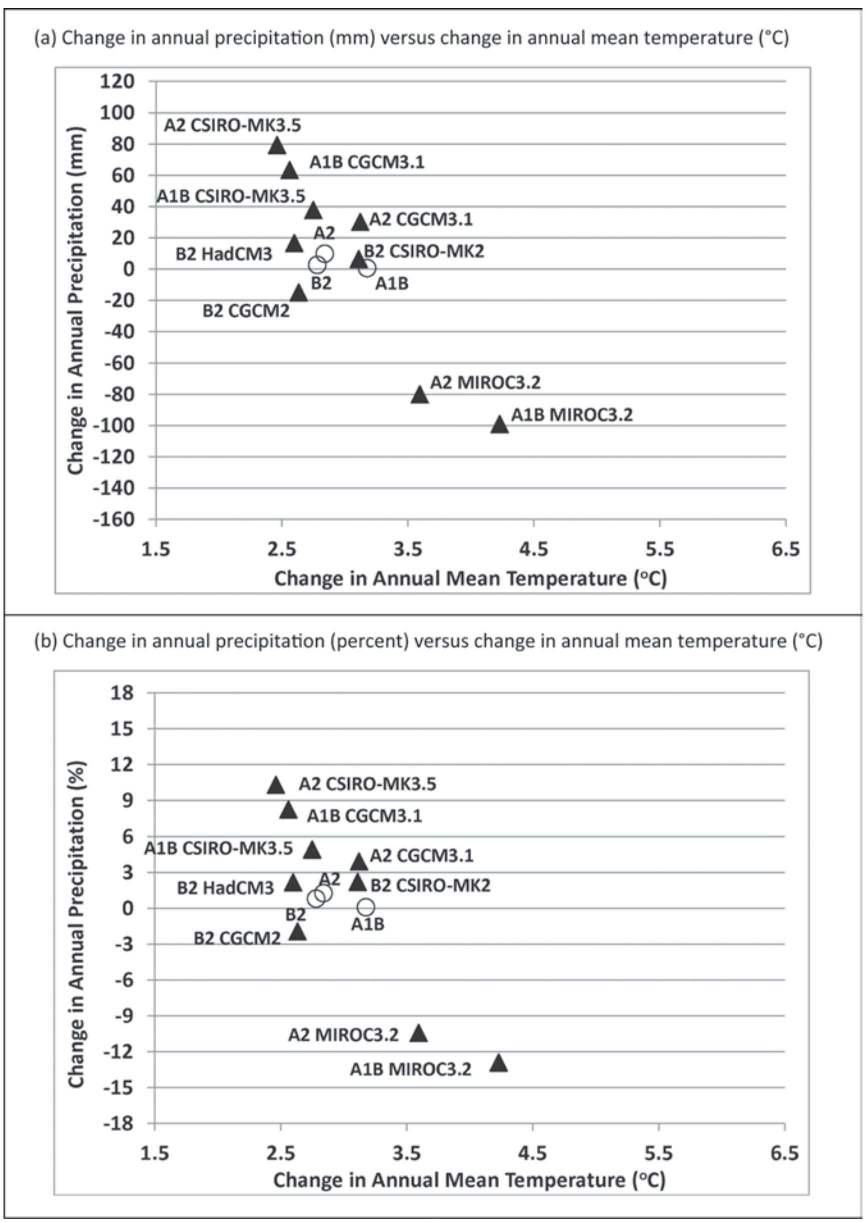

Figure 5. Change in mean annual precipitation (mm) plotted against change in annual mean daily mean temperature change (°C) for climate model projections (triangles) and scenario projections (open circles) for the conterminous United States (a). Area-weighted changes (a) are computed as the difference between the projected mean for the 2060 period (2055-2064) and the historical mean (1961-1990). Precipitation is shown as percent change (b) where the difference is divided by the mean for the historical period.

differences). The warmest and driest projection is the MIROC3.2 model under the A1B scenario. The wettest projection with the smallest increase in temperature is the CSIRO-MK3.5 model under the A2 scenario. The results for the individual models projecting the B2 scenario are less variable than those for either the A1B or the A2 scenario for the 2060 period. We also show change in temperature against change in precipitation where change is measured as percent change from the historical precipitation (Figure 5b). By the 2060 period, changes in precipitation range from a 10 percent increase to nearly a 15 percent decrease in annual precipitation.

When viewed as a map of changes, annual mean daily temperature increases at least 1 ^{o}C by 2060 in every grid cell across the conterminous United States in all models forced by all scenarios. The projected changes vary spatially by scenario and by model; relative to historical climates, changes of the same magnitude could have relatively different effects depending upon the historical climate (compare Figures 6 and 7). Along the Rocky Mountains in western United States, changes in annual mean temperature are projected to be 2.5 ^{o}C and greater; grid cells with historical temperatures in the range of –1 ^{o}C to 2 ^{o}C will see temperatures rising above freezing, as will some grid cells with historical temperatures between –3.7 ^{o}C to –1.1 ^{o}C. Annual mean daily temperatures increase by more than 3 ^{o}C in parts of the northern and central regions in two of the three models, forced by each scenario, but not always the same two models (Figure 7). For the B2 scenario, CGCM2 and CSIRO-MK2 both show warming in the interior, with CSIRO-MK2 extending this pattern to the eastern coast; however HadCM3 shows the greatest warming in western United States. For the A1B scenario, the greatest warming is projected for the continental interior according to CSIRO-MK3.5 and MIROC3.2. With the A2 scenario, the greatest warming in the interior is projected by MIROC3.2 and to a lesser degree, CGCM3.1. The CSIRO-MK3.5 projection for the A2 scenario shows small increases in annual mean daily temperature, compared to the other A2 projections (Figure 7).

The historical precipitation map shows the gradient of annual precipitation increasing from the Great Plains in the mid-continental region to the East Coast of the United States and increasing throughout the Southern region (Figure 6). The West Coast, particularly the Pacific Northwest region, receives the greatest total annual precipitation in the conterminous United States; the Southwest and Intermountain regions (southern California, Arizona, Utah, New Mexico, Nevada, and the western parts of Texas) show the lowest historical precipitation levels across the United States. Changes in precipitation by 2060 (as measured in millimeters) vary among scenarios and among individual climate models (Figure 8). Nevertheless, precipitation is generally projected to increase in the northern regions of the United States and decrease across the southern United States (Figure 8). Some of the largest increases in precipitation amounts are projected for the Pacific Northwest where annual precipitation historically has also been the greatest. The A1B and A2 individual model projections show a greater spatial similarity than the individual model projections for the B2 scenario. In contrast to the A1B and A2 projections, large parts of the conterminous United States see small changes in precipitation for the B2 projections (Figure 8). The spatial patterns of increases or decreases above 75 mm vary across the conterminous United States by model under the B2 scenario.

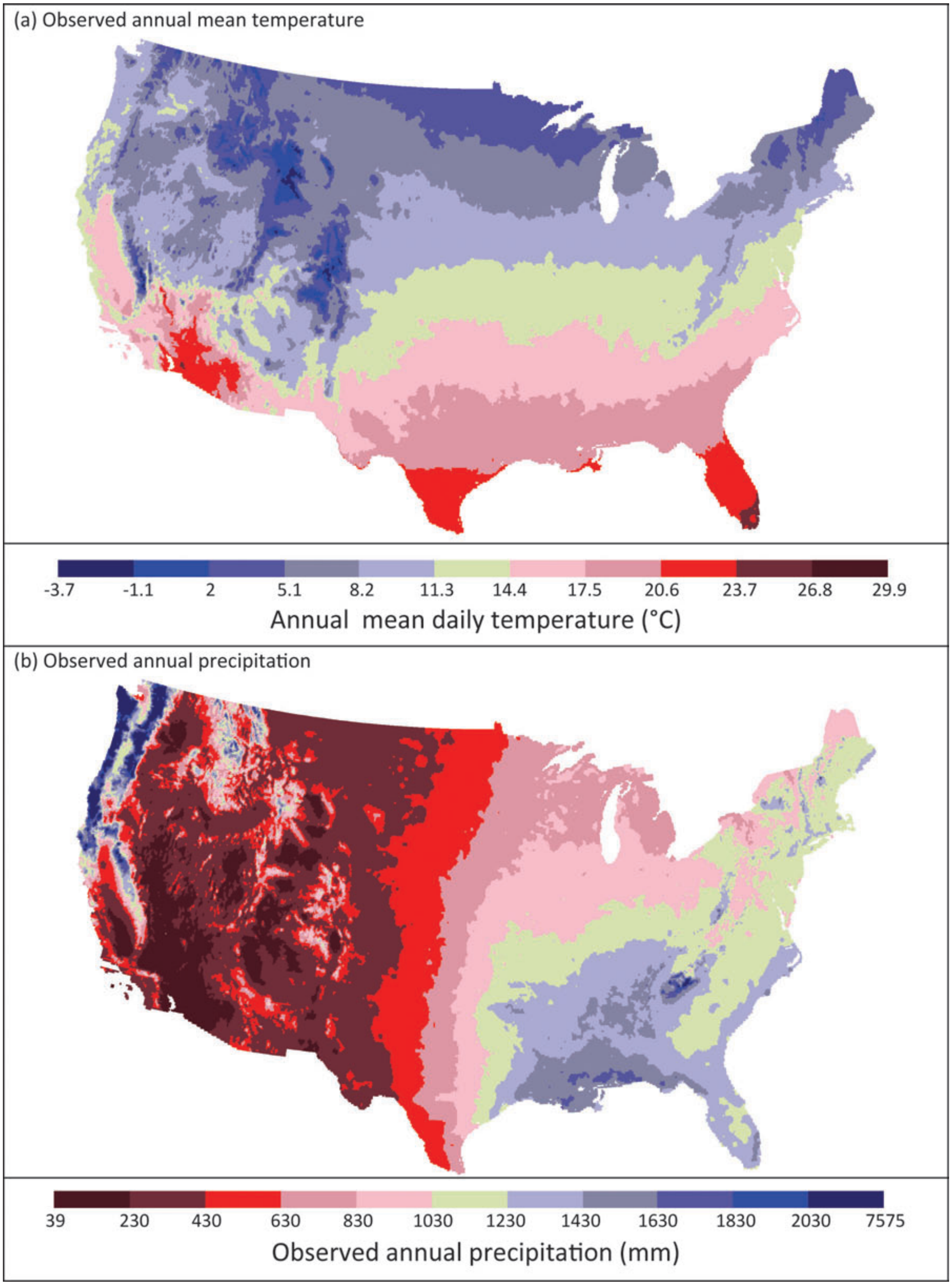

Figure 6. Historical (1961-1990) annual mean daily mean temperature (°C) (a) and annual precipitation (mm) for the conterminous United States based on PRISM climatology.

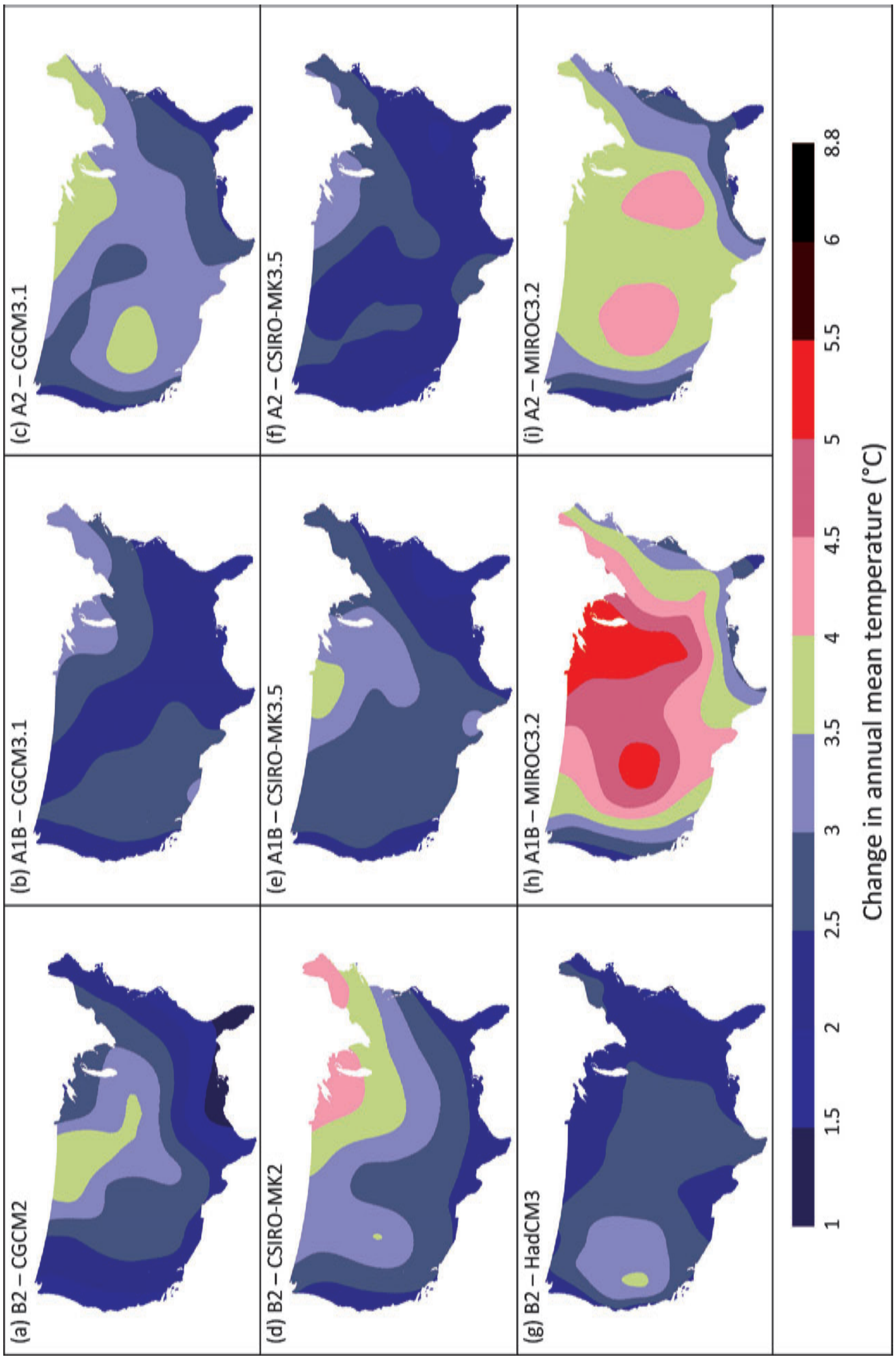

Figure 7. Change in annual mean daily mean temperature (°C) by scenario and climate model for the 2060 period (2055-2064) where change is estimated as the difference between projected annual mean daily mean temperature for the 2060 period and annual mean daily mean temperature for the historical period (1961-1990).

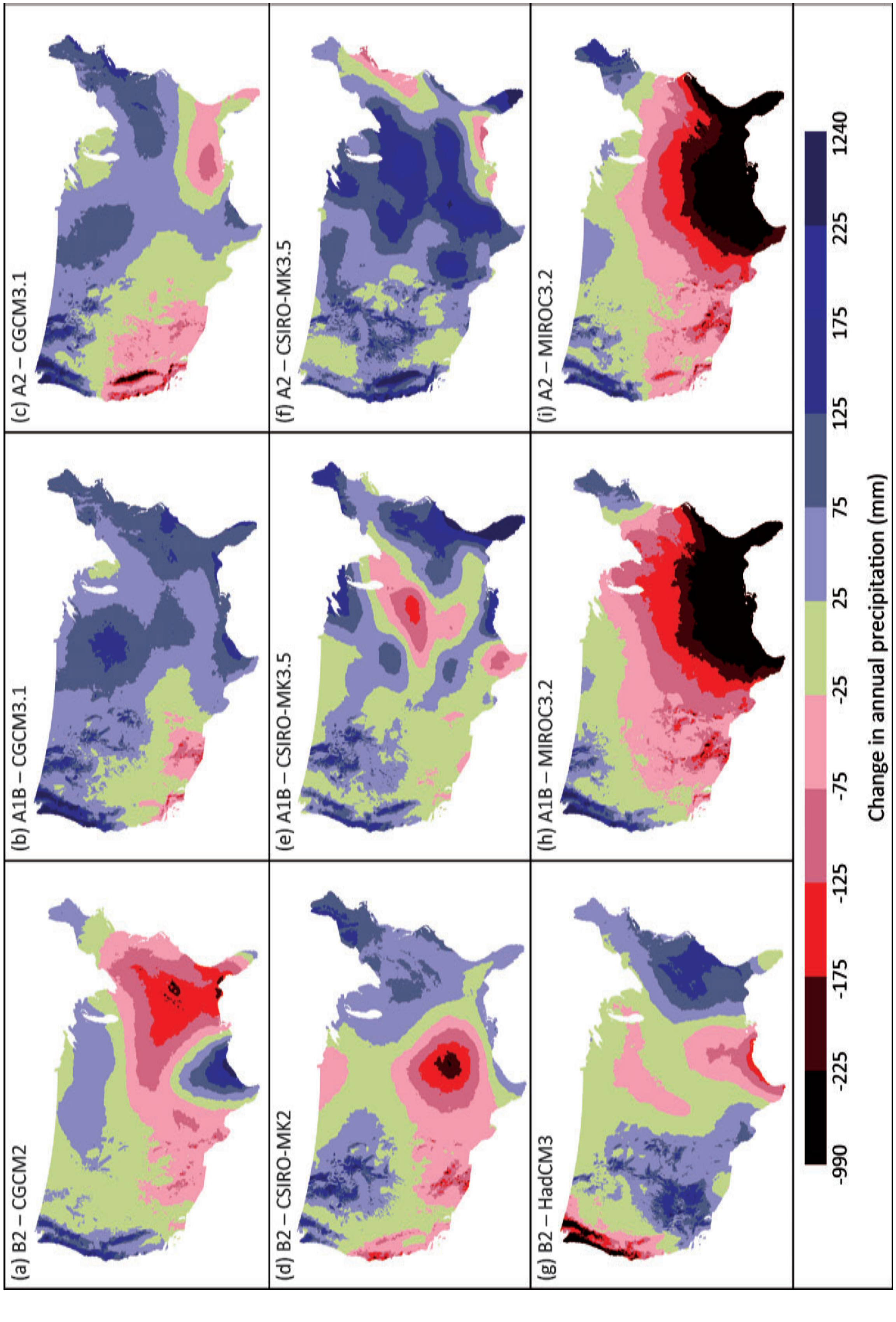

Figure 8. Change in annual precipitation (mm) by scenario and climate model for the 2060 (2055-2064) period. Change is calculated as the difference between projected mean annual precipitation for the 2060 period and mean annual precipitation for the historical period (1961-1990).

When precipitation changes are expressed as percent change from the historical annual precipitation, the percent change provides a benchmark comparison to the historical precipitation (1961-1990) for all nine projections across the conterminous United States. While the differences projected for precipitation change are large in absolute terms (millimeters as the unit), the regional differences when expressed as percent change are more apparent (contrast Figure 8 with Figure 9). The large increases in millimeters of annual precipitation seen in the Pacific Northwest (CGCM3.1 and CSIRO-MK3.5 projections of A1B and A2, Figure 8) represent increases up to 15 percent above historical precipitation. Other parts of the northern region are also projected to see 15 percent and greater increases, even though the absolute change in these areas is smaller than in the Pacific Northwest (compare Figure 8 with Figure 9). Across the Southern region of the United States, though projected changes in mm were in the largest classes, precipitation as percent ranges from 5 to 40 percent.

Mean Temperature and Total Precipitation Projections for the 2071-2100 Period for the Conterminous United States

Relationships between changes in annual mean daily temperature and annual precipitation by scenario vary between the 2060 period and the 2090 (2085-2094) period (Figures 5 and 10). For scenario means, A2 becomes the warmest by 2090, in contrast to A1B in 2060 (reflecting the differences in greenhouse gas [GHG] emissions trajectories assumed for each of these scenarios). The wettest scenario in 2090 is projected with A1B in contrast to A2 in 2060. Temperature differences among the scenario means increase also compared to 2060, with the span between A1B and A2 at 1 ^{o}C in 2090, in contrast to less than 0.5 ^{o}C in 2060.

While all projections show unidirectional increases in temperature by 2090, precipitation changes increase or decrease depending upon the model and scenario (Figure 10). Only two models projected annual mean daily temperature increases of 3.5 ^{o}C or more in 2060; by 2090, seven models project changes greater than 3.5 ^{o}C (Figures 5 and 10). Differences among the models increase by 2090. The wettest individual model projection is the CSIRO-MK3.5 for the A1B scenario, in contrast to the A2 CSIRO-MK3.5 in 2060. The driest is MIROC3.2 for the A2 scenario in 2090, in contrast to the A1B MIROC3.2 in 2060.

At the scale of the conterminous United States, annual mean daily maximum and minimum temperatures for each of the nine projections increase above the range of the 1940 to 2000 historical period (Figure 11); however, projections for annual precipitation mostly remain within historical range (Figure 12). The temporal changes in maximum temperatures at the scale of the conterminous United States are greater than for minimum temperatures over the entire projection period. By the end of the 21st century, projected maximum temperatures and minimum temperatures are largest with the A2 scenario. By 2050, projections for maximum temperature in all scenarios and models rise above 19 ^{o}C, the upper range of the historical maximum temperature (Figure 11). Mean minimum temperature projections exceed the historical maximum of 9 ^{o}C by the mid-2040s. For minimum temperatures, individual model projections for the A2 scenario cluster together very tightly throughout almost the entire period. While the individual model projections may make excursions outside of the historical range for precipitation, no consistent divergence among the three models is apparent in these results. The MIROC3.2 results for the A2 scenario show a decreasing trend in precipitation over time, however this pattern was not repeated by the other two models projecting this same scenario (Figure 12c).

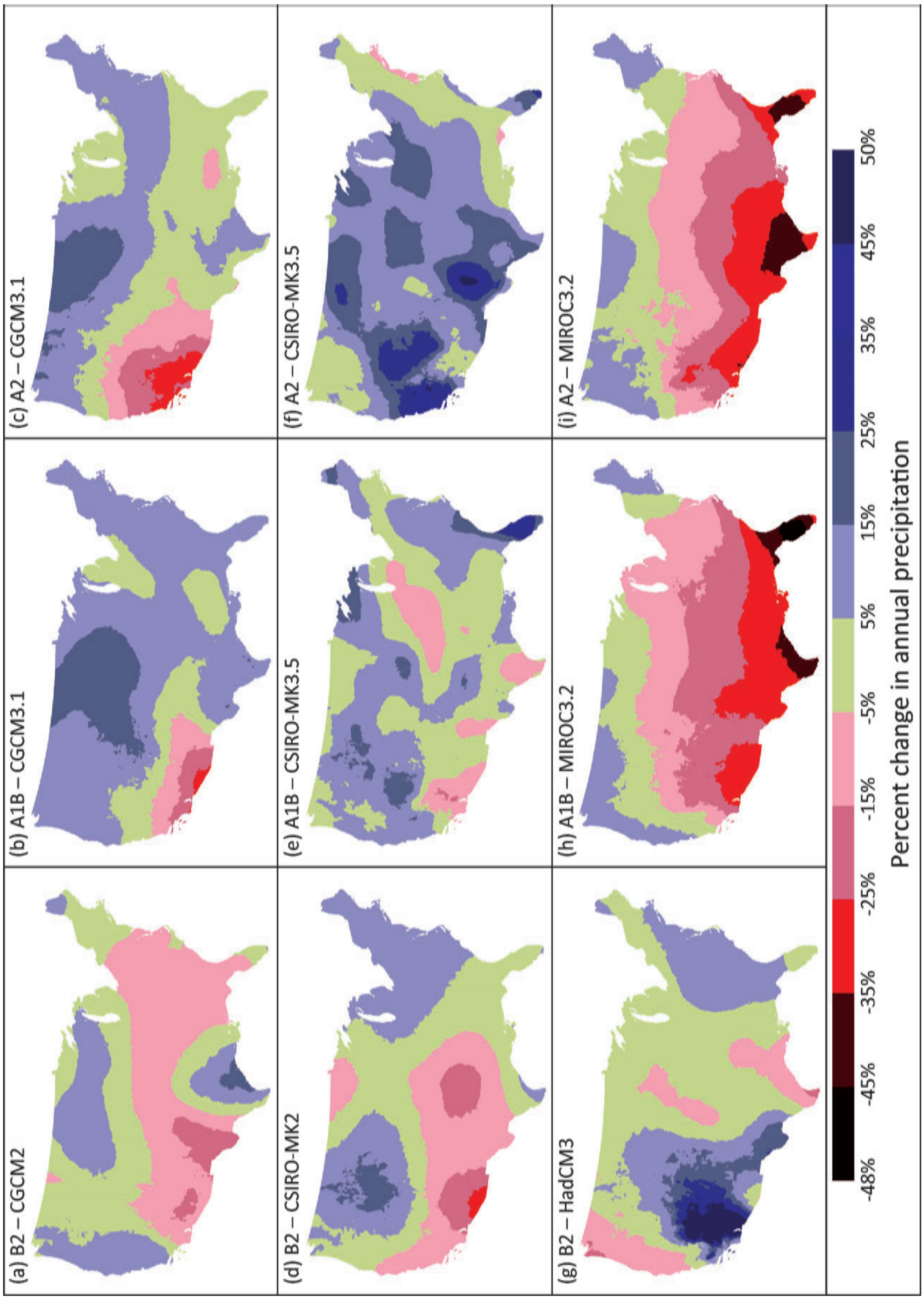

Figure 9. Change in annual precipitation (percent) by scenario and climate model for 2060 period. Change is computed as the difference of projected mean annual precipitation (2055-2064) and historical mean annual precipitation (1961-1990) and divided by the historical mean.

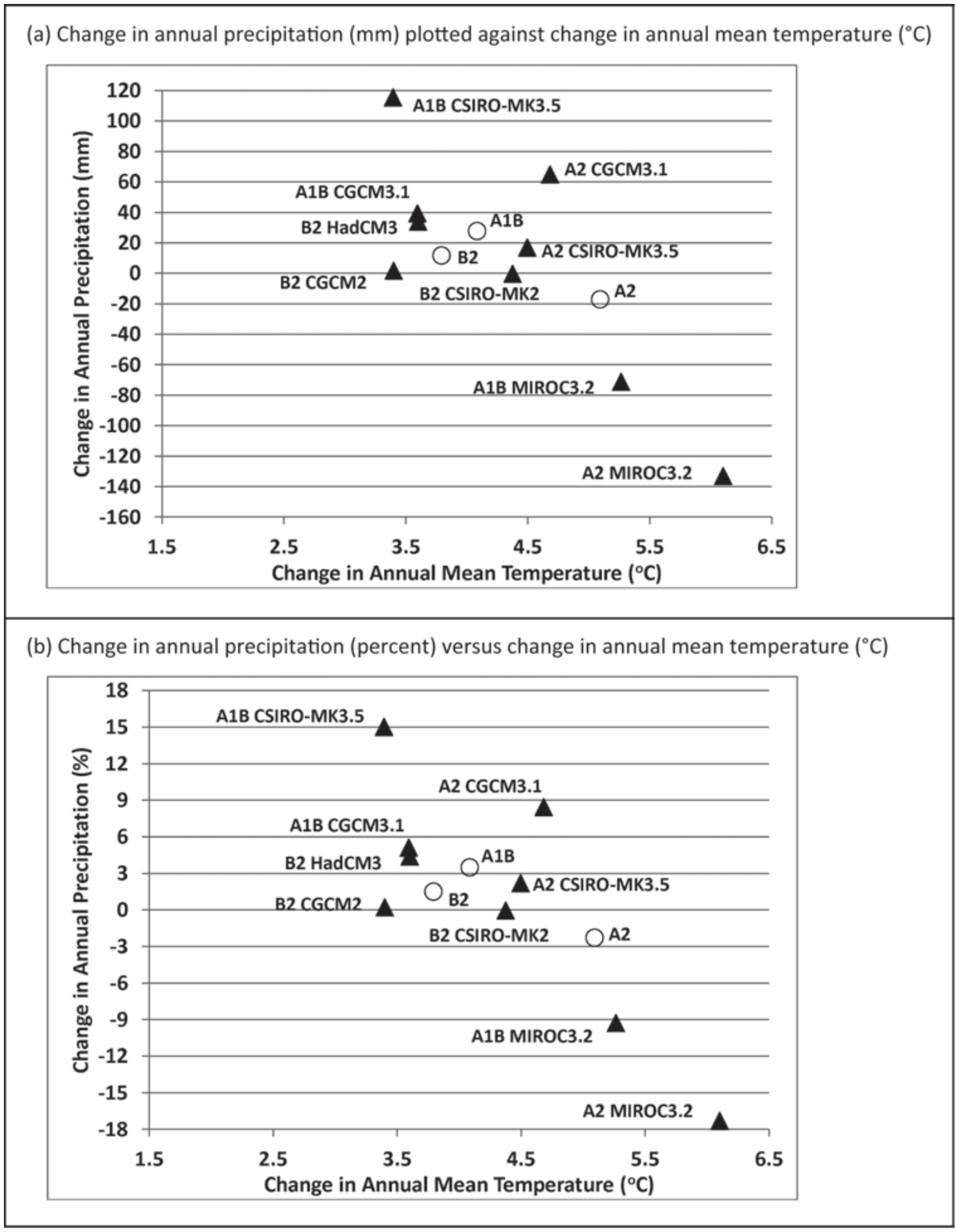

Figure 10. Change in annual precipitation (mm) plotted against change in annual mean daily mean temperature change (°C) for climate model projections (filled triangles) and scenario means (open circles) at the conterminous United States. Area-weighted changes (a) are computed as the difference between the projected mean (2085-2094) and the historical mean (1961-1990). Precipitation is also shown as percent change (b) where the difference in precipitation is divided by the historical mean.

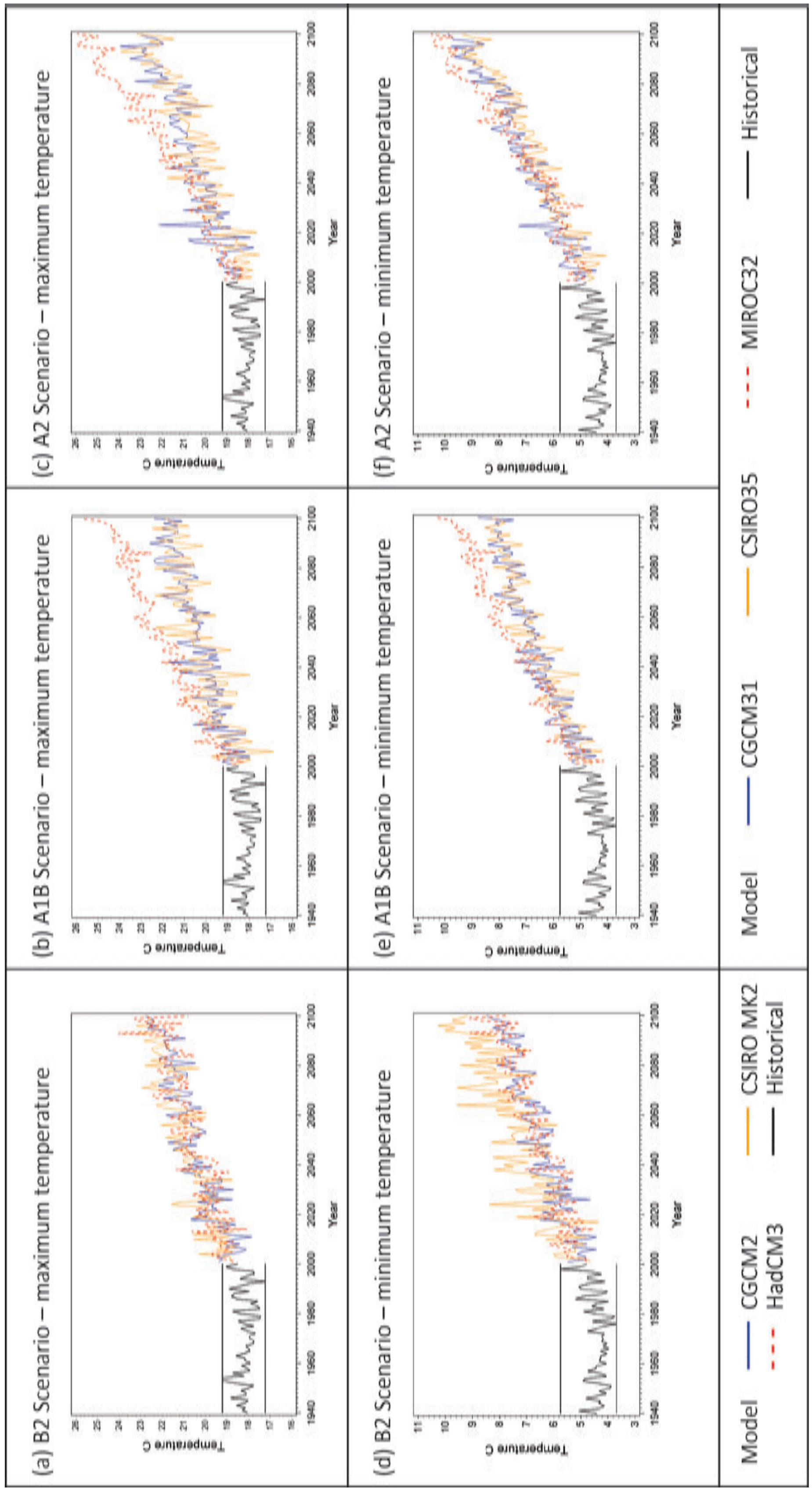

Figure 11. Observed (1940-2006) and projected (2001-2100) annual mean daily maximum mean temperature (°C) (a, b, c) and annual mean daily minimum mean temperature (°C) (d, e, f) for conterminous United States under scenarios B2, A1B, and A2, respectively. Each projection (colors) is the mean of three climate model projections for each scenario. The solid black line is the historical maximum (a) or minimum (b) temperature mean. Horizontal black lines denote the upper and lower range of the historical means.

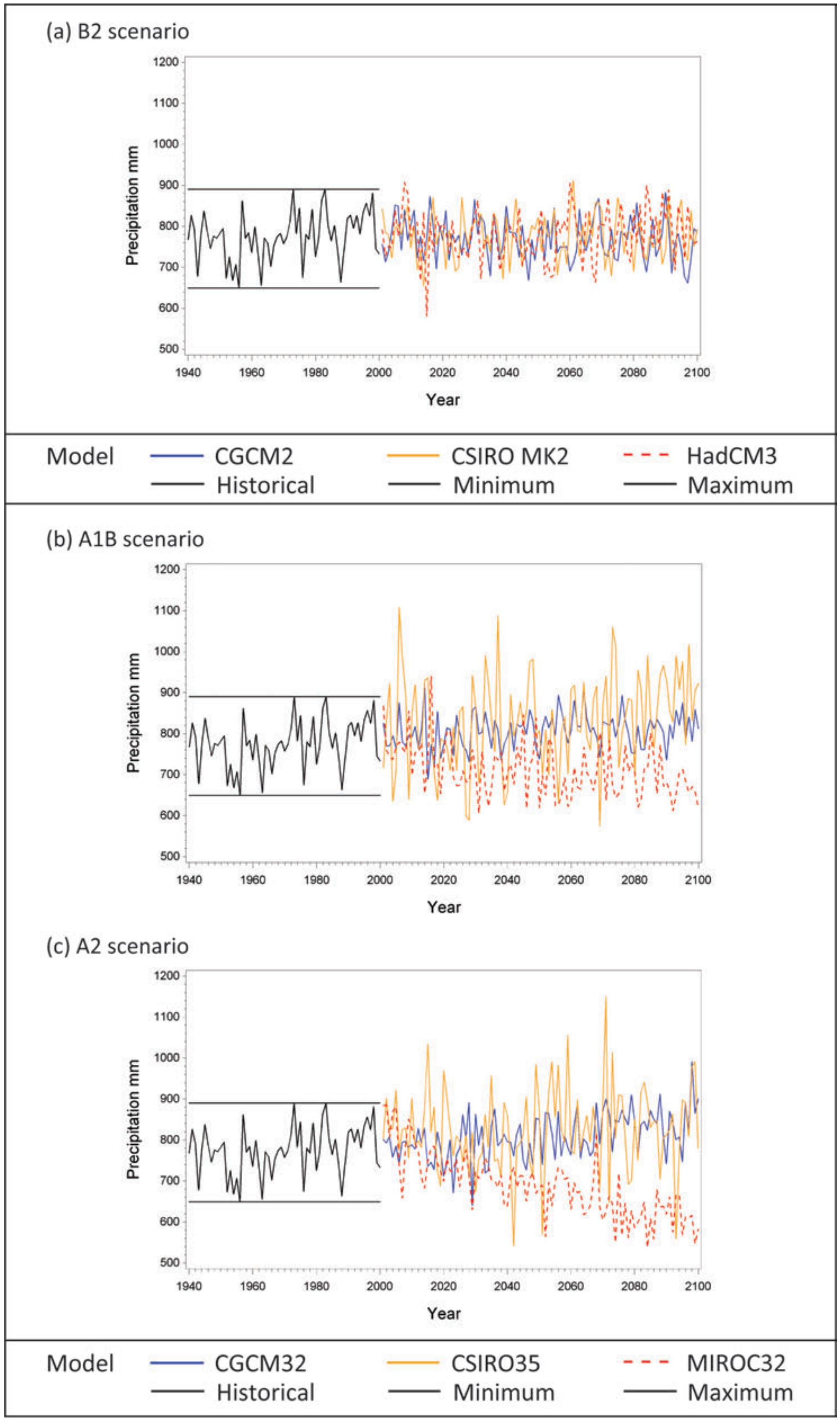

Figure 12. Observed (1940-2006) and projected (2001-2100) mean annual precipitation (mm) (a) for conterminous United States under scenarios B2, A1B, and A2. The solid black line is the historical mean annual precipitation. Horizontal lines denote the upper and lower range of the historical means.

By the end of the 21st century, model projections for the A2 scenario show the most warming. The minimum increases in annual mean daily temperature exceed 1.5 °C across the United States, compared to 1 °C in 2060; the increases do not exceed 5.5 °C anywhere in 2060 but rise above this change in the 2071-2100 period (Figures 7 and 13). As with the 2060 projections, the patterns vary by scenario and model. Coastal areas generally see the smallest increases in temperature, and the continental interior the largest increases (Figure 13).

By the 2071-2100 period, projected change in precipitation show spatial patterns and ranges similar to those in the 2060 period (compare Figure 9 with Figure 14). However for specific areas of the United States, the magnitude of change may be smaller or larger in this later period, and in some regions, projected decreases in 2060 are reversed by the end of the century. As with the 2060 projections, precipitation in the northern regions of the conterminous United States generally increases. Notably, in the A1B-CSIRO-MK3.5 projection, precipitation increases across much of the conterminous United States in the 2090 period in contrast to the 2060 period (compare Figure 9e with Figure 14e). In contrast, the CGCM3.1 model projects less area with increased precipitation for the A1B scenario in 2090 period; but greater area of increases in the A2 scenario. All three models project a decrease in precipitation in the Southern United States in the A2 scenario but for different areas across the region. Precipitation changes in the B2 scenario are least of all three scenarios for both 2060 and end of the 21st century projections. The A2 and A1B scenarios show a more similar spatial pattern to each other than with the B2 precipitation projection (Figure 14).

Regional Patterns in Annual and Seasonal Climate Projections

Southeast

Coastal areas in the conterminous United States are projected to have the smallest changes in annual mean daily temperatures for the 2060 period, especially the southeastern United States (states of Florida, Georgia, North Carolina, South Carolina, and Virginia) (Figure 7). Projected changes in annual mean daily temperature ranged from 1°C to 4.5 °C in this region. For seven of the individual model projections, annual precipitation was projected to remain near historical levels or to increase at most, 15 percent above historical means. For the MIROC3.2 projections in A1B and A2, precipitation decreases below 45 percent of historical mean, resulting in the largest relative decreases in precipitation across the United States (Figure 9).

Historically, observed summer mean daily maximum temperature ranges from 33 °C in the south to 24 °C in the mountainous northwest of the Southeastern region (Figure 15). Cooler temperatures in both the maximum and minimum reflect the mountainous topography. Observed summer mean daily minimum temperature is about 10 °C cooler than mean daily maximum temperature across the region over the historical period 1961-1990. The relatively small difference between daily maxima and minima is related to the generally high humidity in much of the region.

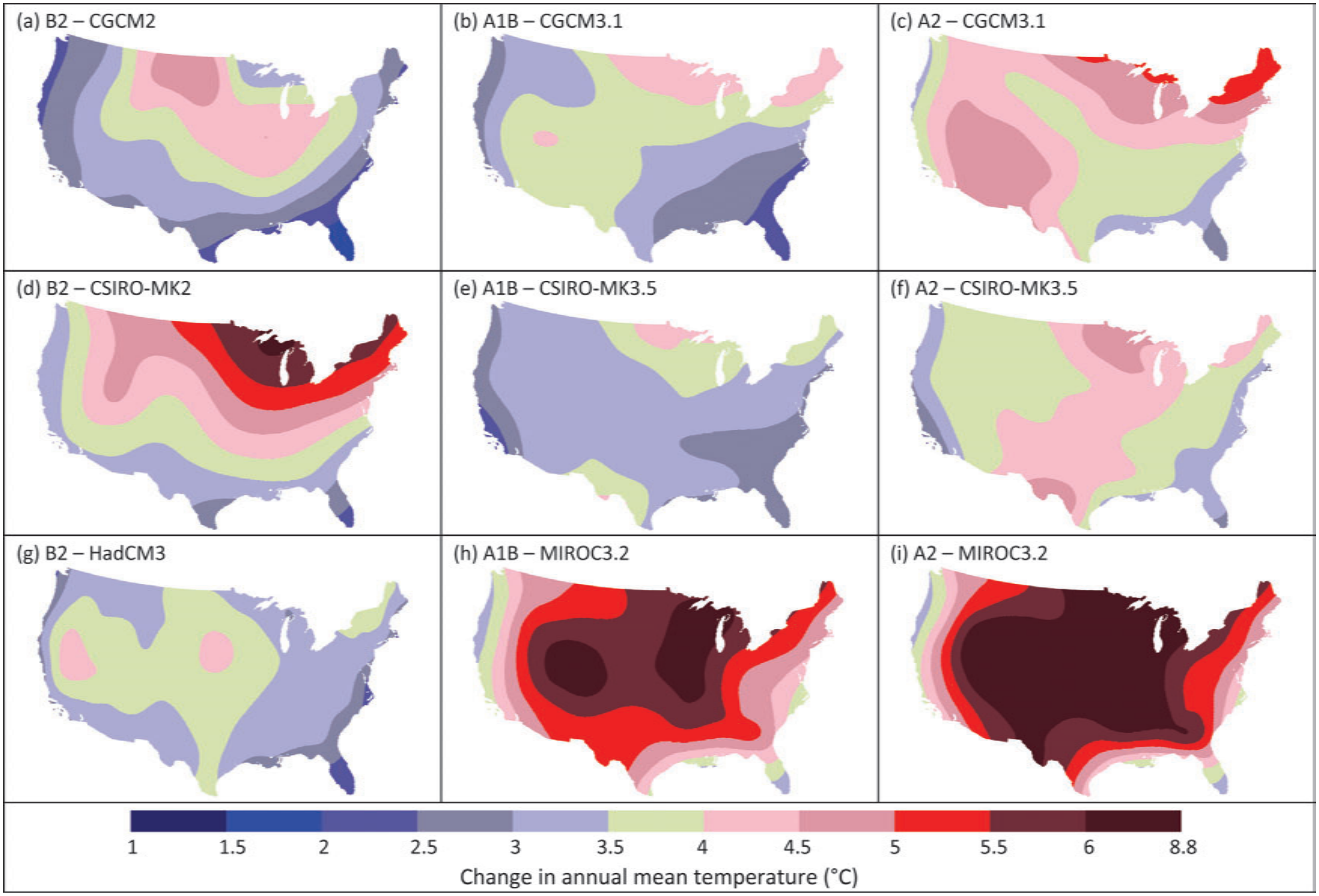

Figure 13. Projected changes in annual mean daily mean temperature (°C) by scenario and climate model for the 2071-2100 period. Change is estimated as the difference between the projected annual mean daily mean temperature (2071-2100) and the historical annual mean daily mean temperature (1961-1990 period).

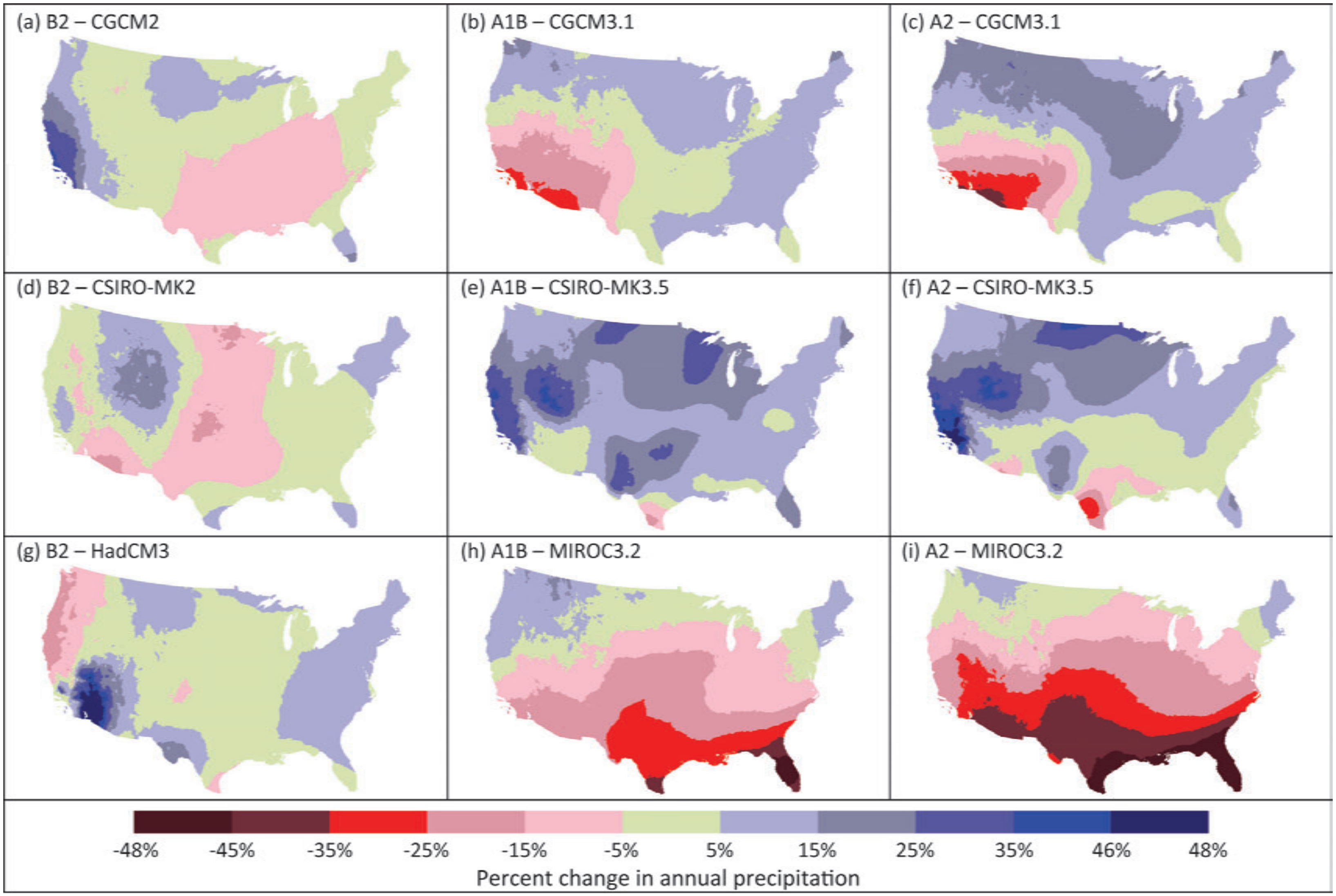

Figure 14. Change in mean annual precipitation (percent change) by scenario (B2, A1B, and A2) and climate model for the 2071-2100 period. Change is computed as the difference between projected annual precipitation (2070-2100 period) and historical annual precipitation (1961-1990 period) divided by the historical mean annual precipitation.

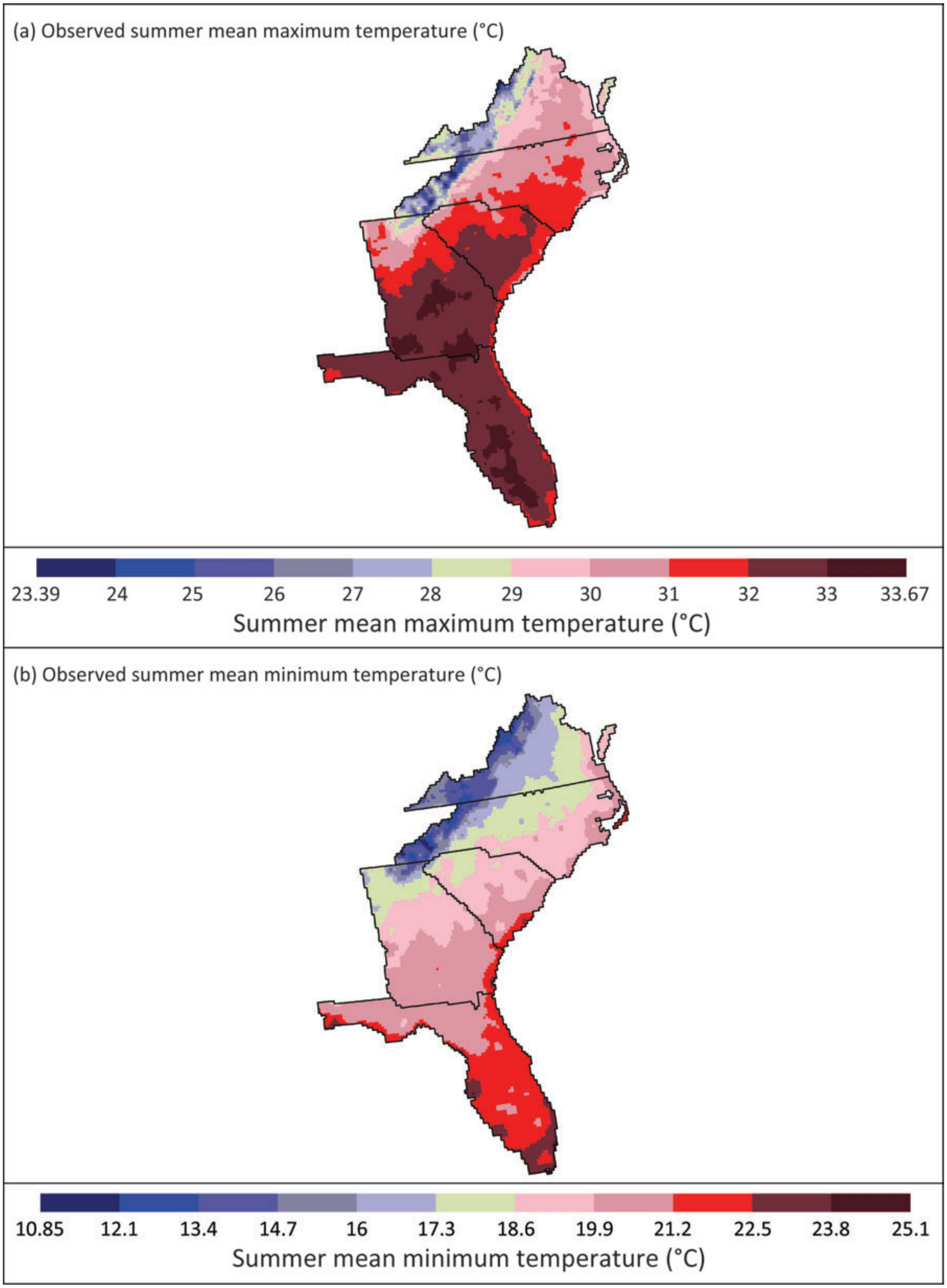

Figure 15. Observed summer mean daily maximum temperature (°C) (a) and summer mean daily minimum temperature (b) for the Southeast region of the United States for the period 1961-1990.

The projected changes in summer mean daily maximum and minimum temperatures for the 2060 period are generally greater than those for the annual means (compare Figure 7 with Figure 16). Projected increases by the 2060 period range from 1.1 ^{o}C for both minimum and maximum temperatures to as much as 7 ^{o}C in the case of the maxima. The relative changes in minimum temperature versus maximum temperature vary considerably among models and scenario. For scenario B2 and the CGCM2 projection, projected increases in summer maximum temperature are as much as 2 ^{o}C greater than for minimum temperature. The MIROC3.2 A1B and A2 project increases in maximum temperature often exceeding those for the minimum by more than 3 ^{o}C (Figure 16h,i). In other cases, minimum temperature increases are projected to be greater than for maximum temperature, e.g., A2 scenario and the CSIRO-MK3.5 projection, and A1B scenario for both CGCM3.1 and CSIRO-MK3.5 projections. Generally, where the greatest changes in minimum temperature are projected across the region, the greatest changes in maximum temperature are also seen (Figure 16)

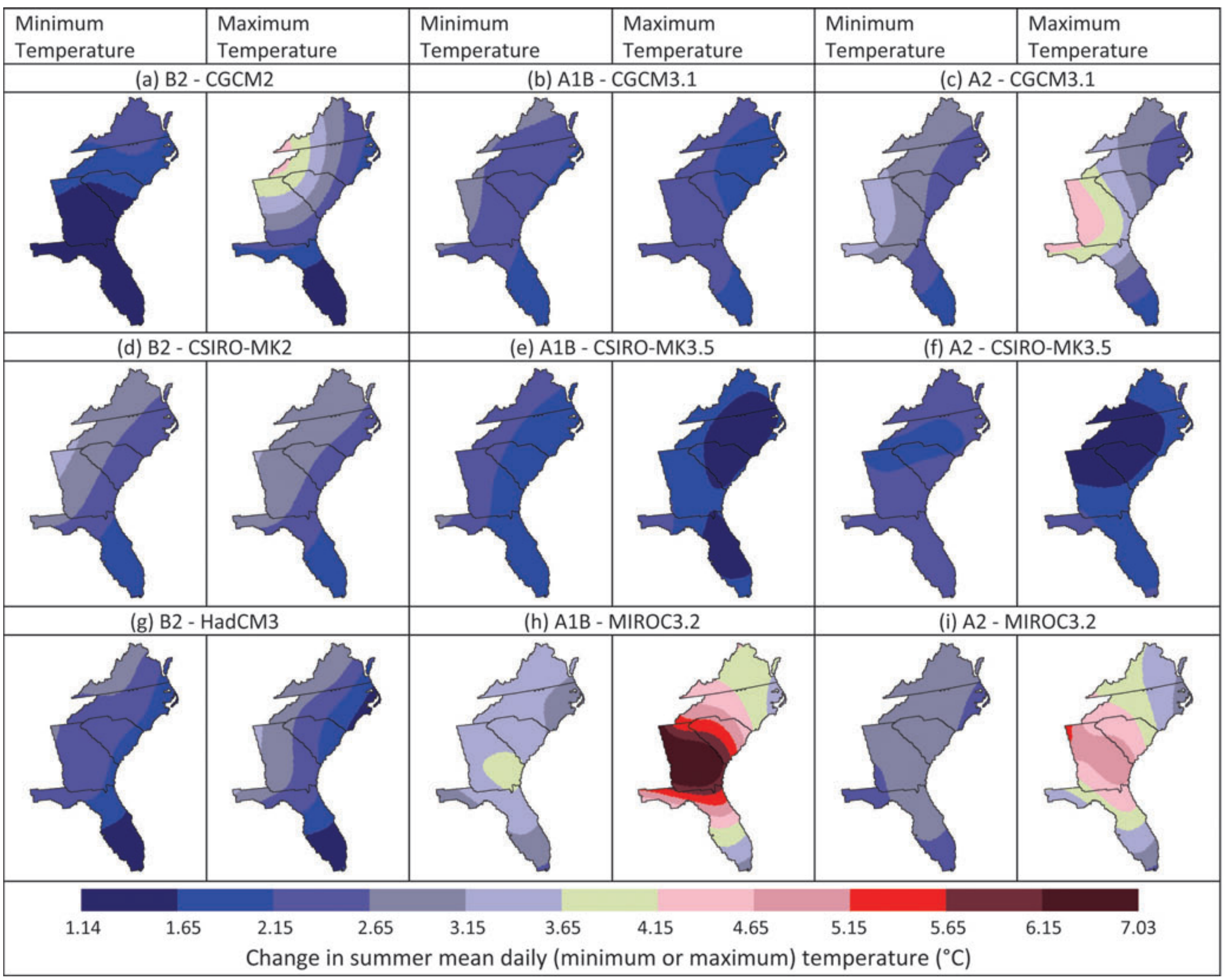

Figure 16. Projected change in summer mean daily minimum temperature and maximum temperatue (°C) by the 2060 period (2055-2064) for the southeastern United States by scenario (B2, A1B, A2) and model.

Great Plains

The means of temperature and precipitation change mapped for specific periods give a general picture of climate change (e.g. for the Southeast, Figure 16); however, variability in those changes across a region may be of interest. For the Northern Great Plains region (states of North Dakota, South Dakota, Nebraska, and Kansas), mean daily temperatures are projected to increase by the 2060 period from 1 °C to 4.5 °C above 1961-1990 means (Figure 7). Across the region, annual precipitation changes vary from minimal change to as much as 25 percent above historical (Figure 9). The major pulse of precipitation in this region occurs during March, April, and May.

Historically, spring mean daily mean temperatures ranged from 14.4 °C to about freezing (Figure 17), with colder temperatures reflecting the mountainous terrain of the Black Hills in western South Dakota as well as the U.S.-Canadian border. Figure 18 compares the frequency distributions of spring mean daily temperature for the historical period (1961-1990) with projections from the 2045-2074 period (i.e. centered on 2060) by three different models driven with the A1B scenario. These frequency distributions reflect the regional variation spatially (all grid cells in the region) and temporally (each year in the 30-year period).

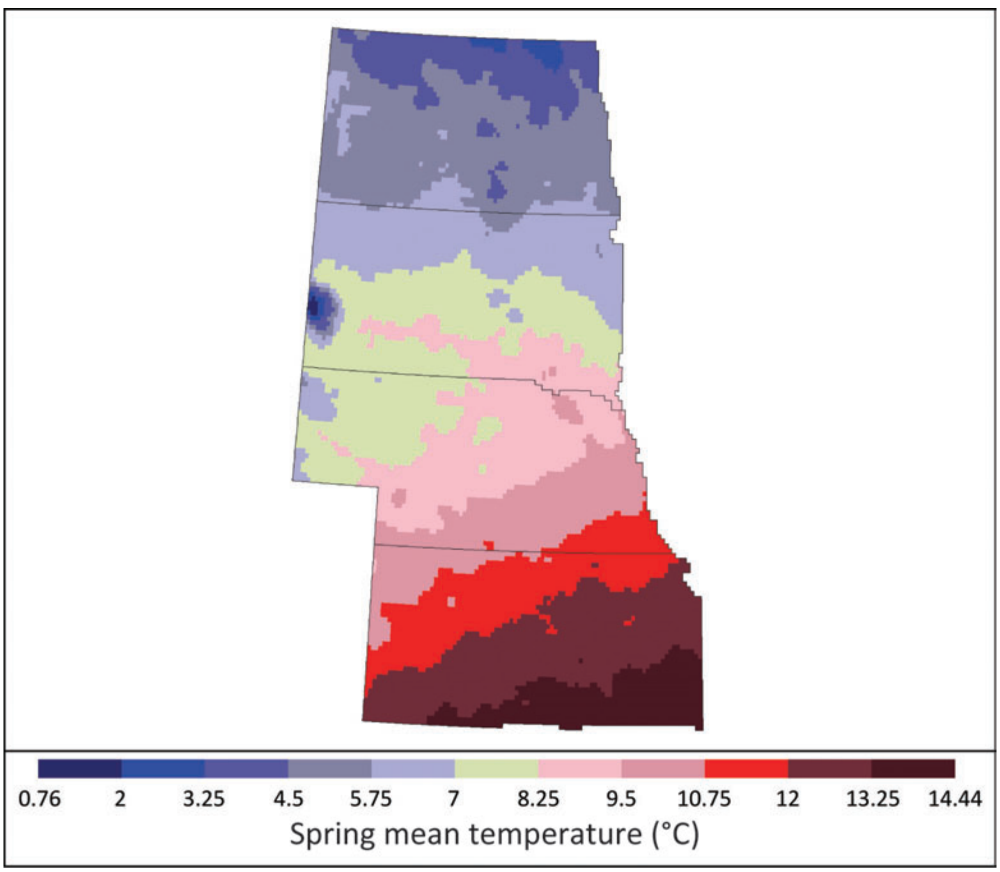

Figure 17. Spring mean daily mean temperature (°C) for the historical period (1961-1990) for the Northern Great Plains region. Spring is defined as the months of March, April, and May.

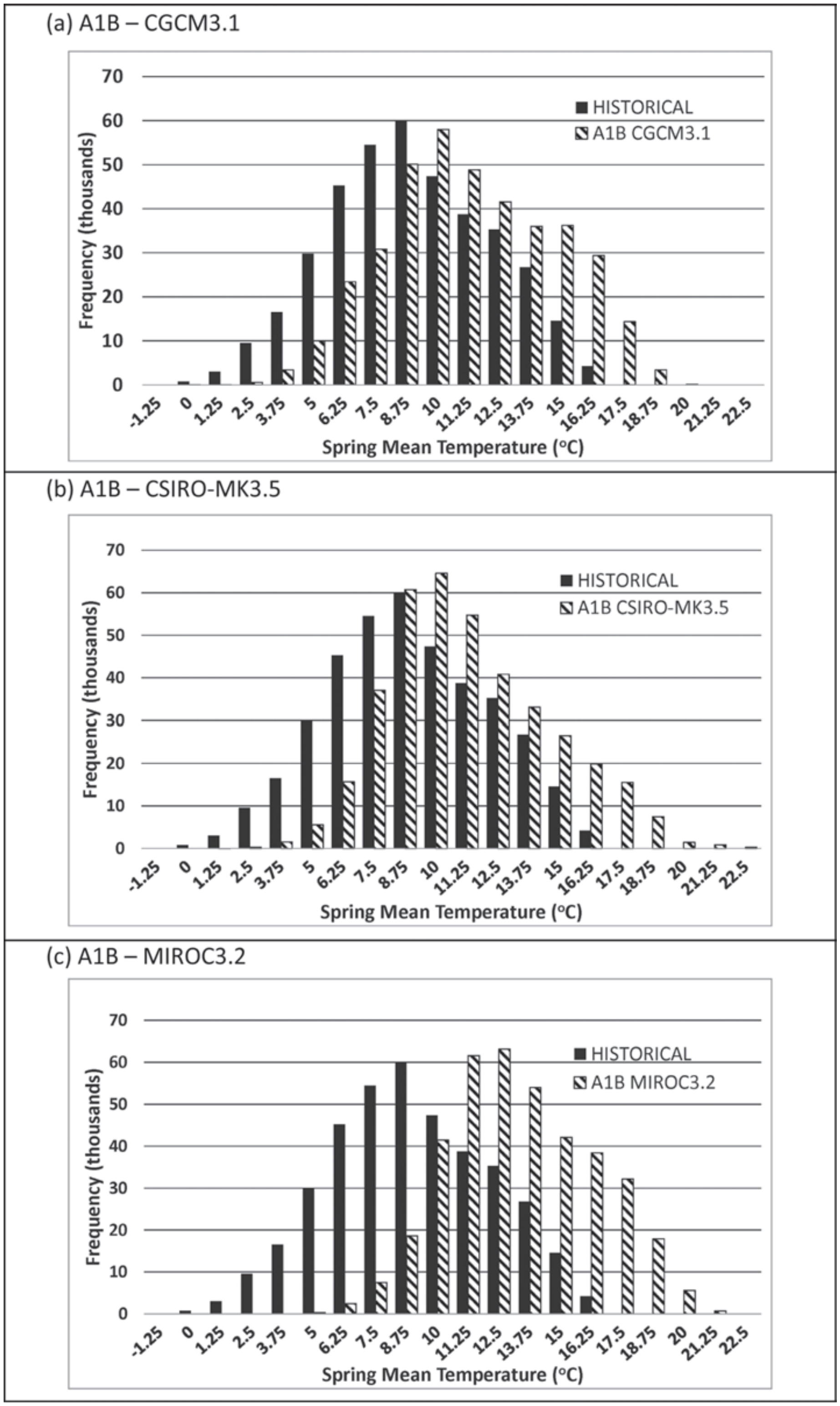

Figure 18. Frequency distribution of spring mean daily mean temperature (°C) in the Northern Great Plains for the historical period (1961-1990) and projected for the 30-year period surrounding 2060 (2045-2074) for the A1B scenario and climate models: (a) CGCM3.1, (b) CSIRO-MK3.5, and (c) MIROC3.2.

Though infrequent, spring mean daily temperatures for some grid cells in the historical period could be below 0 ^{o}C. By 2060, all models for the A1B scenario project a general upward shift in the frequency distribution by at least 1.25 ^{o}C (Figure 18). Spring mean temperatures are projected to stay above zero in seven out of nine projections (not shown), with the CGCM3.1 model being the exception for the A1B (Figure 18a) and the A2 (not shown). The projected mean spring temperatures frequently exceed the warmest historical temperatures (17.5 ^{o}C) seen in the region.

Spring minimum temperatures are of importance because they can affect the initiation and success of vegetative growth. Also, increases in minimum temperatures will affect the occurrence and severity of 'freeze-thaw' events, which can have serious impacts when plants are at vulnerable stages of development (leaf flushing and flowering). Historically, spring mean daily minimum temperatures below freezing (0 ^{o}C) were not infrequent and could be as low as –9.1 ^{o}C (Figure 19). By the 2060 period, all models project fewer occurrences of below freezing with the projected lowest temperature (CGCM3.1) about –4 ^{o}C. This pattern is also common in all models projecting the A2 and the B2 scenario (not shown). Historically, for the spring mean minimum temperature, approximately 40 percent of grid cells and years were below freezing and by 2060, more than 90 percent of the grid cells and years are projected to be above freezing according to the A1B scenario. The upper tail of the frequency distribution for the projected spring mean minimum temperature begins to approach the lower tail of the historical spring maximum temperatures (not shown).

In the Southern Great Plains (states of Texas and Oklahoma), spring mean daily temperatures for the 1961-1990 period were above 11.7 ^{o}C with the warmest spring temperatures exceeding 23 ^{o}C along the U.S.-Mexican border (Figure 20). Over this historical period, spring temperatures range from 9.1 ^{o}C to 27.5 ^{o}C at the scale of the individual grid cell (Figure 21). By the 2060 period, the frequency distribution of spring mean daily temperature for the A1B scenario shifts so that projected spring mean temperatures are never less than 12.6 ^{o}C and exceed the warmest historical spring temperatures by several degrees in all climate model projections (Figure 21).

In the Southern Great Plains, historical spring mean daily mean maximum temperatures range from about 17 ^{o}C to 35 ^{o}C. According to the CGCM3.1 A1B, these spring maximum temperatures are projected to remain above 22 ^{o}C by 2060 and to exceed 38 ^{o}C (Figure 22a). Summer mean daily temperatures historically ranged from about 20 ^{o}C to 33 ^{o}C and are projected to increase to nearly 24 ^{o}C in the lower end of the range and to exceed the upper historical range by several degrees. Comparison of Figure 22a with Figure 22b shows that spring and summer seasonal temperature ranges begin to overlap in the Southern Great Plains by 2060. Projected spring mean daily maximum temperatures overlap with and exceed the historical summer mean temperatures by as much as 6 ^{o}C.

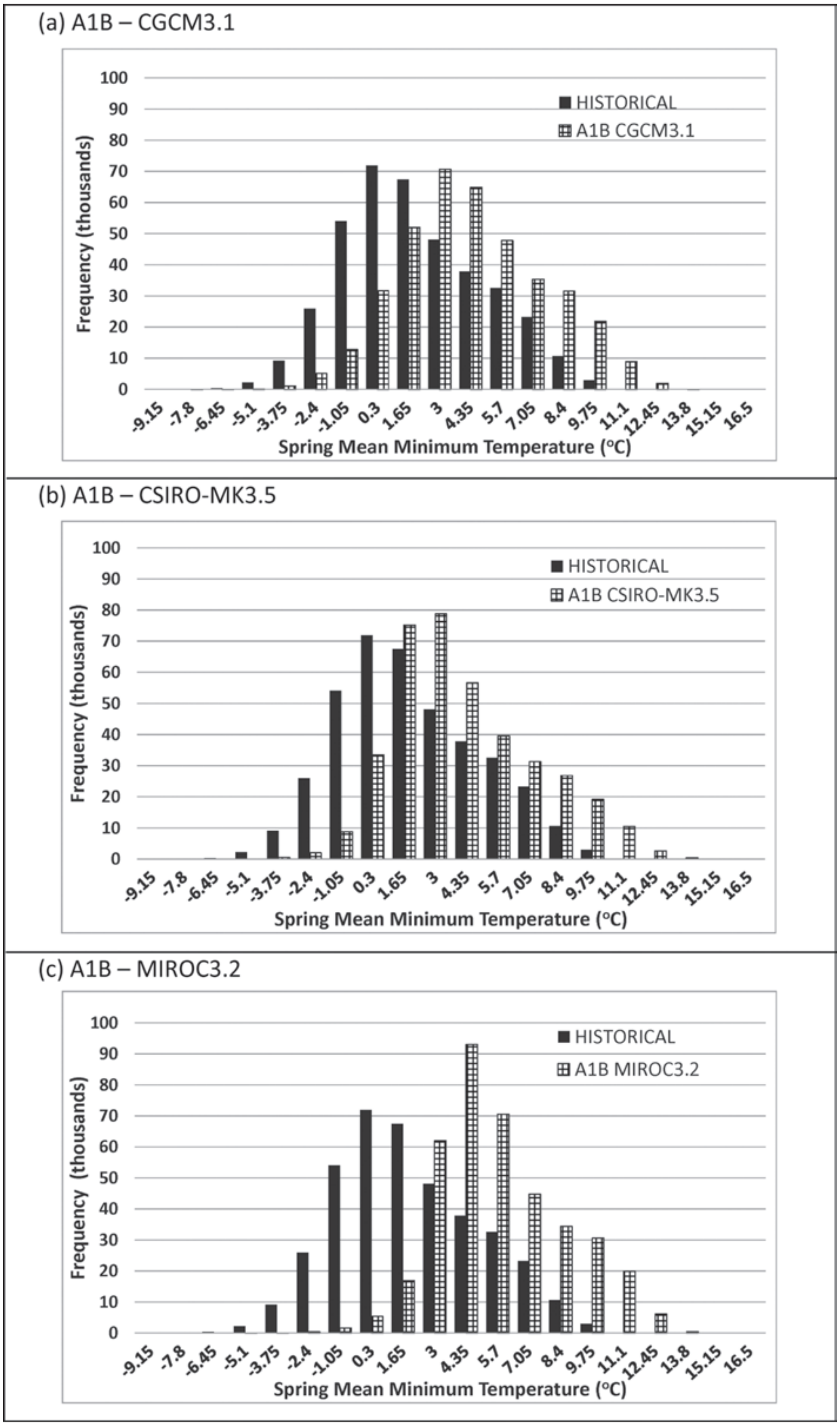

Figure 19. Frequency distribution of spring mean daily mean minimum temperature (°C) in the Northern Great Plains for historical period (1961-1990) and projected for the 30-year period surrounding 2060 (2045-2074) for the A1B scenario and climate models: (a) CGCM3.1, (b) CSIRO-MK3.5, (c) MIROC3.2.

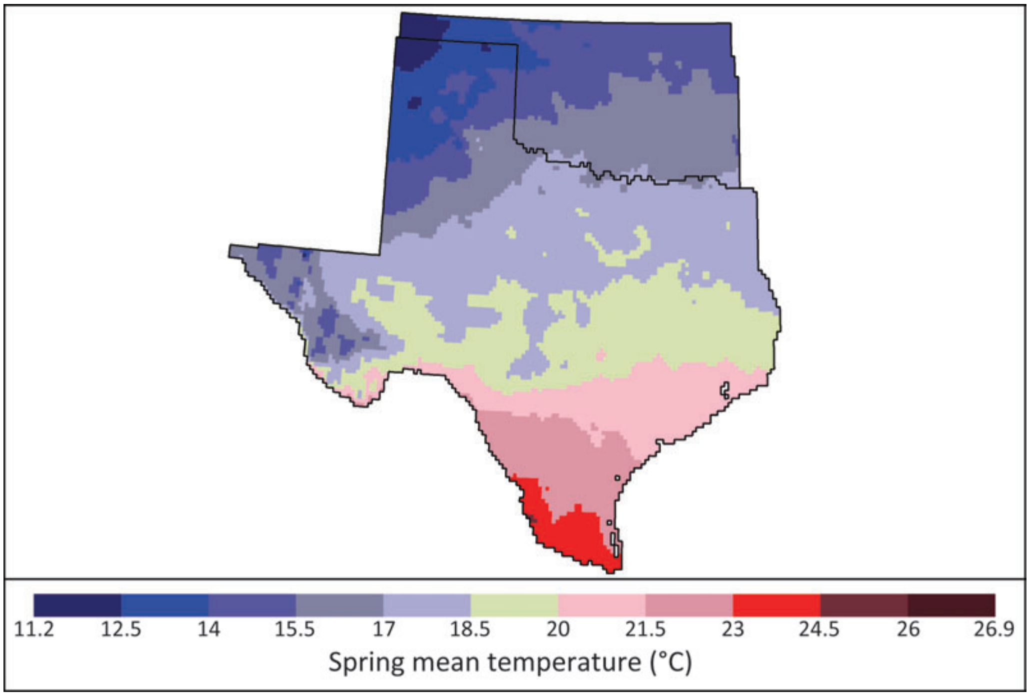

Figure 20. Spring mean daily mean temperature (°C) for the Southern Great Plains based on PRISM climatology for the 1961-1990 period.

Colorado

A comparison of future projections in the context of past observed variability can assist managers and others in planning for climate change. Following the work in Ray and others (2008), we calculated the projected mean daily mean temperature and annual total precipitation for grid cells within a 35-km by 45-km region surrounding the town of Lamar, Colorado, located in eastern Colorado. We compare the nine projections (all scenarios and all models used in the current study) for the 2060 period (2045-2074) with the historical climate record (1950-1999) from the Lamar weather station (Figure 23). The variability in the historical record for precipitation is high—the black dashed lines represent the 10th and 90th percentile values of all monthly observations in the historic period 1950-1999 (Figure 23a). Simulated monthly precipitation data for all nine projections lie completely within the variability of the historical record. At the temporal scale of the 20-year moving averages for precipitation (represented by vertical black lines), the projections for some months are encompassed by this variability or for other months, projections extend beyond this historical variability. Relative to historical precipitation, projected patterns are within the historical ranges. In contrast, projections for July and August mean daily temperature are outside of the historical range; for all other months, projections are within the historical range. The patterns for July and August are very similar to what Ray and others (2008) show for Grand Junction in western Colorado. As Ray and others (2008) described for Grand Junction, as the model consensus is above the 90th percentile of the historical record, the implication is that mean temperatures for July and August in the Lamar area for the 2060 period could be similar to the five warmest years observed in the last 50 years.

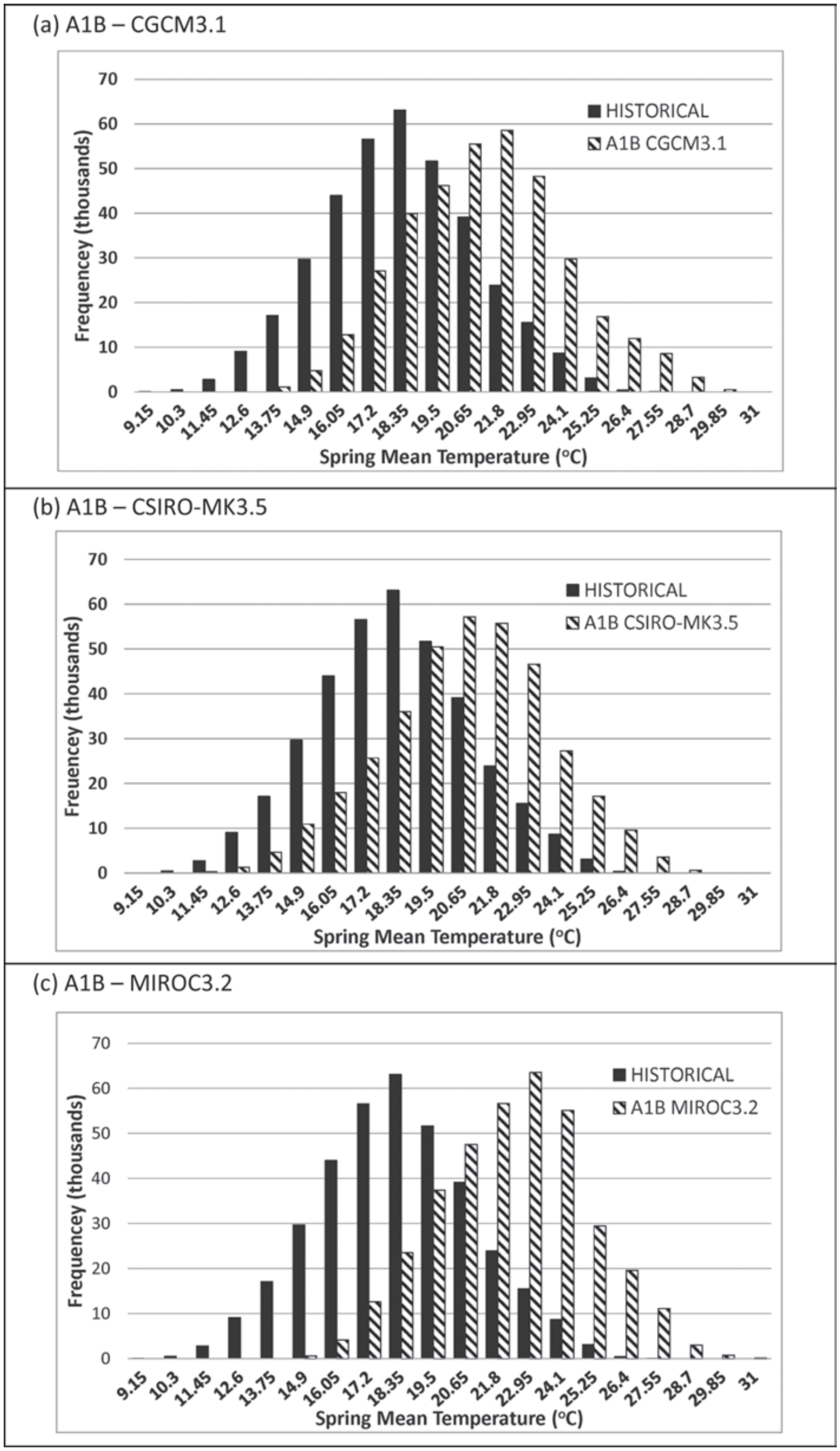

Figure 21. Frequency distribution of spring mean daily temperature (°C) in the Southern Great Plains for the historical period (1961-1990) and projected for the 30-year period surrounding 2060 (2045-2074) for the A1B scenario and climate models: (a) CGCM3.1, (b) CSIRO-MK3.5, (c) MIROC3.2.

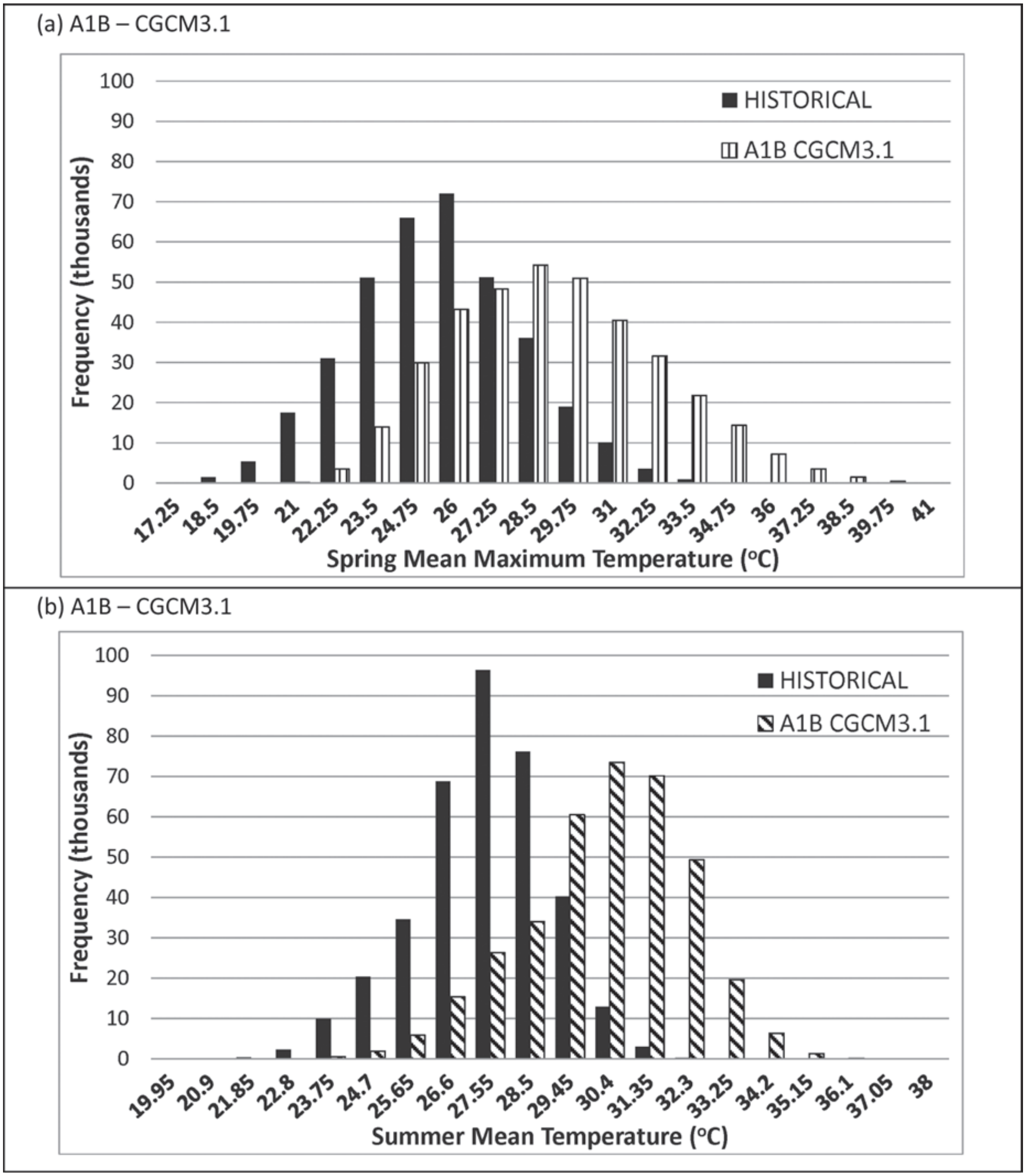

Figure 22. Frequency distribution of spring mean daily mean maximum temperature (a) and summer mean daily mean temperature (b) in the Southern Great Plains for the historical period (1961-1990) and projected for the 30-year period surrounding 2060 (2045-2074) for the A1B scenario and climate model CGCM3.1.

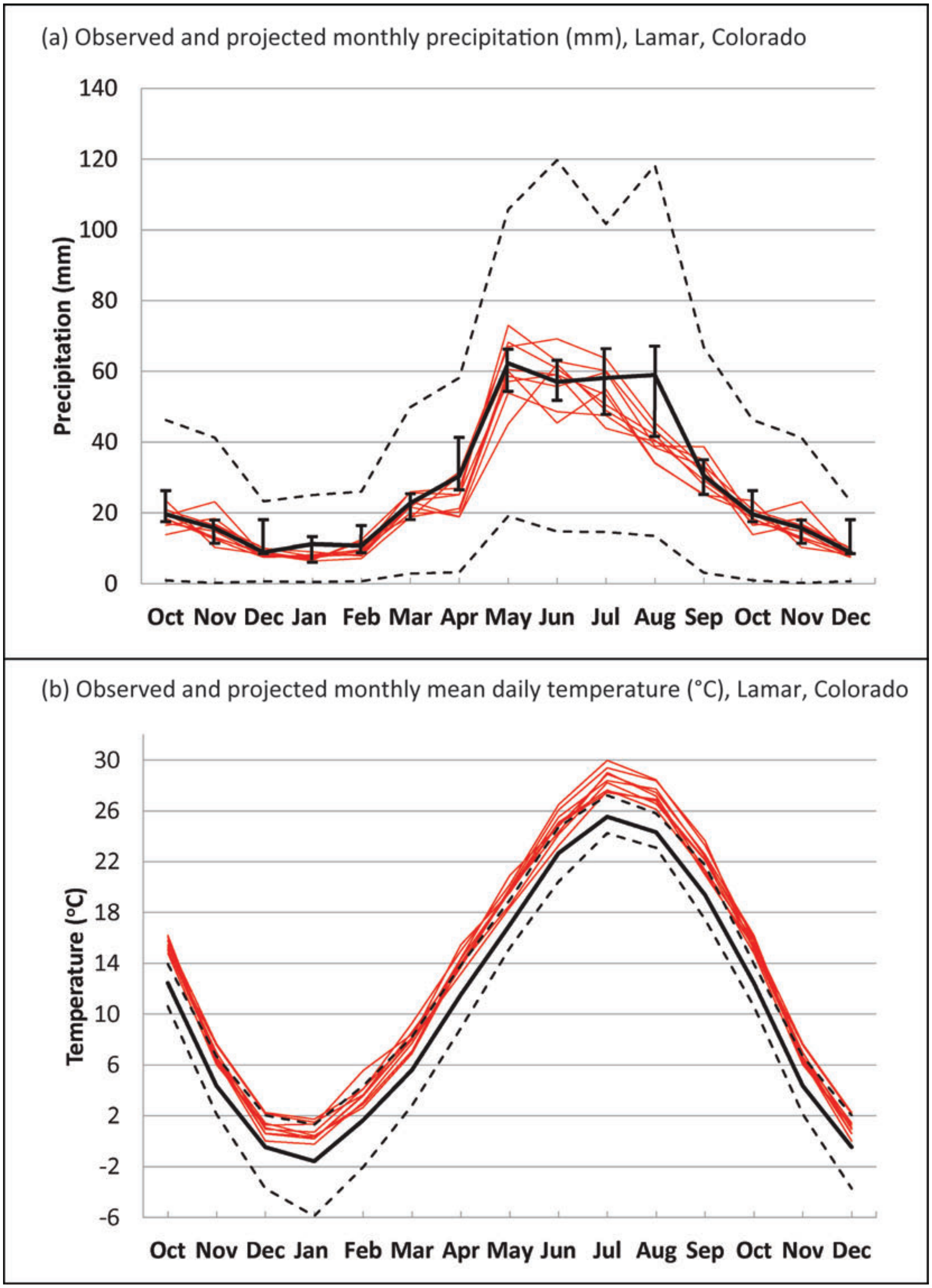

Figure 23. Observed mean annual precipitation (mm) (a) and monthly mean temperature (°C) (b) from the Lamar, Colorado, weather station compared with projections for 2060 (2045-2064) from a region (approximately 30 km by 45 km) surrounding Lamar. The observed monthly 50-year mean (solid black lines) and 10th and 90th percentile values (dashed black lines) are based on all observations over the period 1950-1999. Projected mean daily temperature (°C) and annual total precipitation (mm) (solid red lines) are from the nine scenario-model projections in this study for grids surrounding Lamar, CO. The black bars on historical precipitation represent the 10th and 90th percentiles of the 20-year moving averages from 1897 to 2010.

For Colorado, we summarize the seasonal and annual results for all variables for each emissions scenario (i.e., mean of the three climate model projections) by 30-year periods into the future (Table 7). By the 2061-2090 period, annual mean daily maximum and minimum temperatures are projected to rise 3.3 to 6.2 °C above those during 1971-2000, depending upon the scenario. The changes in annual minimum and maximum temperature in the first 30-year period (2001-2030) are similar across scenario and across temperature variable, ranging from 0.9 °C to 1.1 °C for minimum temperature and from 1.3 °C to 1.6 °C for maximum. The increase in annual minimum temperature is sufficient to raise it slightly above freezing by the 2030 period, depending upon the scenario. By 2061-2090, the projected increase over the 1971-2000 mean is 3.2 °C to 3.8 °C for minimum temperature and 3.4 °C to 4.9 °C for the maximum. By that time, minimum temperature is projected to be 3 °C to nearly 4 °C above freezing.

Changes by season vary from the annual patterns (Table 7). The historical spring mean daily minimum temperature is –1.7 °C. Projections for all scenarios by the 2031-2060 period take spring minimum temperature above freezing and by the end of the 21st century, the projected mean is at least 1 °C above freezing in all scenarios. Similarly, fall mean minimum temperatures are projected to exceed freezing by the 2001-2030 period, and remain above freezing by the end of the 21st century. As noted previously, the seasonal mean daily maximum temperatures increase more than the corresponding minima (Table 7). For example, spring mean maximum temperatures rise 3.1 °C to 4.7 °C by 2061-2090, in contrast to an increase of 2.5 °C to 3.2 °C for spring mean minimum temperatures. Winter temperature increases are similar across all scenarios by 2060-2090. The largest increases in seasonal mean daily maximum temperature occur primarily in the summer. By the end of the 21st century, summer maximum temperatures are projected to be 3.6 °C to 6.9 °C above the historical means. The 100-year change by season varies; the greatest increase (in both maximum and minimum temperature) is seen in summer for the A2 scenario, but in fall for the A1B. For the B2 scenario, the greatest increase in minimum temperature is projected for winter, whereas the greatest increase in maximum temperature is projected for summer.

Annual and seasonal precipitation amounts for Colorado are projected to decline with all emission scenarios, with only the exception of winter showing slight increases (Table 7). By 2061-2090, annual precipitation is projected to decrease from 10 to 35 mm relative to the 1971-2000 period, corresponding to a 7 percent decline (Table 7). Historically, most precipitation occurs in spring and summer; these seasons are generally projected to see the greatest decline over the 21st century. The interannual variability of seasonal and annual precipitation is greater than that of temperature.

Table 7—Climate change outlook for Colorado, based on the mean of three climate models within each scenario.

Climate variable	A2 Emissions scenario					A1B Emissions scenario					B2 Emissions scenario				
Mean Daily Tmin (°C)	Spring	Summer	Fall	Winter	Year	Spring	Summer	Fall	Winter	Year	Spring	Summer	Fall	Winter	Year
Baseline 1971-2000	-1.7	9.5	-0.6	-10.8	-0.9	-1.7	9.5	-0.6	-10.8	-0.9	-1.7	9.5	-0.6	-10.8	-0.9
Change by 2001-2030	0.6	1.2	1.2	0.7	0.9	0.9	1.3	1.2	0.8	1.0	0.8	1.2	1.1	1.4	1.1
Change by 2031-2060	1.6	2.6	2.6	1.9	2.2	2.0	2.6	2.7	1.9	2.3	2.0	2.5	2.3	2.5	2.3
Change by 2061-2090	3.2	4.4	4.3	3.4	3.8	2.9	3.8	3.9	3.3	3.5	2.5	3.3	3.3	3.9	3.2
100-year change	4.6	5.5	5.2	4.9	5.0	3.1	4.3	4.3	4.0	3.9	3.0	3.4	3.4	4.3	3.5
100-year variability (%)	3.9	2.5	3.7	4.9	2.1	5.2	3.2	3.6	5.1	2.7	7.7	4.4	6.3	10.0	4.6
Mean Daily Tmax (°C)	Spring	Summer	Fall	Winter	Year	Spring	Summer	Fall	Winter	Year	Spring	Summer	Fall	Winter	Year
Baseline 1971-2000	14.3	26.6	15.6	4.1	15.1	14.3	26.6	15.6	4.1	15.1	14.3	26.6	15.6	4.1	15.1
Change by 2001-2030	1.1	1.8	1.7	0.6	1.3	1.6	2.0	1.9	0.9	1.6	1.3	1.8	1.7	0.95	1.4
Change by 2031-2060	2.7	3.5	3.3	1.9	2.9	3.0	3.5	3.5	2.0	3.0	2.7	2.9	2.7	1.8	2.5
Change by 2061-2090	4.7	5.8	5.5	3.5	4.9	4.1	4.9	5.0	3.3	4.3	3.1	3.9	3.8	2.8	3.4
100-year change	6.2	6.9	6.5	5.3	6.2	4.2	5.0	5.2	4.1	4.6	3.1	3.6	3.6	2.9	3.3
100-year variability (%)	4.4	4.8	4.8	4.8	2.8	7.8	6.8	3.8	5.8	4.2	9.8	8.7	7.3	9.3	5.5
Total Precipitation (mm)	Spring	Summer	Fall	Winter	Year	Spring	Summer	Fall	Winter	Year	Spring	Summer	Fall	Winter	Year
Baseline 1971-2000	139	145	103	77	465	140	145	103	77	465	139	145	103	77	465
Change by 2001-2030	-11	-5	-4	4	-17	-13	-11	-9	0	-33	-15	-9	-7	4	-27
Change by 2031-2060	-22	-9	-3	1	-34	-17	-8	-5	3	-26	-14	0	-3	2	-16
Change by 2061-2090	-19	-16	-11	11	-35	-17	-5	-10	8	-24	-8	-3	-4	4	-10
100-year change	-16	-15	-12	10	-33	-7	0	-4	11	-1	17	25	6	2	29
100-year variability (%)	-33	-44	-49	44	-36	-86	2169	-129	37	-1350	30	176	94	199	43

Pacific Northwest

The Pacific Northwest (Washington, Oregon, and Idaho) is a region where precipitation has a strong seasonal pattern, with summers typically being much drier across the entire region than the other three seasons (Figure 24a,b,c,d). There is also a strong west-to-east precipitation gradient where the coastal and western parts of this region, as well as northern Idaho, have much higher precipitation each season than the central and southern parts. Focusing on the A1B scenario and the 2060 period, the models project the large decreases in precipitation during summer (comparing across Figure 24e,f,g,h). These decreases are projected to occur throughout the northern coastal, northwestern interior, and scattered areas in the central interior parts of this region (Figure 24g). For winter, fall, and spring, the majority of the region sees anywhere from a slight decrease to an increase of 20 percent above the seasonal mean historical (1961-1990) precipitation. The greatest increases generally are in the eastern parts of the region in winter and spring and scattered across the region in fall.

Seasonal mean daily minimum temperatures reflect coastal influences, mountainous topography, and the continental nature of climate in the eastern interior parts of the region. The coldest temperatures in all seasons are found in the eastern mountainous areas (Figure 25a,b,c,d). Seasonal minimum temperatures are projected to increase 1.4 ^{o}C or more across the region, with the greatest increases occurring in winter and summer in the southeastern part of this region (Figure 25). Projected increases greater than 3 ^{o}C would bring spring and fall mean daily minimum temperatures in the eastern parts of the region close to, if not above, freezing (Figures 25f and h).

The relative temperature and precipitation changes by projection and scenario are often used to identify scenarios for climate impact analysis. We explore these relationships in the Pacific Northwest region for each season (Figure 26). As noted earlier, the A1B scenario is the warmest scenario for the conterminous United States in the 2060 period. However while that trend generally holds for the Pacific Northwest, the seasonal scenario means for A1B, A2, and B2 differ by less than 0.5 ^{o}C, except for winter where the A1B and A2 scenario means are nearly 1.0 ^{o}C greater than the B2 mean.

Overall, the greatest warming is projected for summer along with some relatively large seasonal declines in precipitation (Figure 26). The scenario mean changes in temperature (A1B, A2, and B2) are above 3 ^{o}C in summer with decreases of 5 to 18 percent in summer precipitation (Figure 26c). Across all scenarios, seven of the individual model projections show decreases in summer precipitation. The HadCM3 B2 projected the greatest decrease in summer precipitation and the largest temperature increase for summer of all nine projections. Of the seven projections with decreases in summer precipitation, summer temperature increases range above 2 ^{o}C with several projections exceeding 3.3 ^{o}C.

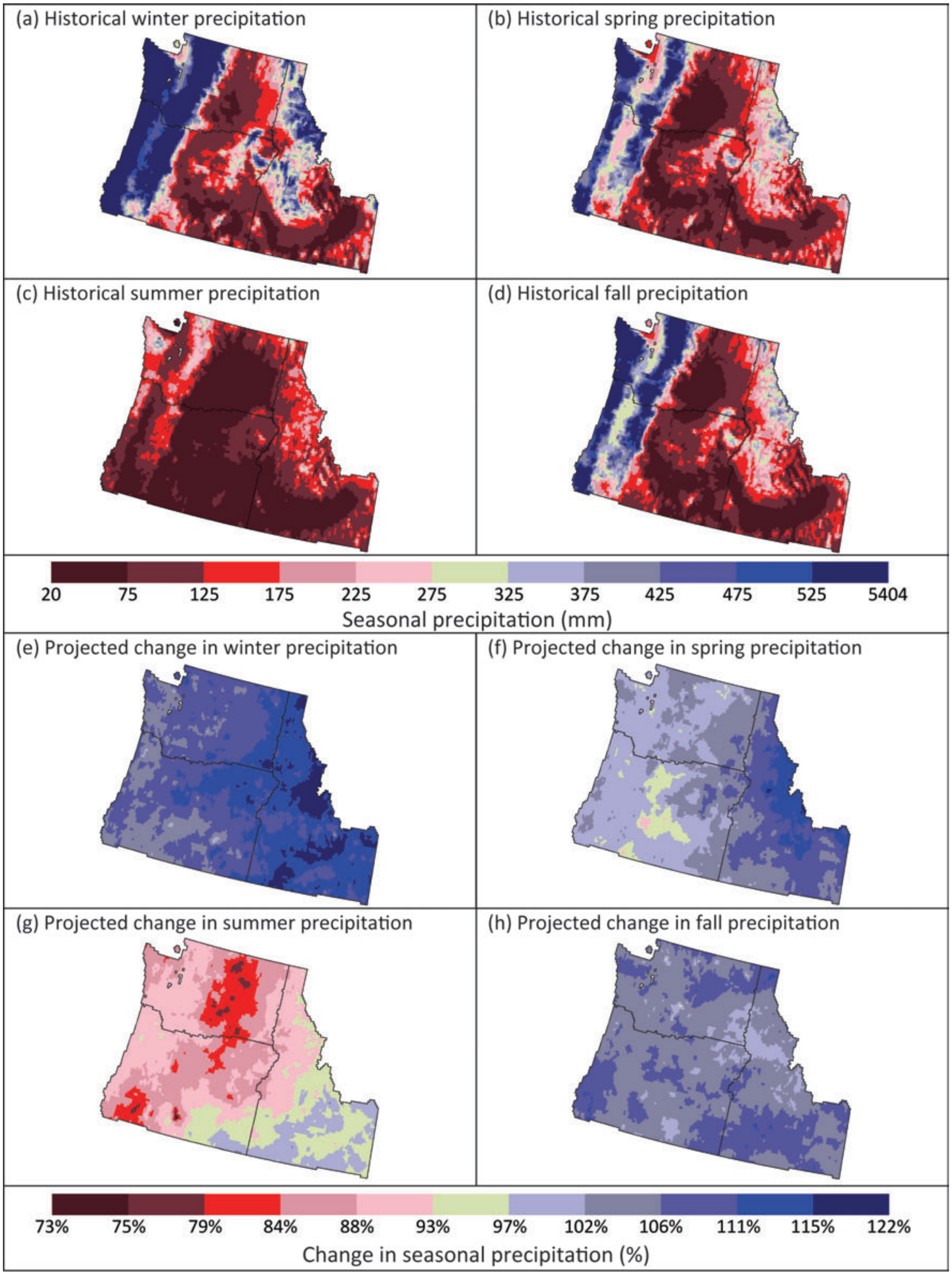

Figure 24. Seasonal observed precipitation (mm) based on PRISM climatology for the historical period (1961-1990) (a, b, c, and d) and projected change in precipitation (percent) by the 2060 period (2055-2064) for the A1B scenario (e, f, g, and h) for the Pacific Northwest region in the United States. Change for precipitation is the mean of changes in three climate model projections.

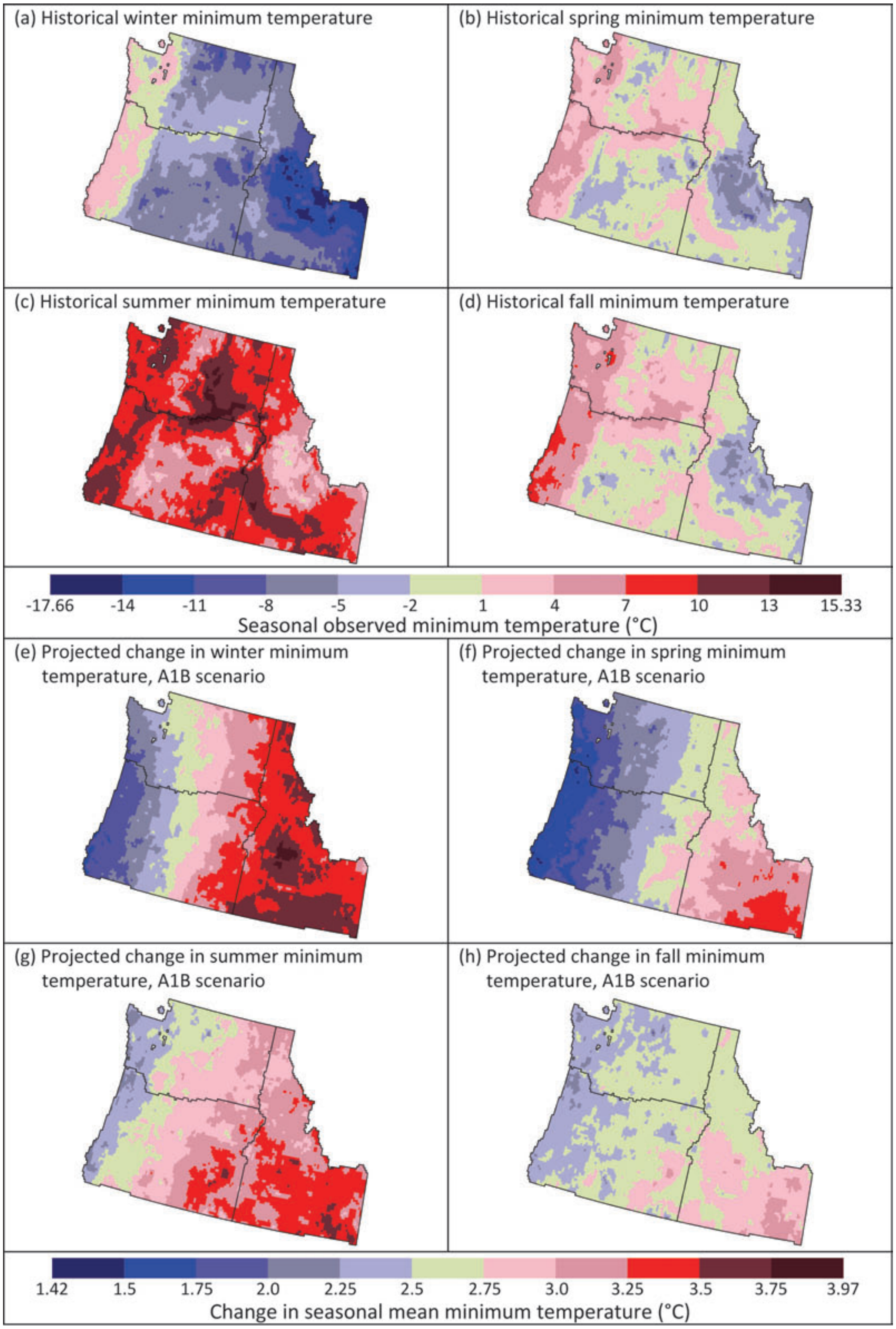

Figure 25. Seasonal observed minimum temperature (°C) based on PRISM climatology for the historical period (1961-1990): (a) winter, (b) spring, and (c) summer, (d) fall, and projected change in minimum temperatures (°C) by 2060 period (2055-2064) for the A1B scenario: (e) winter, (f) spring, (g) summer, and (h) fall. Change is estimated as the mean of change from the three climate model projections for the A1B scenario.

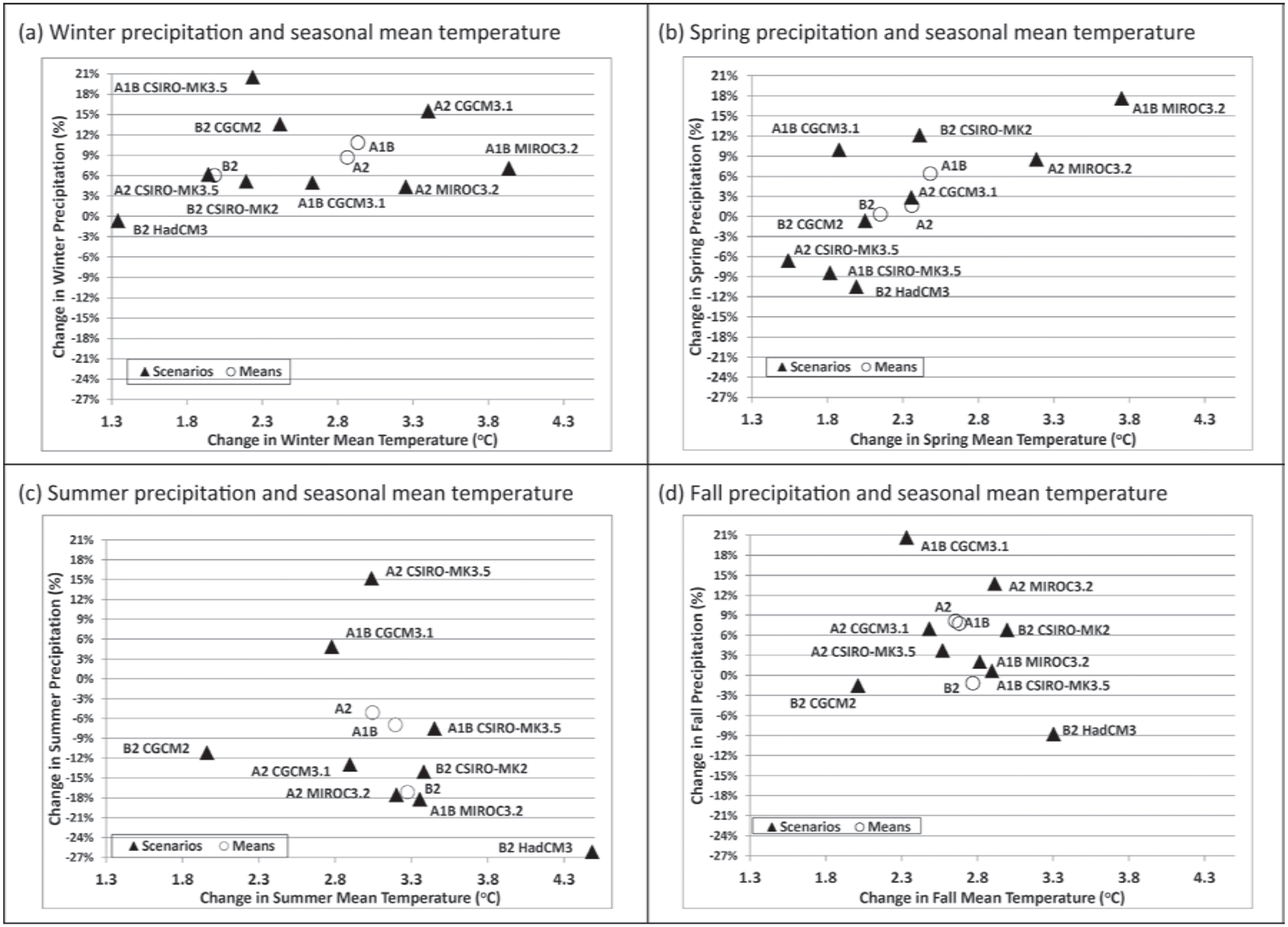

Figure 26. For the Pacific Northwest region, percent change in seasonal precipitation plotted against changes in seasonal mean daily temperature (°C) from historical period (1961-1990) to 2060 period (2055-2064) for nine projections (filled triangles) and three scenario means (open circles) for winter (a), spring (b), summer (c), and fall (d) seasons.

Mean projected temperature increases in winter are close to 3 ^{o}C (A2 and A1B), and smaller in fall and spring (Figure 26). Winter and fall projections generally resulted in increased precipitation. The largest relative increase in precipitation across all seasons is projected for the A1B scenario mean projection for winter at 11 percent above the 1961-1990 mean. Eight of the nine models project increases in winter precipitation, with only the HadCM3 B2 projecting a slight decrease. The CSIRO-MK3.5 A1B projection for winter was the greatest seasonal increase (20 percent) projected by an individual model across all seasons (Figure 26a). Only two models for the B2 scenario projected decreases in fall precipitation.

Seasonally, the individual model projections vary in their relative order for temperature and precipitation changes, suggesting caution is needed when identifying which scenario-model projection to use in an impact analysis. If a 'warmest' projection was the goal for selection, the A1B MIROC3.2 projection would be selected for winter and spring, but the B2 HadCM3 projection generates the largest increases in summer and fall temperature of all nine projections. The wettest projection for winter comes from A1B CSIRO-MK3.5 and the driest is the B2 HadCM3 projection; paradoxically both are also the two driest for spring.

We explore the nine projections for a block of grid cells surrounding the town of Lakeview in south-central Oregon in the context of the historical variability (Figure 27). Unlike Lamar, Colorado (Figure 23) or Grand Junction, Colorado (Ray and others 2008), the 10th and 90th percentile values of 50-year observations of historical monthly mean temperature and monthly total precipitation generally exceeds the projected changes. The historical precipitation pattern reflects the general Pacific Northwest pattern, with most of the precipitation coming during the fall-winter-spring months, resulting in a relatively dry summer. All nine projections remain mostly above the 20-year moving average ranges (vertical bars) for monthly precipitation with a few dropping below the mean during the summer months (Figure 27a). This pattern contrasts with that seen for Lamar (Figure 23a). For mean annual temperature, all nine projections are above the long-term monthly means for all months (solid black line) but, in contrast with the projections for Lamar, Colorado, they still fall within the 50-year range of variability (compare Figures 27b and 23b).

Northeast

Historical temperature patterns in the Northeast region (states of Maine, Vermont, and New Hampshire) vary spatially with annual means ranging from 1.5 ^{o}C at high elevations in the center of the region to around 9 ^{o}C along the southern coast (Figure 28a). Annual precipitation is generally greatest along the coastal areas, but ranges from about 800 mm in the extreme north and west to over 2000 mm at locations in the south (Figure 28b).

The spatial patterns in projected mean daily temperature are visually similar across the three scenario means (Figure 29a,b,c). By 2060, the northern part of Maine is projected to see temperatures in the range of 6.5 ^{o}C to 7.5 ^{o}C, reflecting a 3 to 4 ^{o}C shift above the historical ranges of 2.5 ^{o}C to 4.5 ^{o}C. Historical temperatures seen only in the very southern part of New Hampshire (8.5 ^{o}C to 9.5 ^{o}C) are projected to occur by 2060 as far north as central and coastal Maine (Figure 29a,b,c), where 1961-1990 means ranged from 5.5 ^{o}C to 6.5 ^{o}C.

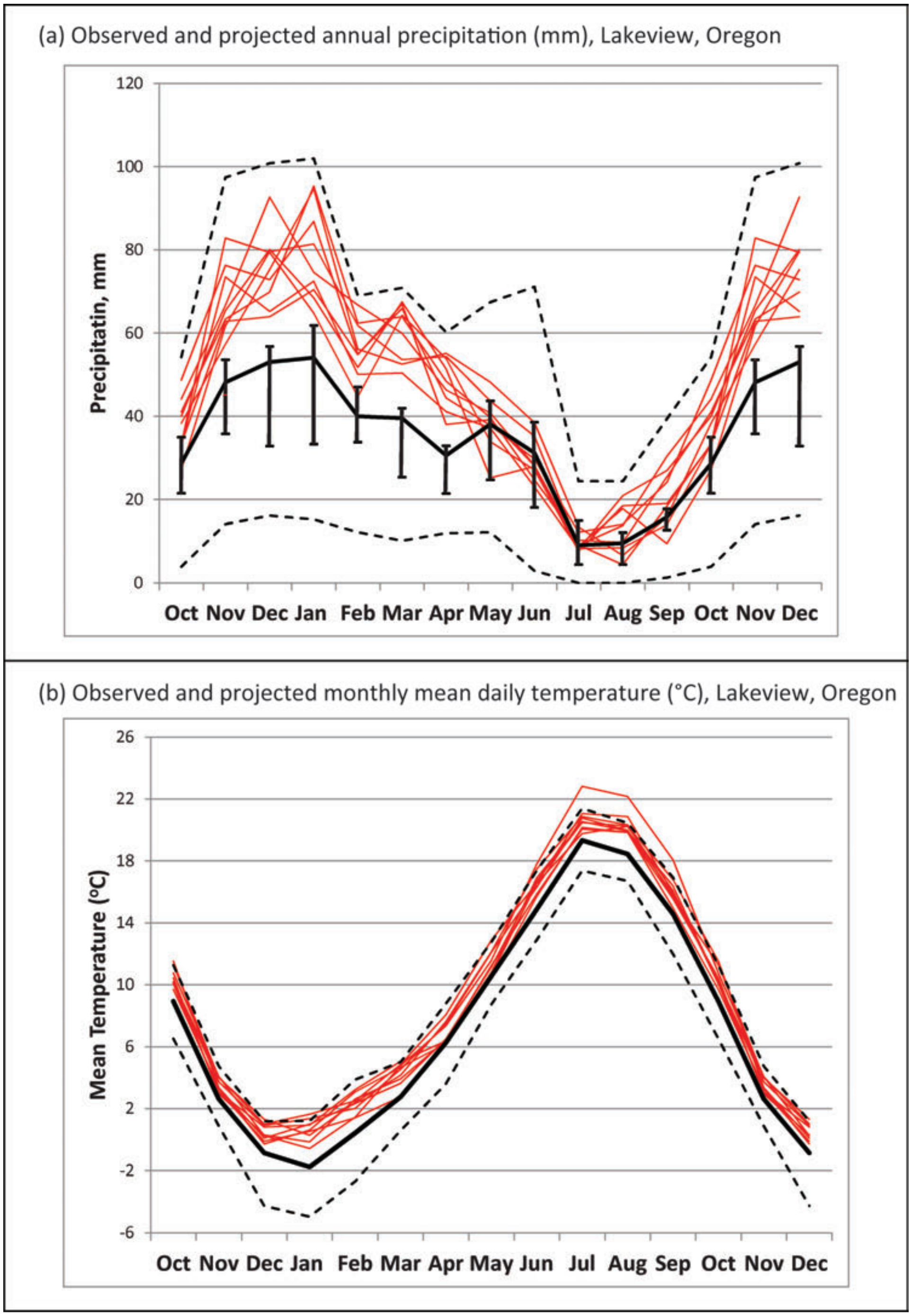

Figure 27. Observed annual precipitation (mm) (a) and monthly mean temperature (°C) (b) from the weather station at Lakeview, Oregon, compared with projections for 2060 (2045-2064) of annual precipitation (mm) and mean daily temperature (°C) for a 30 by 45 km region surrounding Lakeview. Projected monthly mean daily temperature (°C) and annual total precipitation (mm) (solid red lines) are from the nine scenario-model projections in this study. The historical monthly average (solid black) and 10th and 90th percentile values (dotted black lines) are based on all observations over the 1950-1999 period. The black bars on historical precipitation represent the 10th and 90th percentiles of the 20-year moving averages starting from 1897 through 2010.

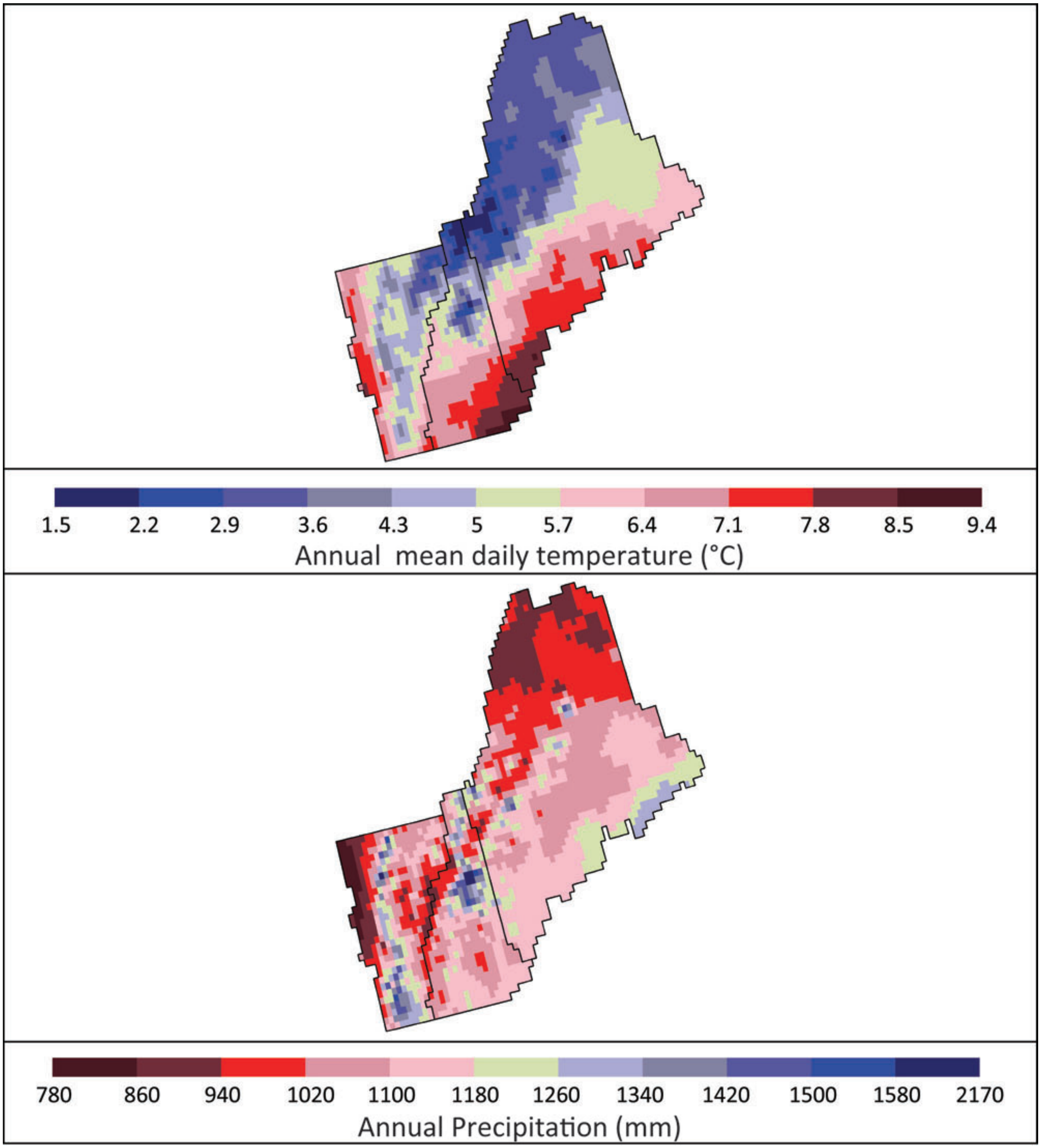

Figure 28. Annual mean daily temperature (°C) (a) and mean annual precipitation (mm) (b) for the historical period (1961-1990) based on PRISM climatology for the Northeastern region in the United States.

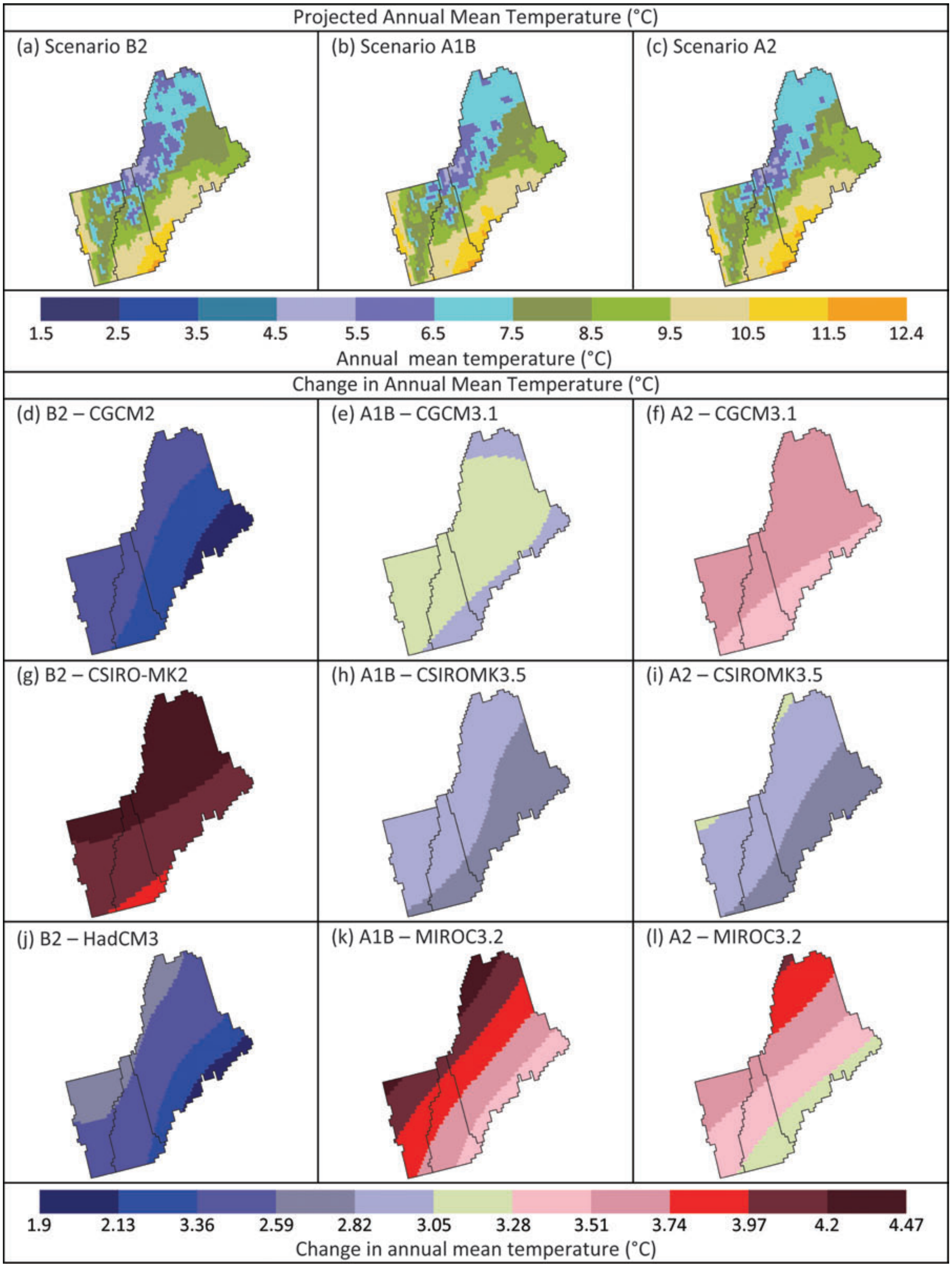

Figure 29. Projected annual mean temperatures (°C) for scenarios: B2, A1B and A2 (a, b, c), and change in mean daily temperature (°C) from historical period (1961-1990) to the 2060 period (2055-2064) as projected by models for B2 scenario: CGCM2, CSIRO-MK2, HadCM3 (d, g, j); for A1B scenario: CGCM3.1, CSIRO-MK3.5 and MIROC3.2 (e, h, k), and for A2 scenario: CGCM3.1, CSIRO-MK3.5, MIROC3.2 (f, i, l) for the Northeastern region in the United States.

All model projections indicate increases in annual mean daily temperatures of 1.9 ^{o}C or more (Figure 29d,e,f,g,h,i,j,k,l), in a very consistent spatial pattern, although the magnitudes of these increases vary inconsistently among the scenarios. For the B2 scenario, two models project changes less than 3 ^{o}C in annual mean daily mean temperature (Figure 29d, CGCM2 and Figure 29j, HadCM3). Conversely, the CSIRO-MK2 model with the B2 scenario (Figure 29g) projects the greatest increases of all models and scenarios in the Northeastern region. Increases in annual mean temperature by 2060 projected by individual models differ somewhat for A1B and A2: CGCM3.1 projects slightly larger increases than CSIRO-MK3.5 when forced by the A2 (compare Figure 29f with Figure 29i), while the MIROC3.2 projects markedly greater warming with the A1B (Figure 29k). The change in temperature figures provide a clearer picture of climate change in the northeastern region than the figures showing projected temperatures where the underlying patterns of historical temperature dominate the patterns (Figure 29b versus Figure 29e, h, and k, for example).

We explore the frequency distributions of summer mean daily minimum temperature for all models projections for the A1B and A2 scenarios, comparing the historical period (1961-1990) with the 30 years centered on 2060 (2045-2074) (Figure 30). The six projections are very consistent: historical minima range from about 6 ^{o}C, but by 2060, the lowest temperatures are projected to exceed nearly 9 ^{o}C. At the higher temperature end of the distributions, historical summer mean temperatures rarely exceeded 16 ^{o}C but these temperatures are projected to increase to around 20 ^{o}C by 2060. Consistent with other results, the A1B projections for the 2060 period show warmer temperatures overall than the A2 projections (compare Figure 30a with Figure 30b). Among the different models, the overlap between the historical and the projected is greater for CGCM3.1 and CSIRO-MK3.5 than for MIROC3.2.

Developing Composite Indices with the Downscaled Climate Projection Data: Aridity

Much of the western United States is classified as hyper-arid, arid, and semi-arid (Figure 31a) for the 1971-2000 period. Areas with higher rainfall, such as the Pacific Northwest region, are classified as humid. When the aridity classes are estimated for the 2060 period, relatively few grid cells in the West increase in aridity (where increase is defined as the shift into at least one more arid class). However there is a major consensus (seven or more projections agree) that large areas in the Midwest will increase in aridity (Figure 31b). Areas within the eastern United States that are projected to become more arid include the western parts of New York State, Pennsylvania, and Ohio, following areas along the Ohio River and to east of where the Ohio River meets the Mississippi River, including eastern Arkansas, north and central Missouri, and Alabama. The pattern in the western United States reflects the complex topography of this region.

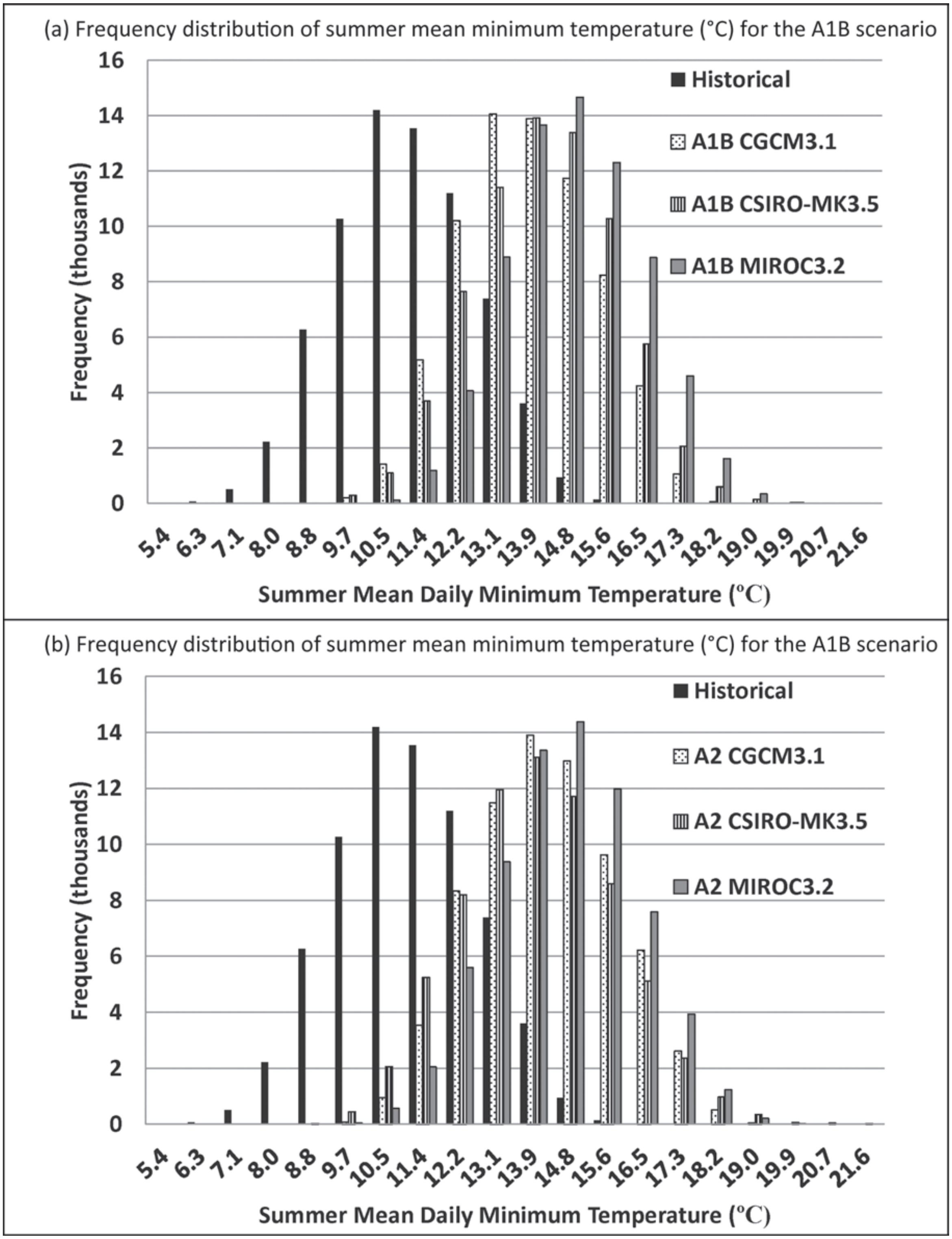

Figure 30. Frequency distribution of summer mean minimum temperature (°C) across the Northeastern region for the historical period (1961-1990) based on PRISM climatology and projected for the 30-year period surrounding 2060 (2045-2074) by three climate models using the A1B scenario (a) and the A2 scenario (b).

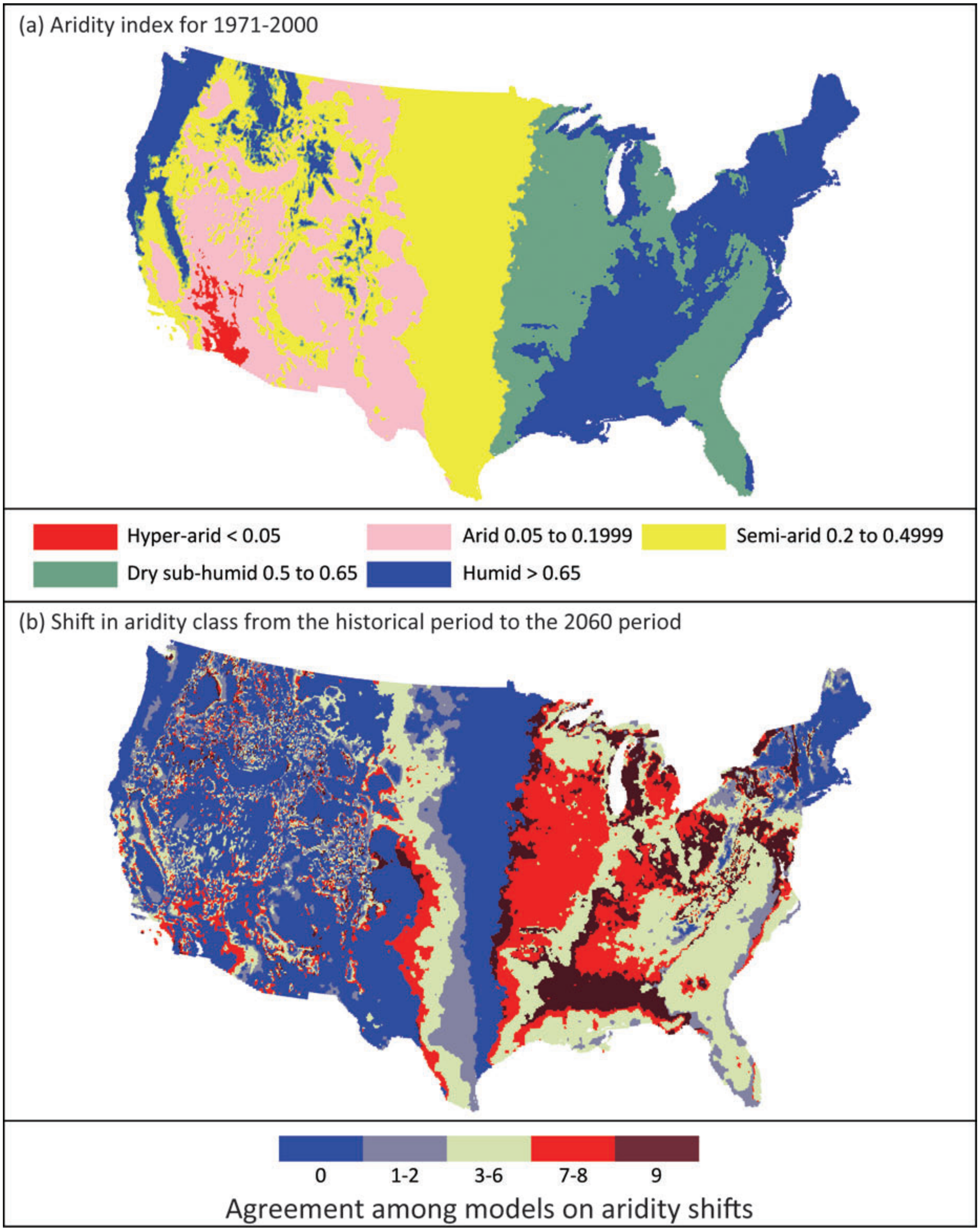

Figure 31. Aridity in the conterminous United States over the 1971-2000 period based on the UNEP aridity index (a) and agreement on projected changes in the aridity index by the 2060 period (2055-2064) where the shift in classification is to a more arid zone (could be more than 1 aridity zone). The scale is the number of projections that agree. If all nine agree, the grid is coded 9.

County-Level Projection Data

The gridded climate data (historical, projected) were aggregated to county level to help facilitate interpretations at that scale (Figures 32 and 33). Typically, such data will be valuable for county scale analyses, such as economic or recreational analyses where the primary data are also available at the county spatial scale. One caution about summarizing county climate data to larger spatial scales is that, given that counties vary greatly in size across the conterminous United States, these data must be area-weighted if they are to be used to calculate regional or conterminous U.S.-scale averages. The gridded data will often be more appropriate to explore regional or national climate dynamics.

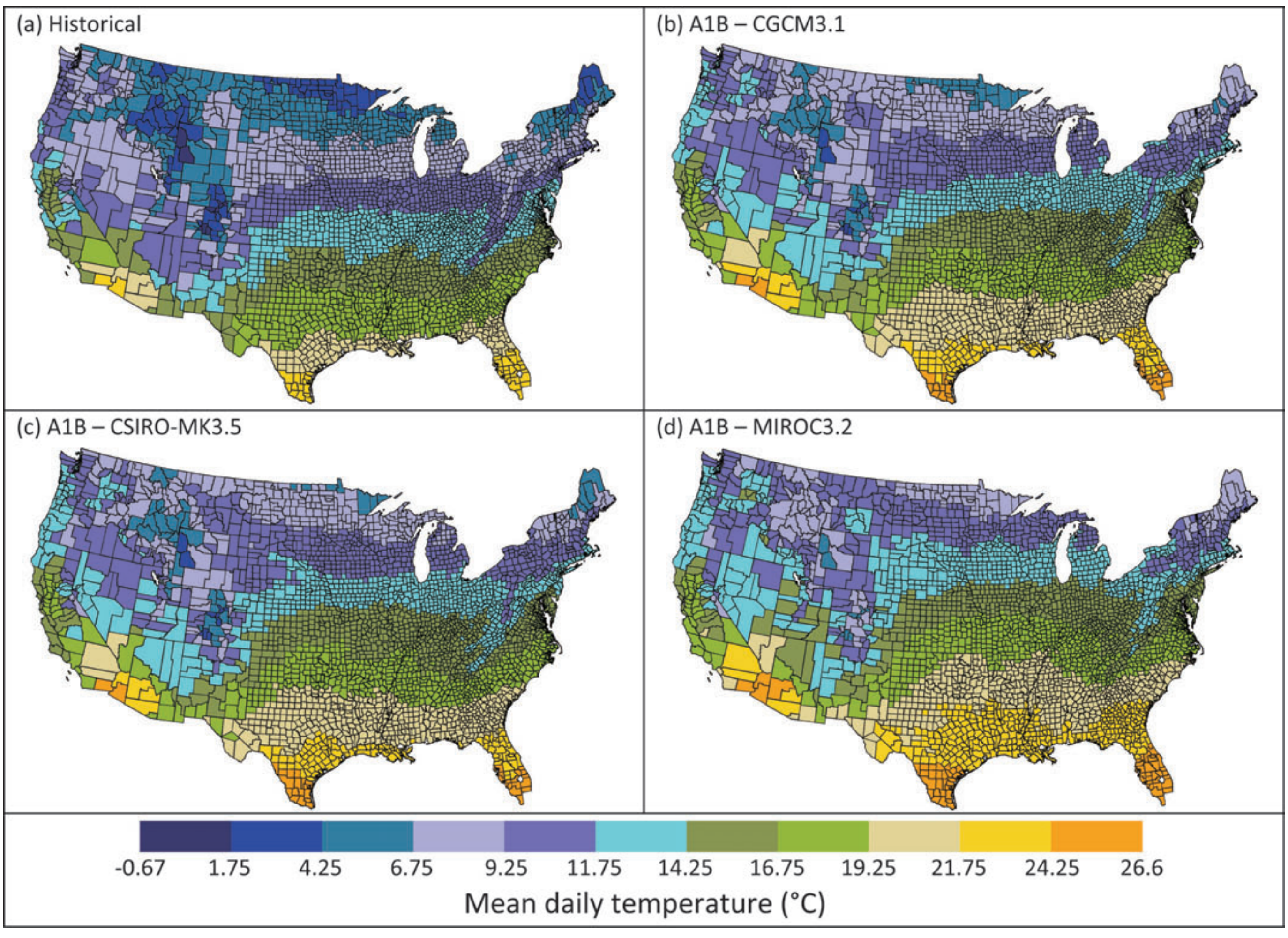

Figure 32. Observed mean daily temperature (°C) for the historical period (1961-1990) based on PRISM climatology (a) and projections of mean daily temperature (°C) based on the A1B scenario for the 2060 decade (2055-2064) at the county spatial scale for conterminous United States. The three models projecting the A1B scenario are (b) CGCM3.1, (c) CSIRO-MK3.5, and (d) MIROC3.2

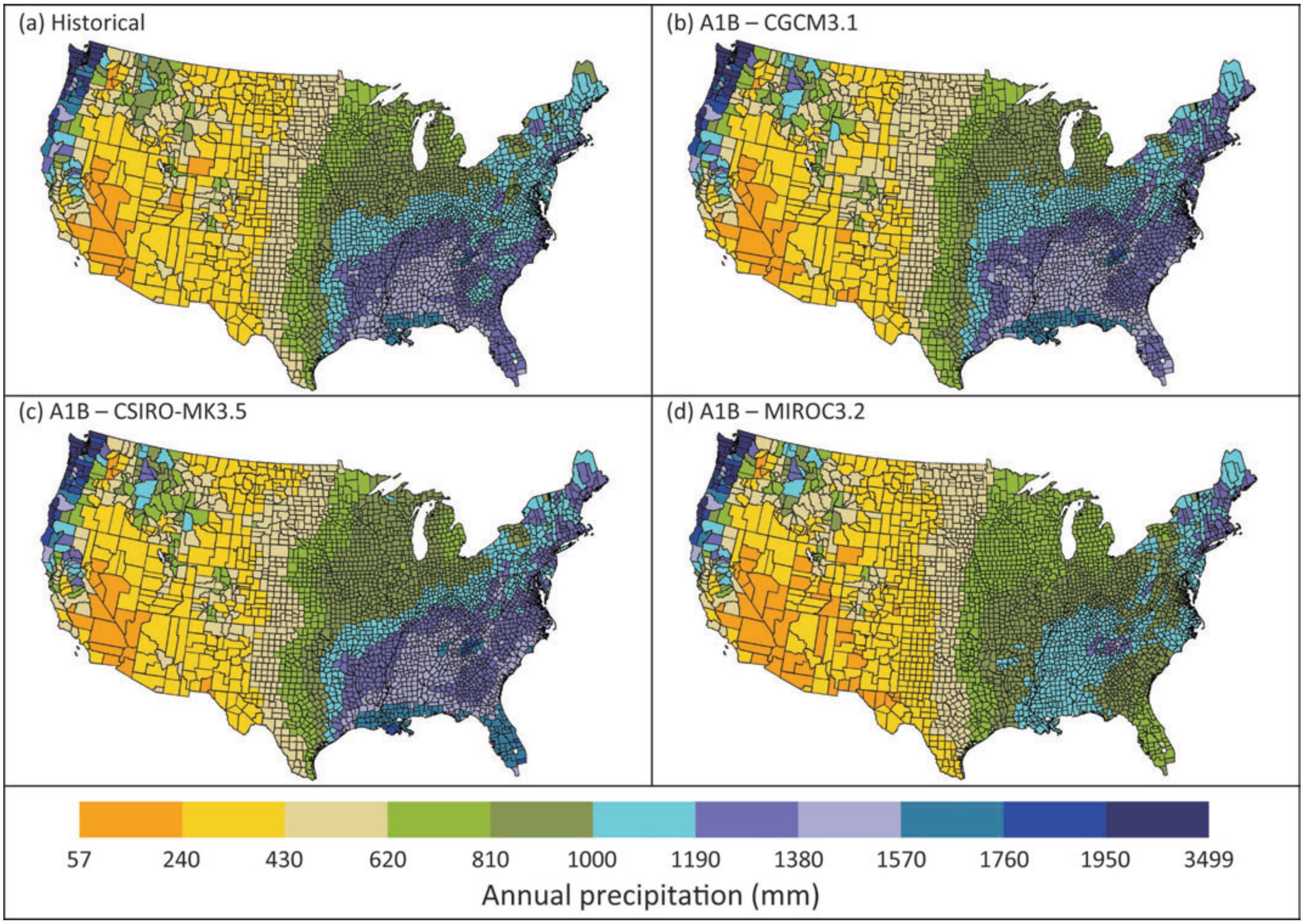

Figure 33. Observed annual precipitation (mm) for the historical period (1961-1990) based on PRISM climatology (a) and projections of mean annual precipitation (mm) based on the A1B scenario for the 2060 decade (2055-2064) at the county spatial scale for conterminous United States. The three models projecting the A1B scenario are (b) CGCM3.1, (c) CSIRO-MK3.5, and (d) MIROC3.2

Discussion

Model Robustness

The reliability of individual climate models has been explored by asking many different questions, including: How well do they simulate historical climate or extreme events? Do they capture well-known global climate phenomena such as the El Nino-Southern Oscillation or transient climate phenomena? How sensitive are the models to changes in atmospheric chemistry? How do results from different models compare in projecting large-scale patterns of climate change (e.g., vertical patterns (atmospheric) of temperature change, land-sea contrasts)? A number of complicated metrics have been developed to integrate and synthesize these many individual tests. Two points are important here. First, there is a growing sense of the challenge to identify the best model. Gleckler and others (2008) note:

> Finally, in spite of the increasing use of metrics in the evaluation of models, it is not yet possible to answer the question often posed to climate models: "What is the best model?"

Second, Gleckler and others (2008) concluded that the answer to the above question *"almost certainly will depend on the intended application."* Mote and others (2011) identify this consideration as the first on their list of criteria for selecting climate scenarios:

> 1) Understand to which aspect of climate your problem or decision is most sensitive (e.g., which climate variables, which statistical measures of these variables, and at what space and time scales).

We suggest that the reader consider carefully the intended application and how climate affects that renewable resource, management strategy, or policy under development. Such information will help identify which climate variables and projections will be most useful.

The RPA climate projections reported here were developed specifically to support U.S. national-level renewable resource analyses exploring the influence of drivers of change such as population dynamics, economic growth patterns, and climate (U.S. Forest Service 2012a,b). These climate data are being used as input both for new renewable resource models under development and existing climate impact models. Socioeconomic analyses typically use county-level data, so this data set is available at the U.S. county scale and at the 5-arcminute grid scale. The climate variables identified for this analysis were monthly mean daily values of maximum and minimum temperature and monthly total precipitation. We discuss further potential uses of these RPA climate projection data in the next section.

Here, we review studies that have contrasted and compared the climate models used in this study with observed climate data, and with the dynamics of other climate models over small and large regions, over historical periods and with respect to future periods. Because use of these data focuses on the United States, we review literature focused on that geographic area as we are relying on the availability of tests that are relevant to our situation, e.g., comparisons focused on North America rather than other parts of the globe.

Climate Sensitivity

Climate sensitivity is a metric that has been used to quantify the potential degree of warming at the global scale associated with a doubling of atmospheric concentrations of greenhouse gases. Using observed climate data and proxy data for periods before the modern instrument record (e.g., ice cores), this metric explores the sensitivity of the global climate to past changes in greenhouse gases or other radiative forcings. Controlled experiments can be carried out with each climate model to assess the simulated climate sensitivity and to compare the sensitivities of different models to changes in the same forcing. Equilibrium climate sensitivity is defined as the equilibrium change in the annual mean global surface temperature following a doubling of the atmospheric equivalent CO_2 concentration (IPCC 2007b).

Randall and others (2007) and Meehl and others (2007b) review the different methods used to determine the climate sensitivity: (1) analysis of the historical transient evolution of temperature (observed surface and upper air temperatures, ocean temperatures, proxy data), and (2) experiments using current global climate models. Based on these different lines of evidence, Meehl and others (2007b) conclude that the global mean equilibrium warming for a doubling of equivalent CO_2 concentration, or equilibrium climate sensitivity, is likely to lie in the range of 2 ^oC to 4.5 ^oC, with a most likely value of about 3 ^oC. In other words, if GHG emissions were to stabilize at a doubling of pre-industrial levels of CO_2, then the global mean temperature is likely to increase and eventually stabilize at a level about 3 ^oC above the long-term global average temperature that would have been measured if GHG concentrations had been maintained at pre-industrial levels. The range (2 ^oC to 4.5 ^oC) reflects the variability in the observed data and modeling studies as well as current knowledge about the processes that determine global climate.

The Multi-Model Data (MMD) study explored the equilibrium climate sensitivity of 23 global climate models (Randall and others 2007). The mean climate sensitivity in this modeling study was 3.3 ^oC with a 5 to 95 percent range of 2.1 ^oC to 4.4 ^oC. Models with greater climate sensitivity project greater warming per CO_2 doubling when compared to models with a lower sensitivity. Three models used here were included in the MMD study, namely CGCM3.1(T47), MIROC3.2(medres), and HadCM3. Their climate sensitivities were about and above the mean; CGCM3.1(T47) had a climate sensitivity of 3.4 ^oC and MIROC3.2(medres), 4.0 ^oC, and HadCM3, 3.3 ^oC. The CGCM3.1(T47) model and the HadCM3 model are close to the 3.3 ^oC mean of all models analyzed. In this study, we used the CSIRO-MK3.5 whereas the MMD study included the earlier CSIRO-MK3.0 with a climate sensitivity of 3.1 ^oC. Climate sensitivity was also discussed in the IPCC's Third Assessment Report by Cubasch and others (2001). They focused on 15 models in active use in the 2001 IPCC assessment and summarized the equilibrium climate sensitivity as having a mean of 3.5 ^oC and a standard deviation of 0.9 ^oC. The three models used here were included among those 15 models, but equilibrium sensitivities were provided only for CSIRO-MK2, 4.3 ^oC, and HadCM3, 3.3 ^oC.

New studies using observed and proxy data or modeling experiments contribute to our understanding of climate, and climate sensitivity. Randall and others (2007) note that the climate sensitivity of some climate models changed when newer versions used in the AR4 were compared to earlier versions of the same GCMs used in the TAR. Increased sensitivity was reported for the more recent UKMO-HadGEM1 compared to the HadCM3 model (used for B2 scenarios here). Decreased sensitivity was reported for the CSIRO-MK3.0 model compared to the CSIRO-MK2 (used for B2 scenarios here) while sensitivity of the CGCM3.1(T47) (used here for A1B and A2 scenarios) remained relatively unchanged from the earlier version CGCM1. Randall and others (2007) conclude that cloud radiative feedbacks are the primary source of inter-model differences in climate sensitivity, although water vapor and surface albedo feedbacks are also important. Similarly new analyses of observed and proxy data explore further the transient evolution of temperature in response to past events. Mote and others (2011) note that "most studies estimate that there is at least a 5 percent chance that the sensitivity exceeds 7 ^oC to 9 ^oC for a doubling of atmospheric CO_2" (see also Hegerl and others 2007). No climate model in the CMIP3 archive, where we obtained our projections, represents such a low-likelihood, high-sensitivity future climate. Mote and others (2011) also suggest that a "full description of response uncertainty would also involve uncertainties in the time-evolving response, and in responses at subglobal scales and of variables other than temperature, which may be proportional to the climate sensitivity, whether on global or regional scales."

We can conclude that the climate models used for the RPA Scenarios have climate sensitivities close to or slightly above the mean of the ranges determined for models used in the IPCC's Third and Fourth Assessment Reports. For the B2 scenario, the HadCM3 model falls slightly below the mean and the CSIRO-MK2 model above the mean and both within the range identified by Cubasch and others (2001). For the A1B and A2 scenarios, the CGCM3.1(T47) and the HadCM3 fall on the mean or just above and the MIROC3.2 falls above the mean but well within the range identified in Randall and others (2007). The CSIRO-MK2 and the MIROC3.2 models clearly have higher sensitivity but are still well within the expected ranges. The higher sensitivity of the MIROC3.2(medres) model to increasing greenhouse gas emissions caused it to produce the warmest projections for some regions in this study, particularly the southern United States. Price and others (2011) found the results from MIROC3.2 to be very similar to or even slightly cooler than the U.S. National Center for Atmospheric Research (NCAR) CCSM3 model when applied to Canada; Joyce and others (2011) found these similarities did not extend to the southern United States, where MIROC3.2 projects distinctly more warming than two other climate models. It is worth noting that MIROC3.2 has been shown to perform well according to studies discussed in this section, so it should not be dismissed simply because it is more climate-sensitive than most other GCMs applied to North America (see next section for further discussion of this point).

Model Agreement with Observations Globally and Regionally

Comparing the dynamics of global climate models with the dynamics of observed climate is an important step to determine model confidence (Reichler and Kim 2008), yet what to compare has been a much-discussed topic in the literature. Gleckler and others (2008) state that "it remains largely unknown what aspects of observed climate must be correctly simulated in order to make reliable predictions of climate change." In other words, accurate modeling of the current mean and variability of one climate variable, for example precipitation, may or may not imply that the same model can make reliable temperature or precipitation projections of future climate. And while a suite of climate variables can be compared with observed data, Gleckler and others (2008) warn against using a single index (composite of many climate variables) to gauge model performance. Further, individual models, their different versions, different climate variables (precipitation versus zonal wind), historical periods (100 years or 20 years), and the region of focus (global or individual regions) all influence the ranking of performance among climate models (Gleckler and others 2008). For example, when temperature versus sea level pressure is used to establish performance for multiple models, the model rankings differ. Models that simulate the 20th century well for the Northern Hemisphere (north of the tropics) can have lower skill in the tropics (Gleckler and others 2008). The observed climate record also has challenges: a lack of reliable and consistent observation over time in some regions of the world; and for some model output variables, atmospheric processes occurring at temporal or spatial scales that are not monitored or monitored routinely (Reichler and Kim 2008). Nonetheless, comparisons have been made to satisfy a number of different interests. Climate modelers are often interested in comparing the performance of multiple models whereas users of climate projection data may be more interested in the performance of a small number of carefully selected models applied to a particular region.

Reichler and Kim (2008) quantify agreement between the global results and observations for 57 models representing three generations of climate models. Using 14 climate variables and late 20th century simulations, they develop an aggregated index by first computing a normalized error variance of each climate variable (e.g. air temperature, zonal wind, precipitation, specific humidity, etc.) as compared to the observed interannual variance and averaging the grid results globally. The final model performance index is developed by taking the mean over all climate variables using equal weights. In this index, values greater than 1.0 represent underperforming models (i.e., relative to the mean) and values less than 1.0 represent models that agree with observed data better than the mean. Four of the six models used in our study were included in the analysis by Reichler and Kim (2008). Three of those models have an index less than 1.0, namely HadCM3 (CMIP3 and an earlier CMIP intercomparison project), CGCM3.1(T47), and MIROC3.2. In our study, we selected projections from the CSIRO-MK3.5 model version, but the Reichler and Kim (2008) study reported only on the CSIRO-MK3.0 version, which also achieved an index less than 1.0. Reichler and Kim (2008) concluded that the most recent generation of climate models, represented in AR4, would generally simulate present-day climate more realistically than the models associated with IPCC TAR or earlier assessments. Models used to simulate response to the B2 scenario in this study came from the TAR generation of models; this choice reflected the objective to have a breadth of socioeconomic futures in the RPA Assessment. Of these TAR-generation models, Reichler and Kim (2008) did not report on the CGCM2, while the HadCM3, previously mentioned, achieved an index of less than 1.0, and the CSIRO-MK2, an index of greater than 1.0

Global and regional comparisons were made by Gleckler and others (2008). Here we focus on their results for the Northern Hemisphere (north of the tropics). They compared the mean values of 26 climate variables from the CMIP3 20th century simulations (20C3M) of 22 climate models with observed data over the 1980-1999 period. Relative model performance was ranked using a normalized root mean square error for each model and the mean of the relative errors of each climate output variable for all of the models considered. According to their analysis, the HadCM3 model performed better than the typical model for 18 of the 26 climate variables analyzed, including air temperature at two heights (850 and 200 hectopascals) and precipitation. The CGCM3.1(T47) model performed better for 17 climate variables, also including air temperature at two different heights (850 and 200 hectopascals) and precipitation. The MIROC3.2 model performed better than the typical model for 13 climate variables, including temperature at 850 hectopascals and precipitation. The Gleckler and others (2008) study reported only on the CSIROMK3 model (CSIRO-MK3.5 was used in our study); CSIROMK3 performed better in six climate variables, including precipitation and temperature at one height.

While good performance in capturing mean observed values provides some confidence in a model, Gleckler and others (2008) suggest that other aspects of climate dynamics may also be important to assess. Using two indices, they compare ability of each of 22 models to capture interannual variability (variability skill) as well as their ability to capture the mean annual cycles (climate skill) for the Northern Hemisphere (north of the tropics). The UKMO HadCM3, and the CGCM3.1(T47) had relative errors less than the typical model for both variability skill and climate skill. The CSIRO-MK3 model performed better than the typical model for climate skill but less so for variability skill. Conversely, the MIROC3.2(medres) model was less skillful than the typical model in both climate skill and variability skill. Given caveats expressed by Gleckler and others (2008) concerning indices and performance, the key point in this comparison is that the performance based on annual means does not imply an equal skill in capturing climate variability.

Radic and Clarke (2011) focused on North America and the western region of North America, for the 1980-1999 period in their comparison of 22 models from the CMIP3 data base. Models that performed well over North America also performed well for the western region of North America (both United States and Canada). As with other studies, model ranking varied with the metric used. For example, while most models simulated the frequencies of daily anomaly patterns associated with the 20-year average daily pattern, few models could reproduce occurrences of characteristic daily weather patterns in the reference database on a seasonal basis. Using the variety of metrics studied, the top five performing models are ECHAM5 (Max Planck Institute-Ocean Model), MIROC3.2(medres), MIROC3.2 (high resolution), CGCM3.1(T47), and CGCM3.1(t63) (Radic and Clarke 2011, Table 5). This list includes two of the models used in this study: MIROC3.2(medres) and CGCM3.1(T47).

Regional responses of the 23 models in the MMD study (Randall and others 2007) were compared to a global historical observed climate data set (Christensen and others 2007). For the western North American region (i.e., western Canada and the western United States), the median bias of all models in estimating annual mean temperature was –1.3 ^{o}C, i.e., the climate models generally estimated annual temperature to be cooler than historical observations. Bias of the models for central North America region was –0.5 ^{o}C, and for eastern North America, –1.2 ^{o}C. Bias in the individual climate simulations for the 20th century has been attributed to many limitations in the models. Regardless of the causes, this bias was removed (as far as possible) in the downscaling process used in our study, by subtracting out the means of the climate model estimates for the 1961-1990 period and using historical climate data for the same period at the 5-arcminute scale to provide the spatial context when constructing the future projections.

We can conclude that the models used to create future climate projections for the AR4 are, in general, likely to simulate present climate more accurately than the models used in the TAR report. Further, the AR4 models used in this study perform reasonably well when compared with many other AR4 models, and several independent studies indicate, depending upon the particular metrics used for comparison, that the models used here were in the top performing ranks. Of the models used for the B2 scenario in our study, HadCM3 is likely to be a more accurate model with respect to historical climate estimations than the CSIRO-MK2 model while little information is available to assess the performance of the CGCM2.

Model Agreement with Observations Regionally

For the specific use of this data in the national analysis of renewable resources, it was critical to have a consistent data set at the national level. Hence, the climate projections developed here were used for all regions of the United States in the RPA analyses, in contrast to other studies using different climate models for different areas of the United States. Users of the RPA climate data are likely to be interested in the ability of these models to simulate regional climates. Hence, we review a variety of efforts that have compared different models or selected climate models for their analyses based on some criteria.

Focusing on the Pacific Northwest, Mote and Salathe (2009) used a number of metrics to compare the performance of 20 climate models hindcasting 20th century climate for an area including Washington, Oregon, Idaho, western Montana, and a small slice of adjacent states in the United States and British Columbia in Canada. Three of the models used in this study were included in the Mote and Salathe comparison: CGCM3.1_t47, MIROC_3.2 medium resolution, and HADCM (in our terminology CGCM3.1(T47), MIROC3.2(T42), and HadCM3 respectively). Mote and Salathe (2009) compared the annual mean difference, or bias, between model output and the historical climate data for 1970-1999, and found that all models have a cold bias (mean of –1.8 ^{o}C) in replicating the historical mean annual temperature. Two models used in this study (CGCM3.1(T47) and MIROC3.2(medres)) showed a mean bias very similar to the overall model mean bias. Five of the 20 models had smaller biases than the two used here (i.e., they replicated the historical temperature of the region more closely). With respect to precipitation, CGCM_t47 (CGCM3.1(T47) in this study) was one of the top five models with the smallest bias. All 20 models had a wet bias in the Pacific Northwest, ranging from less than 10 mm to more than 60 mm (meaning mean annual precipitation simulated by each model exceeded the observation by any amount within this range). Mote and Salathe (2009) also compare the 20th century trend of each model's annual mean temperature for the Pacific Northwest with the observed trend calculated from data from the U.S. Historical Climate Network. The observed trend was 0.8 ^{o}C over the last 100 years compared to 1.1 ^{o}C for CGCM3t_47 and only 0.1 ^{o}C for MIROC32. Finally, they used a Taylor diagram to compare the performance of all 20 models in simulating sea level pressure, precipitation and temperature of a larger geographic domain including much of the western United States, Canada, and the Pacific Ocean (Figure 6 in Mote and Salathe 2009). Overall, CGCM3.1(T47),which was used in this study, ranked the best, and MIROC32, also used in this study, ranked 9th out of the 20 models.

For the Northeastern United States, Hayhoe and others (2007) used nine climate models, including CGCM3.1 and HadCM3, both used in this study. They also used results from MIROC(medres), but no model version number was provided. They analyzed the ability of the nine models to reproduce historical climate and concluded that most were able to reproduce 100-year and 30-year trends in annual temperature. Annual temperatures over the 1900-1999 period have risen 0.08 ^{o}C, ±0.01 ^{o}C per decade, compared to the nine model ensemble average of 0.08 ^{o}C, ±0.06 ^{o}C per decade. For projections of future temperature trends, inter-scenario and seasonal differences were consistent across 23 simulations (scenario and model combinations): temperature increases were projected to be greater under higher, as compared to lower emissions scenarios, with equal or greater increases in summer relative to winter; winter precipitation was projected to increase by 10-15 percent and summer precipitation showed either little change or a decrease. Hayhoe and others (2007) also noted that regional processes may be acting to enhance warming trends in the northeastern United States relative to the global average in a way not captured by these global-scale models.

Users of climate projection data may also be interested in studies that have explored the performance of the climate projections for specific resource uses. This literature is expanding and we point the reader to a few key papers. Brekke and others (2008) evaluated the ability of 17 climate models from the CMIP3 data base for their credibility in hydroclimatological risk assessments. While they identified specific models as more capable of recreating some aspects of 20^{th} century climate, when several of 19 metrics were combined (as in an index), all model performances were comparable among the 17 models. Anandhi and others (2011) analyzed the performance of 19 climate models from the CMIP3 database for their ability to estimate snow water equivalent in New York watersheds. They included details on which model version and realization were used in the study and categorized the models into three classes, based on skill in capturing snow water equivalent. Recognizing the importance of low-frequency variability in rainfall in water resource applications, Johnson and others (2011) assessed the ability of 23 climate models to represent interannual variability and found significant differences in performance.

Models used in this study have been used in many studies exploring the effects of climate change. Rogers and others (2011) used climate projections from MIROC3.2(medres), HadCM3 (both used in this study), and CSIRO-Mk3 forced by the A2 scenario to explore the effects of climate change on vegetation in the Oregon-Washington area using the MC1 dynamic vegetation model. Their representative range of projected future temperatures was the rationale for selecting these three climate models. For California, Cayan and others (2006) identified three climate models that captured a range of climate sensitivities: NCAR Parallel Climate Model (low climate sensitivity), Geophysical Fluids Dynamics Laboratory CM2.1 (medium sensitivity), U. K. Hadley Centre Climate Model, version 3 (with higher sensitivity). Zhu and others (2011) used three climate models in a study of the potential effects of climate change on carbon dynamics in the Great Plains, including MIROC3.2(medres) and CGCM3.1, though they did not state which resolution; the medium resolution CGCM3.1 model was used in this study.

Use of the Climate Projection Data

Change Factor Data

We use the change factor data developed for the conterminous United States by Price and others (2011a) and Joyce and others (2011); these data can be found online (http://www.fs.usda.gov/rds/archive/, Price and others 2011b). Change factors have been developed for Canada (Price and others 2011a). Change factors were also developed for Alaska (Joyce and others 2011) and can be found online (http://www.fs.usda.gov/rds/archive/, Price and others 2011c). The historical climate data used in this study were based on the PRISM historical gridded climatology (available: http://www.fs.usda.gov/rds/archive/, Coulson and Joyce 2010a,b). The change factor data have utility to users who have their own historical climatology or wish to use one of the many historical climatologies that are available, such as VEMAP

(Kittel and others 2004), Rehfeldt (2006), and DAYMET (see http://www.daymet.org/default.jsp). Price and others (2011a) and Joyce and others (2011) used the North American climatology developed by McKenney and others (2006b, 2011) and the same climate model data sources used in the present study to develop projections for Canada and the continental United States, including Alaska.

Climate Projection Data

Projections of possible climatic outcomes are not *predictions*, but should be considered as equally likely alternative scenarios of future climate. The process of creating these data begins with global climate models shown to give reasonably correct representations of observed climate at very coarse scales, as described in the previous section. Bias in each model's ability to simulate 20th century mean values is removed by converting all data to "change values" calculated relative to a reference period (taken in the present study as 1961-1990), and then downscaled to a 5-arcminute grid. These change values (ratios or differences) are then applied to the historical climatology to produce data that capture the spatial characteristics of observed climate variables combined with the changes in these variables projected by each climate model. Each projection attempts to capture trends that would occur under a given set of socioeconomic assumptions (i.e., the IPCC SRES emissions scenarios). The data should not be considered as forecasts, but as a single plausible outcome for a given set of assumptions.

With each step in the modeling process and in the downscaling process, assumptions enter into the analysis (Meehl and others 2007b; Price and others 2011a). Each climate model has an underlying set of assumptions/caveats, e.g., in the parameterizations of "sub-gridscale processes" such as cloud dynamics. Further assumptions are captured in their individual input data, such as the representation of global soils and vegetation types (Randal and others 2007). When the climate model simulations are completed, the output data can be viewed as estimates of the average of each prognostic variable over a large area. The process of decomposing these "averages" to a finer scale incorporates additional assumptions, while basing the work on station data gives a greater sense of realism. Station data are not necessarily the "truth" as there are underlying issues with data quality, measurement errors, and missing data. Further, station data are not uniformly distributed across a heterogeneous landscape. The interpolation used to bring these data to a common grid is itself a form of modeling. It is important to recognize these underlying assumptions and limitations when using the data.

While the data are presented at the grid level, these data are modeled and interpolated data from coarser grids. As such, they probably should not be viewed as a precise estimate of the grid average. Rather the data are best viewed as a point value within the grid, much as station data are point-based measurements of many possible outcomes in an area and not necessarily the average value for the area. Using these grid level data in models is appropriate; however, reporting of trends is only recommended across an aggregation of grid cells.

With these nine model projections presented here, researchers can examine the effects of alternative climate futures in their own assessment methods (or models). Users should also keep in mind that each scenario reflects a set of assumptions about global population growth and economic development. Three climate model projections are available for each of the three IPCC SRES scenarios. We recommend that each projection be used as separate input to the resource model(s); such an approach allows the researcher/analyst to capture a range of possible outcomes from the effects of changes in temperature and precipitation as well as from the socioeconomic drivers that determine the projected greenhouse gas emissions levels. Results from multiple simulations of the resource model could then be averaged if the analysis warrants it. If nine runs of the resource model are prohibitive, selecting those climate scenarios that seem the best match/fit to the researcher's needs (e.g. provide a range of outcomes over the region of interest) is prudent. One approach would be to plot all the model projections using a graph, such as Figures 5, 10, or 26 for the region of interest, to determine a small subset of the nine scenarios that best cover the complete range of possibilities. Another approach would be to average the three climate projections within a given emissions scenario, recognizing that such averaging will suppress a lot of the simulated year-to-year variability generated by each model individually. As seen in Figures 7 and 9 (also Figures 13 and 14), the individual models within each scenario can differ greatly in their projected changes. Harding and others (2012) suggest that impact analyses relying on one or a few climate scenarios are unacceptably influenced by the choice of projections. Hence, if the use of an ensemble (average) of projections is desired, Mote and others (2011) recommend using the ensemble to characterize consensus not only about the projected mean but also about the range and other aspects of variability. If the analysis also uses the underlying socioeconomic projections, averaging across SRES scenarios is not recommended as that could be viewed as averaging different socioeconomic assumptions (Manning and others 2010).

Availability of Climate Projection Data

The historical climate data and the downscaled climate projections are available online both as gridded and as county level (aggregated grid cells) data (Table 8). Data for four climate variables (monthly mean daily minimum temperature, monthly mean daily maximum temperature, monthly total precipitation, and mean daily potential evapotranspiration) are included in the gridded and the county level data sets. The gridded climate change factors are also available separately for Alaska and the conterminous United States (Table 8). Metadata documentation following international standards is available for each climate data set.

We provide these data in ASCII text format for the convenience of most users, rather than formats commonly used by large-scale modelers, such as netCDF. The projection data set for the county spatial scale is available in nine files where each zipped file contains the climate projection data (2001-2100) for one scenario (A1B, A2, or B2) as modeled by one climate model (GCGM3.1, CSIRO-Mk3.5, MIROC3.2 for scenarios A1B and A2, or CGCM2, CSIROMK2 or HadCM3 for scenario B2) for all counties in the conterminous United States. The gridded data set is available in ten individually downloadable zipped files, where each file contains the projection data for the specified scenario (A1B, A2, B2) as modeled by the three climate models associated with each scenario (GCGM3.1, CSIRO-MK3.5, MIROC3.2 for scenarios A1B and A2, or CGCM2, CSIR-MK2 or HadCM3 for scenario B2) for all grid cells in the conterminous United States. Each of the ten zipped files contains three comma-delimited ASCII text files, one for each model and for one decade.

Table 8—RPA climate change projections, source climate models, and spatial scale at which the downscaled results are available through the RMRS archive website (www.fs.fed.us/rm/data_archive/).

Spatial scale	Climate data	Citation for meta-documentation and weblink
5-arcminute	Climate projections using SRES scenarios A1B and A2 and PRISM climatology for conterminous United States	Coulson, David P.; Joyce, Linda A.; Price, David T.; McKenney, Daniel W.; Siltanen, R. Martin; Papadopol, Pia; Lawrence Kevin. 2010c. Climate Scenarios for the conterminous United States at the 5 arc minute grid spatial scale using SRES scenarios A1B and A2 and PRISM climatology. Fort Collins, CO: U.S. Department of Agriculture, Forest Service, Rocky Mountain Research Station. Available: http://dx.doi.org/10.2737/RDS-2010-0017
5-arcminute	Climate projections using SRES scenarios B2 and PRISM climatology for conterminous United States	Coulson, David P.; Joyce, Linda A.; Price, David T.; McKenney, Daniel W. 2010d. Climate Scenarios for the conterminous United States at the 5 arc minute grid spatial scale using SRES scenario B2 and PRISM climatology. Fort Collins, CO: U.S. Department of Agriculture, Forest Service, Rocky Mountain Research Station. Available: http://dx.doi.org/10.2737/RDS-2010-0018
5-arcminute	Change factors for SRES Scenarios A1B, A2 for Alaska	Price, David T.; McKenney, Daniel W.; Siltanen, R. Martin; Papadopol, Pia; Lawrence, Kevin; Joyce, Linda A.; Coulson, David P. 2011c. High resolution interpolation of climate scenario change factors for Alaska derived from AR4 General Circulation Model simulations. Fort Collins, CO: U.S. Department of Agriculture, Forest Service, Rocky Mountain Research Station. Available: http://dx.doi.org/10.2737/RDS-2011-0022
5-arcminute	Change factors for SRES Scenarios A1B, A2 for the conterminous United States	Price, David T.; McKenney, Daniel W.; Siltanen, R. Martin; Papadopol, Pia; Lawrence, Kevin; Joyce, Linda A.; Coulson, David P. 2011b. High resolution interpolation of climate scenario change factors for the conterminous USA derived from AR4 General Circulation Model simulations. Fort Collins, CO: U.S. Department of Agriculture, Forest Service, Rocky Mountain Research Station. Available: http://dx.doi.org/10.2737/RDS-2011-0023
5-arcminute	Historical climate data (1946-2006) using PRISM climatology for conterminous United States	Coulson, David P.; Joyce, Linda A. 2010b. Historical climate data (1940-2006) for the conterminous United States at the 5 arcminute grid spatial scale based on PRISM climatology. Fort Collins, CO: U.S. Department of Agriculture, Forest Service, Rocky Mountain Research Station. Available: http://dx.doi.org/10.2737/RDS-2010-0011
County	Climate projections using SRES scenarios A1B and A2 and PRISM climatology for conterminous United States	Coulson, David P.; Joyce, Linda A.; Price, David T.; McKenney, Daniel W.; Siltanen, R. Martin; Papadopol, Pia; Lawrence, Kevin. 2010a. Climate Scenarios for the conterminous United States at the county spatial scale using SRES scenarios A1B and A2 and PRISM climatology. Fort Collins, CO: U.S. Department of Agriculture, Forest Service, Rocky Mountain Research Station. Available: http://dx.doi.org/10.2737/RDS-2010-0008
County	Climate projections using SRES scenarios B2 and PRISM climatology for conterminous United States	Coulson, David P.; Joyce, Linda A.; Price, David T.; McKenney, Daniel W. 2010b. Climate Scenarios for the conterminous United States at the county spatial scale using SRES scenario B2 and PRISM climatology. Fort Collins, CO: U.S. Department of Agriculture, Forest Service, Rocky Mountain Research Station. Available: http://dx.doi.org/10.2737/RDS-2010-0009
County	Historical climate data (1940-2006) based on PRISM climatology for conterminous United States	Coulson, David P.; Joyce, Linda A. 2010a. Historical Climate data (1940-2006) for the conterminous United States at the county spatial scale based on PRISM climatology. Fort Collins, CO: U.S. Department of Agriculture, Forest Service, Rocky Mountain Research Station. Available: http://dx.doi.org/10.2737/RDS-2010-0010

The individual gridded data files are still large, and as a result, most text reading software, such as Notepad, Wordpad, and Microsoft Word, are unable to open or completely open these files for viewing or processing. This is also true for Access and Excel. However, Excel 2007 will load the front end of the file for viewing, but as it has a limit of 1,048,578 lines of data, only 10 percent of the file will be loaded. Thus, users should ensure the software they are planning to use to process the data has the capability to handle files of this magnitude (the authors used SAS (Statistical Analysis System)).

Summary and Conclusons

This study developed historical climate data and downscaled climate scenario data (derived from climate model projections) to be used in concert with population projections, economic growth projections, and land use projections in the 2010 RPA Assessment. These data were developed for researchers and others who are interested in using climate data to model or assess the effects of climate change on natural resources within the conterminous United States. The specific applications of this data in the RPA Assessment are in the resource models of forest condition, water supply/use projections, wildlife habitat, recreation participation, and amenity migration analyses. These data will also be useful input for other applications exploring the impact of climate change on resource management issues in other settings.

In order to provide a broad set of alternative socio-economic futures for the RPA analysis, SRES scenarios A1B, A2, and B2 were selected. This study used projections from the following climate models: CGCM3.1(T47), CSIRO-MK3.5(T63) and MIROC3.2 (T42), each forced using the A1B and A2 emissions scenarios, as used in the IPCC's Fourth Assessment. For the B2 forcing scenario, we selected simulations generated by the CGCM2, CSIRO-MK2, and HadCM3 global climate models, as used in the IPCC's Third Assessment. These models have been used in a number of climate change impact studies and they have been compared with other climate models extensively in the literature. Generally, we can conclude from the literature that climate models used in the Fourth IPCC Assessment are likely to simulate present climate more accurately than the models used in the Third Assessment. The models used for the A1B and A2 scenarios in this study, as evaluated in the literature, perform reasonably well for a variety of tests when compared with many other AR4 models, and depending upon the metric used for comparison, models used here were among the top performers. Of the models used for the B2 scenario in our study, HadCM3 is likely a more accurate model with respect to historical climate estimation than the CSIRO-MK2 model. Little information was available from published literature to assess the performance of the CGCM2 model. The global climate data were downscaled for the conterminous region of the United States to a 5-arcminute grid using the delta technique for downscaling. In total, nine individual model projections (three scenarios and three models each) were developed.

All model projections forced by each of the three emissions scenarios project increased temperatures across the entire conterminous United States. Results for the A1B and A2 model projections are generally similar in magnitude over the next 50 years (i.e., consistent with long-term trends projected by other climate models) both regionally and globally. By 2100, however, simulations forced with the A2 scenario generally project the greatest warming, again consistent with projections of most climate models. On average, models forced by the

B2 scenario project the least warming by 2060 and 2100. Precipitation projections have less consistency among models and among scenarios and at the conterminous U.S. scale, it is difficult to detect a trend over the next 50 or 100 years. However, precipitation at regional scales shows some trends; generally projections show increases in precipitation for the northern regions.

We explore the use of different types of summarizations and graphical presentations at regional scales to show variation in temperature and precipitation projections at the regional scale. In the Southeast, both summer maximum and minimum temperatures are projected to increase across the region by at least 1.1 ^{o}C by mid-21st century and by up to 7 ^{o}C in the case of maximum temperature. Using the frequency distribution to explore temperature change in the Northern Great Plains indicates the spring mean daily minimum temperature will drop below 0 ^{o}C less frequently in the future. Historically, 40 percent of spring mean minimum temperature observations in the Northern Great Plains were below freezing, but by mid-century, more than 90 percent of the grid cell temperatures are projected to be above freezing. In the Southern Great Plains by mid-century, projected spring maximum temperatures overlap with and exceed the historical summer mean temperatures by as much as 6 ^{o}C. Results of a point-based comparison for two climate stations (Lamar, Colorado, and Lakeview, Oregon) project upward shifts in mean temperatures for all months at both locations; however, only the July and August mean temperature projections for the Lamar, Colorado, site are statistically outside of the 90th historical percentile. In the Pacific Northwest region, changes in minimum temperature across all seasons are projected to be greater than 1.4 ^{o}C by mid-century. Projected temperature increases in winter and spring brings these seasonal minimum temperatures close to, if not above, freezing in the eastern parts of this region.

The climate projection data are available for all nine projections at the 5-arcminute grid scale as well as aggregated to the U.S. county scale. Monthly projection data are available from 2001 to 2100. The change factor data (“the deltas”) are available for users who may wish to apply these factors to their own historical climatology or other available climatologies. These data are available online through the U.S. Forest Service Research and Development data archive website (http://www.fs.usda.gov/rds/archive/).

References

Anandhi, A.; Frei, A.; Pradhanang, S.M.; Zion, M.S.; Pierson, D.C.; Schneiderman, E.M. 2011. AR4 climate model performance in simulating snow water equivalent over Catskill Mountain watersheds, New York, USA. Hydrological Processes 25: 3302-3311.

Bachelet, D.; Neilson, R.P.; Hickler, T.; Drapek, R.J.; Lenihan, J.M.; Sykes, M.T.; Smith, B.; Sitch, S.; Thonicke, K. 2003. Simulating past and future dynamics of natural ecosystems in the United States. Global Biogeochemical Cycles 17: 1045. doi:10.1029/2001GB001508, 2003.

Bachelet, D.; Lenihan, J.; Drapek, R.; Neilson, R.P. 2008. VEMAP vs VINCERA: A DGVM sensitivity to differences in climate scenarios. Global and Planetary Change 64: 38-48.

Bowker, J.M.; Askew, A.E.; Cordell, H.K.; Betz, C.J.; Zarnoch, S.J.; Seymour, L. 2012. Outdoor Recreation Participation in the United States – Projections to 2060: A technical document supporting the Forest Service 2010 RPA Assessment. Gen. Tech. Rep. SRS-GTR-160. Asheville, NC: U.S. Department of Agriculture, Forest Service, Southern Research Station. 34 p.

Brekke, L.D.; Dettinger, M.D.; Maurer, E.P.; Anderson, M. 2008. Significance of model credibility in estimating climate projection distributions for regional hydroclimatological risk assessments. Climatic Change 89: 371–394.

Cayan, D.; Luers, A.L.; Hanemann, M.; Franco, G. 2006. Scenarios of climate change in California: an overview. CEC-500-2005-1896-SF. California Energy Commission. Online: http://www.energy.ca.gov/2005publications/CEC-500-2005-186/CEC-500-2005-186-SF.PDF (accessed 1-18-2013).

Christensen, J.H.; Hewitson, B.; Busuioc, A.; Chen, A.; Gao, X.; Held, I.; Jones, R.; Kolli, R.K.; Kwon, W.-T.; Laprise, R.; Magaña Rueda, V.; Mearns, L.; Menéndez, C.G.; Räisänen, J.; Rinke, A.; Sarr, A.; Whetton, P. 2007: Regional climate projections. In: Solomon, S.; Qin, D.; Manning, M.; Chen, Z.; Marquis, M.; Averyt, K.B.; Tignor, M.; Miller, H.L. (eds.). Climate change 2007: The physical science basis. Contribution of Working Group I to the Fourth Assessment Report of the Intergovernmental Panel on Climate Change Cambridge, UK: Cambridge University Press: 847-940.

Cordell, H.K.; Heboyan, V.; Santos, F.; Bergstrom, J.C. 2011. Natural amenities and rural population migration: a technical document supporting the Forest Service 2010 RPA Assessment. Gen. Tech. Rep. SRS-GTR-146. Asheville, NC: U.S. Department of Agriculture Forest Service, Southern Research Station. 23 p.

Coulson, D.P.; Joyce, L.A.; Price, D.T.; McKenney, D.W.; Siltanen, R.M.; Papadopol, P.; Lawrence, K. 2010a. Climate scenarios for the conterminous United States at the county spatial scale using SRES scenarios A1B and A2 and PRISM climatology. Fort Collins, CO: U.S. Department of Agriculture, Forest Service, Rocky Mountain Research Station. Online: http://dx.doi.org/10.2737/RDS-2010-0008 (accessed 1-18-2013).

Coulson, D.P.; Joyce, L.A.; Price, D.T.; McKenney, D.W. 2010b. Climate scenarios for the conterminous United States at the county spatial scale using SRES scenario B2 and PRISM climatology. Fort Collins, CO: U.S. Department of Agriculture, USDA Forest Service, Rocky Mountain Research Station. Online: http://dx.doi.org/10.2737/RDS-2010-0009 (accessed 1-18-2013).

Coulson, D.P.; Joyce, L.A.; Price, D.T.; McKenney, D.W.; Siltanen, R.M.; Papadopol, P.; Lawrence, K. 2010c. Climate scenarios for the conterminous United States at the 5 arc-minute grid spatial scale using SRES scenarios A1B and A2 and PRISM climatology. Fort Collins, CO: U.S. Department of Agriculture, Forest Service, Rocky Mountain Research Station. Online: http://dx.doi.org/10.2737/RDS-2010-0017 (accessed 1-18-2013).

Coulson, D.P.; Joyce, L.A.; Price, D.T.; McKenney, D.W. 2010d. Climate scenarios for the conterminous United States at the 5 arcminute grid spatial scale using SRES scenarios B2 and PRISM climatology. Fort Collins, CO: U.S. Department of Agriculture, Forest Service, Rocky Mountain Research Station. Online: http://dx.doi.org/10.2737/RDS-2010-0018 (accessed 1-18-2013).

Coulson, D.P.; Joyce, L.A. 2010a. Historical Climate data (1940-2006) for the conterminous United States at the county spatial scale based on PRISM climatology. Fort Collins, CO: U.S. Department of Agriculture, Forest Service, Rocky Mountain Research Station. Online: http://dx.doi.org/10.2737/RDS-2010-0010 (accessed 1-18-2013).

Coulson, D.P.; Joyce, L.A. 2010b. Historical climate data (1940-2006) for the conterminous United States at the 5 arcminute grid spatial scale based on PRISM climatology. Fort Collins, CO: U.S. Department of Agriculture, Forest Service, Rocky Mountain Research Station. Online: http://dx.doi.org/10.2737/RDS-2010-0011 (accessed 1-18-2013).

Cubasch, U.; Meehl, G.A.; Boer, G.-J.; Stouffer, R.J.; Dix, M.; Noda, A.; Senior, C.A.; Raper, S.; Yap, K.S. 2001. Projections of future climate change. In: Houghton, J.T.; Ding, Y.; Griggs, D.J.; Noguer, M.; van der Linden, P.J.; Dai, X.; Maskell, K.; Johnson C.A. (eds.).Climate change 2001: The scientific basis. Contribution of Working Group I to the Third Assessment Report of the Intergovernmental Panel on Climate Change. Cambridge, UK: Cambridge University Press: 526-582.

Daly C.; Neilson R.P.; Phillips D.L. 1994. A statistical-topographic model for mapping climatological precipitation over mountainous terrain. Journal of Applied Meteorology 33: 140–158.

Daly, C.; Gibson, W.P.; Taylor, G.H.; Johnson, G.L.; Pasteris, P. 2002. A knowledge-based approach to the statistical mapping of climate. Climate Research 22: 99-113.

Daniels, A.E.; Morrison, J.F.; Joyce, L.A.; Crookston, N.L.; Chen, S.C.; McNulty, S.G. 2012. Climate projections FAQ. Gen. Tech. Rep. RMRS-GTR-277WWW. Fort Collins, CO: U.S. Department of Agriculture, Forest Service, Rocky Mountain Research Station. 32 p.

Foti, R.; Ramirez, J.A.; Brown, T.C. 2012. Vulnerability of U.S. water supply to shortage: a technical document supporting the Forest Service 2010 RPA Assessment. Gen. Tech. Rep. RMRS-GTR-295. Fort Collins, CO: U.S. Department of Agriculture, Forest Service, Rocky Mountain Research Station. 147 p.

Gibson, W.; Daly, C.; Kittel, T.; Nychka, D.; Johns, C.; Rosenbloom, N.; McNab, A.; Taylor, G. 2002. Development of a 103-year high-resolution climate data set of the conterminous United States. Proceedings of the 13th AMS Conference on Applied Climatology; May 13-16, 2002; Portland, OR. Boston, MA: American Meteorological Society: 181-183. Online: http://ams.confex.com/ams/13ac10av/techprogram/programexpanded_99.htm or http://prism.oregonstate.edu/docs/index.phtml.

Gleckler, P.J.; Taylor, K.E.; Doutriaux, C. 2008. Performance metrics for climate models. Journal of Geophysical Research: Atmospheres 113: D06104, doi: 10.1029/2007JD008972.

Greenfield, E.J.; Nowak, D.J. 2013. Tree cover and aridity projections to 2060: a technical document supporting the Forest Service 2010 RPA Assessment. Gen. Tech. Rep. NRS-GTR-125. Newtown Square, PA: U.S. Department of Agriculture, Forest Service, Northern Research Station. 35 p.

Hamlet, A.F.; Lettenmaier, D.P. 1999. Effects of climate change on hydrology and water resources in the Columbia River Basin. Journal of the American Water Resources Association 35: 1597-1623.

Harding, B.L.; Wood, A. W.; Prairie, J.R. 2012. The implications of climate change scenario selection for future streamflow projection in the Upper Colorado River Basin Hydrology and Earth System Science: 16, 3989–4007.

Hayhoe, K.; Wake, C.P.; Huntington, T.G.; Luo, L.; Schwartz, M.D.; Sheffield, J.; Wood, E.; Anderson, B.; Bradbury, J.; DeGaetano, A.; Troy, T.J.; Wolfe, D. 2007. Past and future changes in climate and hydrological indicators in the U.S. Northeast. Climate Dynamics 28: 381-407.

Hegerl, G.C.; Zwiers, F.W.; Braconnot, P.; Gillett, N.P.; Luo, Y.; Marengo Orsini, J.A.; Nicholls, N.; Penner, J.E.; Stott, P.A. 2007. Understanding and attributing climate change. In: Solomon, S.; Qin, D.; Manning, M.; Chen, Z.; Marquis, M.; Averyt, K.B.; Tignor, M.; Miller, H.L. (eds.). Climate change 2007: The physical science basis. Contribution of Working Group I to the Fourth Assessment Report of the Intergovernmental Panel on Climate Change. Cambridge, UK: Cambridge University Press: 663-745.

Hutchinson, M.F. 2010. ANUSPLIN Software Version 4.3. Online: http://fennerschool.anu.edu.au/research/software-datasets/anusplin (accessed 1-18-2013).

Hutchinson, M.F.; McKenney D.W.; Lawrence, K.; Pedlar, J.H.; Hopkinson, R.F.; Milewska, E.; Papadopol, P. 2009. Development and testing of Canada-wide interpolated spatial models of daily minimum–maximum temperature and precipitation for 1961–2003. Journal of Applied Meteorology and Climatology 48: 726–741.

IPCC [Intergovernmental Panel on Climate Change]. 2001a. Climate change 2001: Synthesis report. Contribution of Working Groups I, II, and III to the Third Assessment Report of the Intergovernmental Panel on Climate Change. Watson, R.T. and the Core Writing Team (eds.). Cambridge, UK: Cambridge University Press. 398 p.

IPCC [Intergovernmental Panel on Climate Change]. 2001b. Climate change 2001: The scientific basis. Contribution of Working Group I to the Third Assessment Report of the Intergovernmental Panel on Climate Change. Houghton, J.T.; Ding, Y.; Griggs, D.J.; Noguer, M.; van der Linden, P.J.; Dai, X.; Maskell, K.; Johnson, C.A. (eds.). Cambridge, UK: Cambridge University Press. 881 p.

IPCC [Intergovernmental Panel on Climate Change]. 2007a. Climate change 2007: Synthesis report. Contribution of Working Groups I, II and III to the Fourth Assessment. Report of the Intergovernmental Panel on Climate Change. Core Writing Team, Pachauri, R.K and Reisinger, A. (eds.). Geneva, Switzerland: IPCC. 104 p.

IPCC [Intergovernmental Panel on Climate Change]. 2007b. Glossary. In Annex I [A.P.M. Baede (ed)]. In: Contribution of Working Group I to the Fourth Assessment Report of the Intergovernmental Panel on Climate Change. Solomon, S.; Qin, D.; Manning, M.; Chen, Z.; Marquis, M.; Averyt, K.B.; Tignor, M.; Miller, H.L. (eds.). Geneva, Switzerland: IPCC: 941-954.

IPCC-TGICA [Intergovernmental Panel on Climate Change, Task Group on Data and Scenario Support for Impact and Climate Assessment].2007. General guidelines on the use of scenario data for climate impact and adaptation assessment. Online: http://www.ipcc-data.org/guidelines/TGICA_guidance_sdciaa_v2_final.pdf. 66 p.

Johnson, F.; Westra, S.; Sharma, A. 2011. An assessment of GCM skill in simulating persistence across multiple time scales. Journal of Climate 24: 3609-3623.

Joyce, L.A.; Birdsey, R., tech. eds. 2000. The impact of climate change on America's forests. Gen. Tech. Rep. RMRS-GTR-59. Fort Collins, CO: U.S. Department of Agriculture, Forest Service, Rocky Mountain Research Station. 133 p.

Joyce, L.A.; Price, D.T.; McKenney, D.W.; Siltanen, R.M.; Papadopol, P.; Lawrence, K.; Coulson, D.P. 2011. High resolution interpolation of climate scenarios for the conterminous USA and Alaska derived from general circulation model simulations. Gen. Tech. Rep. RMRS-GTR-263. Fort Collins, CO: U.S. Department of Agriculture, Forest Service, Rocky Mountain Research Station. 87 p.

Kingston, D.G.; Todd, M.C.; Taylor, R.G.; Thompson, J.R.; Arnell, N.W. 2009. Uncertainty in the estimation of potential evapotranspiration under climate change. Geophysical Research Letters: 36, L20403, doi:10.1029/2009GL040267.

Kittel, T.G.F.; Rosenbloom, N.A.; Royle, J.A.; Daly, C.; Gibson, W.P.; Fisher, H.H.; Thornton, P.; Yates, D.N.; Aulenbach, S.; Kaufman, C.; McKeown, R.; Bachelet, D.; Schimel, D.S.; VEMAP2 Participants. 2004. VEMAP Phase 2 bioclimatic database. I. Gridded historical (20th century) climate for modeling ecosystem dynamics across the conterminous USA. Climate Research 27: 151-170.

Lamarque, J.-F.; Kiehl, J.; Brasseur, G.; Butler, T.; Cameron-Smith, P.; Collins, W.D.; Collins, W.J.; Granier, C.; Hauglustaine, D.; Hess, P.; Holland, E.; Horowitz, L.; Lawrence, M.; McKenna, D.; Merilees, P.; Prather, M.; Rasch, P.; Rotman, D.; Shindell, D.; Thornton, OP. 2005. Assessing future nitrogen deposition and carbon cycle feedback using a multi-model approach. Part 1: Analysis of nitrogen deposition. Journal of Geophysical Research 110: D19303 Online: doi:10.1029/2005JD005825.

Lenihan, J.M.; Bachelet, D.; Neilson, R.P.; Drapek, R.J. 2008. Simulated response of conterminous United States ecosystems to climate change at different levels of fire suppression, CO_2, and growth response to CO_2. Global and Planetary Change. 64: 16-25.

Linacre, E.T. 1977. A simple formula for estimating evaporation rates in various climates using temperature data alone. Agricultural Meteorology 18: 409-424.

Lobell, D.B.; Bonfils,C.; Duffy, P.B. 2007. Climate change uncertainty for daily minimum and maximum temperatures: A model inter-comparison. Geophysical Research Letters 34: L05715. doi:10.1029/2006GL028726

Manning, M.R.; Edmonds, J, E.; Grubler, A.; Hibbard, K.; Joos, F.; Kainuma, M.; Keeling, R.F.; Kram, T.; Manning, A.C.; Meinshausen, M.; Moss, R.; Nakicenovic, N.; Riahi, K.; Rose, S.K.; Smith, S.; Swart, R.; van Vuuren, D.P. 2010. Misrepresentation of the IPCC CO_2 emission scenarios. Nature Geoscience 3: 376–377.

McKenney, D.W.; Price, D.T.; Papadapol, P.; Siltanen, R.M; Lawrence, K. 2006a. High-resolution climate change scenarios for North America. Frontline Technical Note 107. Sault Ste. Marie, ON, Canada: Canadian Forestry Service, Great Lakes Forestry Centre. 18 p.

McKenney, D.W.; Pedlar, J.H.; Papadopol, P.; Hutchinson, M.F. 2006b. The development of 1901–2000 historical monthly climate models for Canada and the United States. Agricultural and Forest Meteorology 138: 69–81.

McKenney, D.W.; Papadapol, P.; Campbell, K.; Lawrence, K.; Hutchinson, M.F. 2006c. Spatial models of Canada- and North America-wide 1971/2000 minimum and maximum temperature, total precipitation and derived bioclimatic variables. Frontline Technical Note 106. Sault Ste. Marie, ON, Canada: Canadian Forestry Service, Great Lakes Forestry Centre.

McKenney, D.W.; Hutchinson, M.F.; Papadopol, P.; Lawrence, K.; Pedlar, J.; Campbell, K.; Milewska, E.; Hopkinson, R.T.; Price, D.; Owen, T. 2011. Customized spatial climate models for North America. Bulletin of the American Meteorology Society 92: 1611-1622. doi: 10.1175/BAMS-D-10-3-3132.1.

Meehl, G.A.; Covey, C.; Delworth, T.; Latif, M.; McAvaney, B.; Mitchell, J.F.B.; Stouffer, R.J.; Taylor, K.E. 2007a. The WCRP CMIP3 multimodel data set. Bulletin of the American Meteorological Society 88: 1383–1394. doi: http://dx.doi.org/10.1175/BAMS-88-9-1383.

Meehl, G.A.; Stocker, T.F.; Collins, W.D.; Friedlingstein, P.; Gaye, A.T.; Gregory, J.M.; Kitoh, A.; Knutti, R.; Murphy, J.M.; Noda, A.; Raper, S.C.B.; Watterson, I.G.; Weaver, A.J.; Zhao, Z.-C. 2007b: Global Climate Projections. In: Solomon, S.; Qin, D.; Manning, M.; Chen, Z.; Marquis, M.; Averyt, K.B.; Tignor, M.; Miller, H.L. (eds.). Climate change 2007: The physical science basis. Contribution of Working Group I to the Fourth Assessment Report of the Intergovernmental Panel on Climate Change Cambridge, UK: Cambridge University Press:ManningMiller: 747-845

Miller, N.I.; Bashford, K.E.; Strem, E. 2003. Potential impacts of climate change on California hydrology. Journal of the American Water Resources Association 39: 771-784.

Mote, P.W.; Salathé, E.P. 2009. Future climate in the Pacific Northwest. In: The Washington Climate Change impacts assessment: Evaluating Washington's future in a changing climate. Seattle, WA: University of Washington, Climate Impacts Group.

Mote, P.; Brekke, L.; Duffy, P.B.; Maurer, E. 2011. Guidelines for Constructing Climate Scenarios. EOS 92: 257-264.

Nakicenovic, N.; Swart, R. (eds.). 2000. Special report on emissions scenarios. A Special Report of Working Group III of the Intergovernmental Panel on Climate Change. Cambridge, UK: Cambridge University Press. 570 p. Online: http://www.ipcc.ch/ipccreports/sres/emission/index.htm.

Parry M.L.; Canziani O.F.; Palutikof J.P.; and others. 2007. Technical summary. In: Parry, M.L.; Canziani, O.F.; Palutikof, J.P. van der Linden, P.J.; Hanson, C.E. (eds.). Climate Change 2007; Impacts, adaptation and vulnerability. Contribution of Working Group II to the Fourth Assessment Report of the Intergovernmental Panel on Climate Change.Parry. Cambridge, UK: Cambridge University Press: 23-78.

Prentice, I.C.; Farquhar, G.D.; Fasham, M.J.R.; Goulden, M.L.; Heimann, M.; Jaramillo, V.J.; Kheshgi, H.S.; LeQuere, C.; Scholes, R.J.; Wallace, D.W.R. 2001. The carbon cycle and atmospheric carbon dioxide. Chapter 3. In: Houghton, J.T.; Ding, Y.; Griggs, D.J.; Noguer, M.; van der Linden, P.J.; Dai, X.; Maskell, K.; Johnson C.A. (eds.).Climate change 2001: The scientific basis. Contribution of Working Group I to the Third Assessment Report of the Intergovernmental Panel on Climate Change. Cambridge, UK: Cambridge University Press: 183-238 p.

Price, D.T.; McKenney, D.W.; Nalder, I.A.; Hutchinson, M.F.; Kestevan, J.L. 2000. A comparison of statistical and thin-plate spline methods for spatial interpolation of Canadian monthly mean climate data. Agricultural and Forest Meteorology 101: 81–94.

Price, D.T.; McKenney, D.W.; Papadopol, P.; Logan, T.; Hutchinson, M.F. 2004. High resolution future scenario climate data for North America. In: Proceedings of the 26th Conference on Agricultural and Forest Meteorology; August 23-26, 2004; Vancouver, BC. Boston, MA: American Meteorological Society: 7.7.1-7.7.13. Online: http://ams.confex.com/ams/AFAPURBBIO/techprogram/paper_78202.htm.

Price, D.T.; Scott, D. 2006. Project A636: Large scale modelling of Canada's forest ecosystem responses to climate change. 2nd ed. Final report to Government of Canada: Climate change impacts and adaptation program.

Price, D.T.; McKenney, D.W.; Joyce, Linda A.; Siltanen, R.M.; Papadopol, P.; Lawrence, K. 2011a. High resolution interpolation of climate scenarios for Canada derived from general circulation models. Inf. Rep. NOR-X-2011. Edmonton, Alberta, Canada: Canadian Forest Service, Northern Forestry Centre, Natural Resources Canada. 135 p.

Price, D.T.; McKenney, D.W.; Siltanen, R.M.; Papadopol, P.; Lawrence, K.; Joyce, L.A.; Coulson, D.P. 2011b. High resolution interpolation of climate scenario change factors for the conterminous USA derived from AR4 General Circulation Model simulations. Fort Collins, CO: U.S. Department of Agriculture, Forest Service, Rocky Mountain Research Station. Online: http://dx.doi.org/10.2737/RDS-2011-0023.

Price, D.T.; McKenney, D.W.; Siltanen, R.M.; Papadopol, P.; Lawrence, K.; Joyce, L.A.; Coulson, D.P. 2011c. High resolution interpolation of climate scenario change factors for Alaska derived from AR4 General Circulation Model simulations. Fort Collins, CO: U.S. Department of Agriculture, Forest Service, Rocky Mountain Research Station. Online: http://dx.doi.org/10.2737/RDS-2011-0022.

Price, D.T. 2009. [email to L Joyce]. October 21, 2009. RE: FW: Third IPCC Assessment B2 scenarios – question. On file at: USDA Forest Service Rocky Mountain Research Station, Fort Collins, CO, with author.

Radic, V.; Clarke, G.K.C. 2011. Evaluation of IPCC models' performance in simulating late-twentieth-century climatologies and weather patterns over North America. Journal of Climate 24: 5257-5274.

Randall, D.A.,; Wood, R.A.; Bony, S.; Colman, R.; Fichefet, T.; Fyfe, J.; Kattsov, V.; Pitman, A.; Shukla, J.; Srinivasan, J.; Stouffer, R.J.; Sumi, A.; Taylor, K.E. 2007. Climate models and their evaluation. In: Climate change 2007: The physical science basis. In: Solomon, S.; Qin, D.; Manning, M.; Chen, Z.; Marquis, M.; Averyt, K.B.; Tignor, M.; Miller, H.L. (eds.). Climate change 2007: The physical science basis. Contribution of Working Group I to the Fourth Assessment Report of the Intergovernmental Panel on Climate Change Cambridge, UK: Cambridge University Press: 590-662.

Ray, A.J.; Barsugli, J.J.; Averyt, K.B.; and others. 2008. Climate change in Colorado. A synthesis to support water resources management and adaptation. Boulder, CO: CU-NOAA Western Water Assessment. 52 p.

Rehfeldt, G.E. 2006. A spline model of climate for the western United States. Gen. Tech. Rep. RMRS-GTR-165. Fort Collins, CO: U.S. Department of Agriculture, Forest Service, Rocky Mountain Research Station. 21 p.

Rehfeldt, G.E.; Crookston, N.L.; Warwell, M.V.; Evans, J.S. 2006. Empirical analyses of plant-climate relationships for the western United States. International Journal of Plant Science 167: 1123-1150.

Reichler, T.; Kim, J. 2008. How well do coupled models simulate today's climate? Bulletin of the American Meteorology Society 89: 303-311.

Rogers, B.M.; Neilson, R.P.; Drapek, R.; Lenihan, J.M.; Wells, J.R.; Bachelet, D.; Law, B.E. 2011. Impacts of climate change on fire regimes and carbon stocks of the U.S. Pacific Northwest. Journal of Geophysical Research 116: G03037.

Tabor, K.; Williams, J.W. 2010. Globally downscaled climate projections for assessing the conservation impacts of climate change. Ecological Applications 20: 554-565.

USDA Forest Service. 2012a. Future scenarios: a technical document supporting the Forest Service 2010 RPA Assessment. Gen. Tech. Rep. RMRS-GTR-272. Fort Collins, CO: U.S. Department of Agriculture, Forest Service, Rocky Mountain Research Station. 34 p.

USDA Forest Service. 2012b. Future of America's Forest and Rangelands: Forest Service 2010 Resources Planning Act Assessment. Gen. Tech Rep. WO-87. Washington, DC: U.S. Department of Agriculture, Forest Service. 198 p.

USDI Bureau of Reclamation, 2010(draft). Climate change and hydrology scenarios for Oklahoma yield studies. Technical Memorandum 86-68210-2010-01 (draft). Prepared by Technical Service Center, Water Resources Planning and Operations Support Group Water and Environmental Resources Division, Levi Brekke, Tom Pruitt, and Del Smith. 59 p.

VEMAP members [Vegetation/ecosystem modeling and analysis project]. 1995. Comparing biogeography and biogeochemistry models in a continental-scale study of terrestrial ecosystem responses to climate change and CO_2 doubling. Global Biogeochemical Cycles 9: 407-437.

Wear, D.N.; Huggett, R.; Li, R.; Perryman, B.; Liu, S. 2013. Forecasts of forest conditions in regions of the United States under future scenarios: a technical document supporting the Forest Service 2010 RPA Assessment. Gen. Tech. Rep. SRS-GTR-170. Asheville, NC: Department of Agriculture, Forest Service, Southern Research Station. 101 p.

Zhu, Z.(editor); Bouchard, M.; Butman, D.; Hawbaker, T.; Li, Z.; Liu, J.; Liu, S.; McDonald, C.; Reker, R.; Sayler, K.; Sleeter, B.; Sohl, T.; Stackpoole, S.; Wein, A.; Zhu, Z. 2011. Baseline and projected future carbon storage and greenhouse-gas fluxes in the Great Plains Region of the United States. Professional Paper 1787. Reston, VA: U.S. Geological Survey. Online: http://pubs.usgs.gov/pp/1787/.

Appendix I: Carbon Dioxide Concentrations and Nitrogen Emissions Associated with the Scenarios

Development of the storylines and the emission levels for the greenhouse gases is given in Nakicenovic and Swart 2000. The anthropogenic emissions for each greenhouse gas are given in Nakicenovic and Swart 2000 as well as the Appendix II of Working Group I report (IPCC 2001b). Two carbon cycle models (ISAM, Bern-CC) were used in the scenario development process to compute the CO_2 concentrations that develop in the atmosphere as a result of the greenhouse gas emission levels from the A1B, A2, and B2 scenarios (Tables I.1, and I.2).

Table I.1—CO_2 concentrations (ppm) used by AR4 models as projected by the ISAM model reference case. (http://www.ipcc-data.org/ddc_co2.html).

	ISAM model (reference)		
Year	A1B	A2	B2
	- - - - - - - - - - - ppm - - - - - - - - - - -		
1970	325	325	325
1980	337	337	337
1990	353	353	353
2000	369	369	369
2010	391	390	388
2020	420	417	408
2030	454	451	429
2040	491	490	453
2050	532	532	478
2060	572	580	504
2070	611	635	531
2080	649	698	559
2090	685	771	589
2100	717	856	621

Note: A 'reference' case was defined with climate sensitivity 2.5 °C, ocean uptake corresponding to the mean of the ocean model results in Chapter 3, Figure 3.10 (IPCC 2001b), and terrestrial uptake corresponding to the mean of the responses of mid-range models, LPJ, IBIS and SDGM (Chapter 3, Figure 3.10, IPCC 2001b). See Chapter 3, Box 3.7 (IPCC 2001b) for more details on the ISAM model.

Table I.2—CO_2 concentrations (ppm) used by AR4 models as projected by the Bern-CC reference case. (http://www.ipcc-data.org/ddc_co2.html).

	Bern-CC model (reference)		
Year	**A1B**	**A2**	**B2**
	ppm		
1970	325	325	325
1980	337	337	337
1990	352	352	352
2000	367	367	367
2010	388	386	385
2020	418	414	406
2030	447	444	425
2040	483	481	448
2050	522	522	473
2060	563	568	499
2070	601	620	524
2080	639	682	552
2090	674	754	581
2100	703	836	611

Note: A "reference" case was defined with an average ocean uptake for the 1980s of 2.0 PgC/yr. Climate sensitivity was set to 2.5 °C for a doubling of CO2. The Bern-CC model was initialized for observed atmospheric CO2 which was prescribed for the period 1765 to 1999. The CO2 data were smoothed by a spline. Scenario calculations started at the beginning of the year 2000. This explains the difference in the values given for the years up to 2000. Values shown are for the beginning of each year. Annual-mean values are generally higher (up to 7ppm) depending on the scenario and the year. See Chapter 3, Box 3.7 (IPCC 2001b) for more details on the Bern-CC model.

Further information on the carbon cycle models and the development of these concentrations is given in IPCC TAR Working Group 1 report (IPCC 2001b) Box 3.7 (http://www.ipcc.ch/ipccreports/tar/wg1/122.htm). These CO_2 concentrations were then used as forcings in various General Circulation Models reported in the AR4 (Table I.3).

Nitrogen oxide (NO_x) emissions (Table I.4) were also developed in the SRES process using the Integrated Assessment Models (Nakicenovic and Swart 2000). The emission levels are given in Nakicenovic and Swart (2000) as well as in Appendix II of Working Group I report (IPCC 2001b). The abundances (concentrations) were not developed for NO_x (http://www.ipcc.ch/ipccreports/tar/wg1/525.htm)

Table I.3—Climate models using future CO_2 concentrations output from the Integrated Science Assessment Model (ISAM) or the Bern Carbon Cycle model (Bern-CC) (from http://www.ipcc-data.org/ddc_co2.html).

ISAM	MRI:CGCM2_3_2 NASA:GISS-AOM, GISS-EH, GISS-ER GFDL:CM2 GFDL:CM2_1
Bern-CC	BCC:CM1 BCCR:BCM2 CNRM:CM3 INM:CM3 IPSL:CM4 LASG:FGOALS-G1_0 NCAR:CCSM3 NIES:MIROC3_2-HI, MIROC3_2-MED; UKMO:HadCM3, HADGEM1

Table I.4—NO_x emissions (TgN/yr) (from Working Group I Appendix II, http://www.ipcc.ch/ipccreports/tar/wg1/525.htm).

Year	A1B	A1T	A1FI	A2	B1	B2	A1p	A2p	B1p	B2p	IS92a
2000	32.0	32.0	32.0	32.0	32.0	32.0	32.5	32.5	32.5	32.5	37.0
2010	39.3	38.8	39.7	39.2	36.1	36.7	41.0	39.6	34.8	37.6	43.4
2020	46.1	46.4	50.4	50.3	39.9	42.7	48.9	50.7	39.3	43.4	49.8
2030	50.2	55.9	62.8	60.7	42.0	48.9	52.5	60.8	40.7	48.4	55.2
2040	48.9	59.7	77.1	65.9	42.6	53.4	50.9	65.8	44.8	52.8	59.6
2050	47.9	61.0	94.9	71.1	38.8	54.5	49.3	71.5	48.9	53.7	64.0
2060	46.0	59.6	102.1	75.5	34.3	56.1	47.2	75.6	48.9	55.4	67.8
2070	44.2	51.7	108.5	79.8	29.6	56.3	45.1	80.1	48.9	55.6	71.6
2080	42.7	42.8	115.4	87.5	25.7	59.2	43.3	87.3	48.9	58.5	75.4
2090	41.4	34.8	111.5	98.3	22.2	60.9	41.8	97.9	41.2	60.1	79.2
2100	40.2	28.1	109.6	109.2	18.7	61.2	40.3	109.7	33.6	60.4	83.0

Note: NO_x is the sum of NO and NO_2.

Appendix II: CMIP3 Run Numbers for Individual Climate Model Projections

Table II.1—Realization (or run) numbers for each climate model and greenhouse gas forcing scenario in the CMIP3 catalog that were selected for spatial interpolation using ANUSPLIN in this study.

Model and scenario	Run number	Time stamp[a]
CGCM3.1(T47)[b]		
20C3M	Run 5	reformatted 2005-05-12—22:21:09
A2	Run 5	reformatted 2005-05-12—22:21:09
A1B	Run 5	reformatted 2005-05-12—22:21:09
CSIRO-MK3.5(T63)[c]		
20C3M	Run 1	2006-09-20—05:09
A2	Run 1	2006-09-20—04:09
A1B	Run 1	2006-11-04—10:04
MIROC3.2(T42)[d]		
20C3M	Run 3	reformatted 2004-10-14—20:53:37
A2	Run 3	reformatted 2004-12-14—00:22:38
A1B	Run 3	reformatted 2004-12-14—00:02:09

[a]Date and time information extracted from available metadata for the run.
[b]CGCM3.1(T47) = Third Generation Coupled Global Climate Model, version 3.1, medium resolution.
[c]CSIRO-MK3.5(T63) = Commonwealth Scientific and Industrial Research Organisation Climate System Model, Mark 3.5.
[d]MIROC3.2(T42) = Model for Interdisciplinary Research on Climate, version 3.2, medium resolution.

Appendix III: Potential Evaporation Estimation Procedure

Potential evapotranspiration (PET) for vegetation was calculated using a modification of Penman's work by Linacre (1977),

where

$$PET = [500Tm/(100\text{-}A)+15(T\text{-}Td)]/(80\text{-}T)\text{mm day-1}$$

and

T is the mean monthly temperature in units of degrees Celsius (^{o}C),

Tm is the mean monthly temperature adjusted for elevation,

Td is the mean monthly dew point temperature in units of degrees Celsius, and

A is the latitude in degrees.

Tm = T + 0.0006h,

where

h is the elevation in units of meters.

Linacre (1977) provides an alternate for estimating (T-Td) when dew point data are not available. (T-Td) = 0.0023h+0.37T+0.53R+0.35Rann-10.9°C. Rann is the difference between the means of the hottest and coldest months. R is mean daily range of temperature.

Rann is calculated from the projected data by the formula Max(T1-T12)-Min(T1-T12). Ti is the mean monthly temperature of the month, where T1= Jan, T2=Feb…T12=Dec.

Mean R is estimated from PRISM data using mean monthly of maximum air temperature and the minimum air temperature from 1940-2006. This value is used as a surrogate for any given year in the future. The R is calculated for each PRISM grid and then a weighted average is calculated for the 5-arcminute grids as described above.

Note that R = ∑(Dmax – Dmin)/n,

where

R is the monthly average,

Dmax is the daily maximum temperature,

Dmin is the daily minimum temperature,

n is the number of days in the month.

An elevation is obtained from PRISM data, which is available at the 2.5-minute grids (1/24 degree) and a weighted mean is calculated for the 5-arcminute grid.

This methodology provides an estimate of future PET using only the temperature and latitude values from the climate projections, elevation, and average mean daily temperature range from PRISM data.

Appendix IV: Area-Weighting the Climate Data

All regional and conterminous summaries of the climate data were computed using an area-weight calculation. For estimations within the conterminous United States in Geographic 0.08333 degree, area was calculated for latitude of center of cell in Excel (as per http://eos-webster.sr.unh.edu/data_guides/global_model_dg.jsp#equations) shown here:

Convert to radians:
radians = (90.0-(lat))*3.141593/180.0

Calculate cosines:
cosines = cosine(radians)-cosine(radians+(0.083333333333333*3.141593)/180.0)

Calculate area in square kilometers:
area = 6371221.3*6371221.3*3.141593*cosines/(180/0.0833333333333333)*1.0e-6

United States Department of Agriculture

Forest Service

Rocky Mountain Research Station

General Technical Report RMRS-GTR-320

May 2014